***Graphical Abstract**

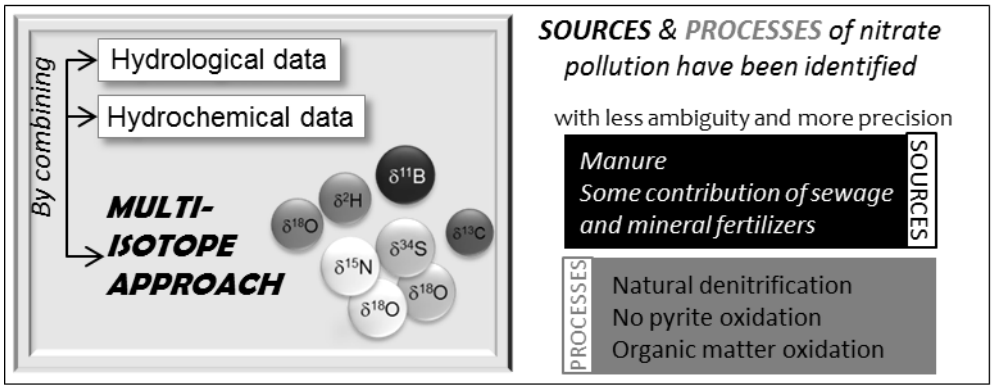

***Highlights (for review)**

- $\delta^{15}N$, $\delta^{18}O_{NO3}$ and $\delta^{11}B$ confirm pig manure as the main vector of NO_3-pollution.
- SO_4^{2-} and B isotopes indicate also contributions from sewage and mineral fertilizers.
- NO_3^- isotopes show that NO_3^- undergoes natural attenuation.
- SO_4^{2-} isotopes confirm that denitrification is not controlled by pyrite oxidation.
- The multi-isotope approach provides a unique and comprehensive approach that allows to characterise the origin of NO_3^- pollution as well as the processes involved.

Characterizing sources and natural attenuation of nitrate contamination in the Baix Ter aquifer system (NE Spain) using a multi-isotope approach

Roger Puig[a], Albert Soler[a], David Widory[b], Josep Mas-Pla[c, d], ~~Neus Otero[a] and~~ Cristina Domènech[a] and Neus Otero[a]

[a]Grup de Mineralogia Aplicada i Geoquímica de Fluids, Dept. de Mineralogia, Petrologia i Geologia Aplicada, Facultat de ~~Geologia~~Ciències de la Terra, Universitat de Barcelona (UB), c/ Martí i Franquès s/n, 08028 Barcelona, Spain.

[b]Département des Sciences de la Terre et de l'Atmosphère, Geotop/UQAM, Montréal, Canada.

[c]Grup de Geologia Aplicada i Ambiental, Centre de Geologia i Cartografia Ambiental, Dept. de Ciències Ambientals, Universitat de Girona, 17003 Girona, Spain.

[d]Catalan Institute for Water Research, c/ Emili Grahit 101, 17003 Girona, Spain.

Corresponfing author: Cristina Domenech (cristina.domenech@ub.edu)

Graphical abstract

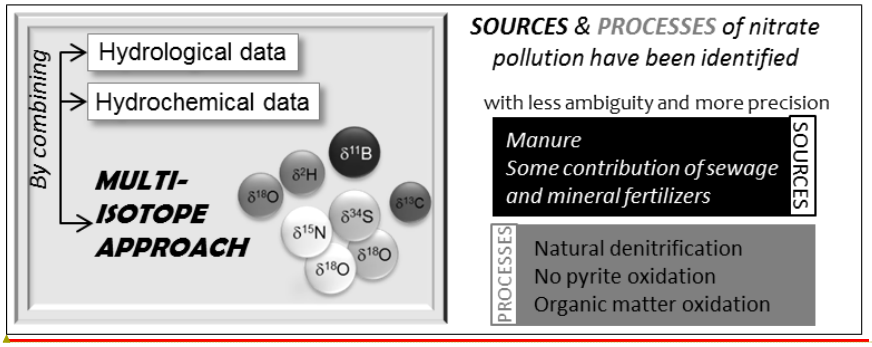

Formatted: Font: 12 pt, Bold

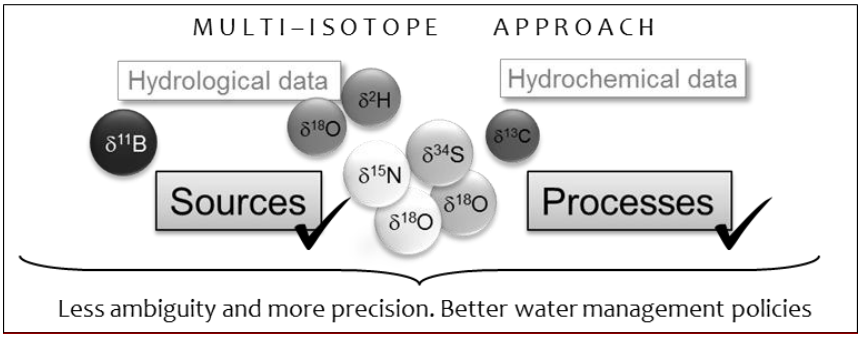

Highlights

~~We applied a multi-isotope approach to characterize nitrate contamination in a large-scale polluted aquifer system.~~

- $\delta^{15}N$, $\delta^{18}O_{NO3}$ and $\delta^{11}B$ confirm pig manure as the main vector of NO_3-pollution.
- SO_4^{2-} and B isotopes indicate also contributions from sewage and mineral fertilizers.
- NO_3^- isotopes show that NO_3^- undergoes natural attenuation.
- SO_4^{2-} isotopes ~~reveal that~~confirm that denitrification is not controlled by pyrite oxidation.
- The multi-isotope approach provides a unique and comprehensive approach that allows to characterise the origin of NO_3^- pollution as well as the processes involved.

Abstract

Nitrate pollution is a widespread issue affecting global water resources with significant economic and health effects. Knowledge of both the corresponding pollution sources and of processes naturally attenuating them is thus of crucial importance in assessing water management policies and the impact of anthropogenic activities. In this study, an approach combining hydrodynamic, hydrochemical and multi-isotope systematics (8 isotopes) is used to characterise the sources of nitrate pollution and potential natural attenuation processes in a polluted basin of NE Spain. δ^2H and $\delta^{18}O$

isotopes were used to further characterize the sources of recharge of the aquifers. Results show that NO_3^- is not homogeneously distributed and presents a large range of concentrations, from no NO_3^- to up to 480 mg L^{-1}. $\delta^{15}N$ and $\delta^{18}O$ of dissolved NO_3^- identified manure as the main source of nitrate, although sewage and mineral fertilizers can also be isotopically detected using boron isotopes ($\delta^{11}B$) and $\delta^{34}S$ and $\delta^{18}O$ of dissolved sulphate, respectively. The multi-isotope approach proved that natural denitrification is occurring, especially in near-river environments or in areas hydrologically related to fault zones. $\delta^{34}S$ and $\delta^{18}O$ indicated that denitrification is not driven by pyrite oxidation but rather by the oxidation of organic matter. This could not be confirmed by the study of $\delta^{13}C_{HCO3}$ that was buffered by the entanglement of other processes and sources.

Keywords

Stable isotopes, nitrate contamination, boron, denitrification, groundwater, manure

1. Introduction

Nitrate (NO_3^-) contamination of groundwater is a problem affecting groundwater quality worldwide (Xu et al., 2016 and references therein) that has proved to affect human health (Bryan et al., 2012; Ward et al., 2005). Because of this, considerable efforts have been made by the European authorities to promote both the reduction of NO_3^- inputs and the enhancement of attenuation processes in groundwater.

However, no decreasing trends in average European nitrate concentration in groundwater have been observed during the last 15 years (EEA, 2015). Thus, ~~Groundwater contamination arising from long-standing agricultural practices is a global water resources problem with adverse economic and health effects. More precisely, nitrate (NO_3^-) contamination of groundwater is a widespread problem given that its~~

~~connitrate~~NO_3 concentrations in groundwater ~~easily~~ often exceed~~s~~ the 50 mg L^{-1} legal ~~threshold~~ guideline ~~value~~ set for drinking water (EC, 1998). NO_3 is currently one of the ~~According to the European Environmental Agency (EEA, 2015), the European average concentration of nitrate in groundwater in 2012 was 19.1 mg L^{-1}, equivalent to the previous average of 2000. In Spain, corresponding mean values are significantly higher: 32.3 mg L^{-1} in 2000 and 34.5 mg L^{-1} in 2012. NO_3^- is thus, one of the~~ main contaminants that may hinder ~~the~~ achiev~~ement~~ing ~~of~~ the goals of the Water Framework (EC, 2000) and of the European Groundwater (EC, 2006) directives. This arises the need for a better knowledge on the overall nitrogen, including nitrate species cycle in surface water and groundwater.

~~Because of this, significant efforts are done to minimise nitrate concentration in groundwater either by reducing its incorporation and/or by enhancing its attenuation (Archna et al. 2012).~~

N~~itrate contamination mainly arises from the biological transformation of the nitrogen~~ incorporated into the soil as a nutrient through mineral fertilizers or manure, each of these sources accounting for ~~. Each of these two sources accounts from~~ nearly 50% of ~~all~~ the N input into the European agricultural soils (EEA, 2012). However, other minor N sources ~~have been reported~~ such as the leakage of sewage from sewer networks in urban environments (~~Barroso et al. 2015;~~ Aravena and Mayer, 2010; Barroso et al., 2015; Sacchi et al., 2013; Vane et al., 2010) have been reported for groundwater.

Once in the soil, nitrogen is transformed ~~Nitrogen transformation~~ through ~~may occur through different~~ microbially mediated redox reactions (nitrogen fixation, nitrification, denitrification, dissimilatory NO_3^- reduction to ammonium, anammox; Borch et al., 2010). Nitrification~~,~~ represents the oxidation of nitrogen (~~as~~ under the form

of ammonia) into nitrate. It, frequently occurs in the unsaturated zone given the availability ofwhere oxygen is available, and explains why most of the nitrogen that reaches groundwater appears as NO_3^-. Denitrification is Tthe transformation of nitrate into $N_2(g)$ and it. It is called denitrification and is considered the main natural process attenuating nitrate concentration in groundwater. This requires The required conditions for natural denitrification include 1) the presence of denitrifying bacteria and electron donors (organic carbon, reduced sulphur and/or reduced iron), 2) abundant presence of NO_3^- and 3) an anaerobic environment (Koba et al., 1997; dissolved oxygen concentrations below 2 mg L^{-1}; Rivett et al., 2008) or an anaerobic microsite within an otherwise oxygenated water body (Koba et al., 1997). Denitrification can be heterotrophic if linked to the oxidation of an organic compound (eq.1) or autotrophic, if linked to the oxidation of an inorganic compound, such as iron sulphide (eq.2).

$$4NO_3^- + 5CH_2O \rightarrow 2N_2 + 4HCO_3^- + CO_2 + 3H_2O \quad (1)$$

$$14NO_3^- + 5FeS_2 + 4H^+ \rightarrow 7N_2 + 10SO_4^{2-} + 5Fe^{2+} + 2H_2O \quad (2)$$

Dilution and dispersion are other processes that can Similar to natural attenuation, the processes of dilution and dispersion can also result in a decrease of groundwater nitrate concentration, but contrarily to . However, only natural attenuation, they do not lead to leads to the mass-reduction of the contaminant within the aquifer making it the most interesting process to achieve water quality management goals.

Knowledge of both the sources of nitrogen contamination and the processes affecting nitrogen once in the aquifer is thus of the utmost importance to better design strategies to ultimately decrease nitrate pollution. The study of the isotope composition of nitrogen compounds has proved to be a viable tool to tackle both issues (e.g. Amiri et al. 2016; Vitòria et al. 2008). Denitrification reactions . This reduction of the nitrate mass according to (eq.1 and/or eq.and 2) also affects the isotopeic composition of the

residual nitrate leading to an ~~causing an~~ enrichment in its heavy isotopes ^{15}N and ^{18}O (Aravena and Robertson, 1998; Fukada et al., 2003; Kendall et al., 2007; Mariotti et al., 1988). The study of the $\delta^{15}N$ and $\delta^{18}O$ isotope compositions and nitrate concentrations (eq. 3 and 4) allow to determine the corresponding ~~. Residual $\delta^{15}N$ and $\delta^{18}O$ are related to the sources initial isotope compositions and to the nitrate concentration according to equations 3 and 4, respectively (Böttcher et al., 1990; Fukada et al., 2003; Mariotti et al., 1981), where ε is the~~ isotopic enrichment factor (ε), used to characterise the extension of the attenuation processes ~~depending on the aquifer characteristics~~ (Böttcher et al., 1990; Fukada et al., 2003; Mariotti et al., 1981). Also, as the initial NO_3^- isotope compositions differ between the different nitrate sources (inorganic fertilizers, manure, soil, …), the $\delta^{15}N$ and $\delta^{18}O$ compositions of nitrate have been used to identify its origin in groundwater (Aravena et al., 1993; Aravena and Mayer, 2010; Clark and Fritz, 1997; Kendall et al., 2007; Panno et al., 2001).

$$\delta^{15}N_{residual} = \delta^{15}N_{initial} + \varepsilon_N \ln([NO_3^-]_{residual}/[NO_3^-]_{initial}) \quad (3)$$

$$\delta^{18}O_{residual} = \delta^{18}O_{initial} + \varepsilon_O \ln([NO_3^-]_{residual}/[NO_3^-]_{initial}) \quad (4)$$

~~Moreover, as the initial $\delta^{15}N$ and $\delta^{18}O$ composition differs within the different nitrate sources (inorganic fertilizers, manure, soil organic…), the isotopic composition of nitrate has been proved to be a useful tool to distinguish between them (e.g. Curt et al., 2004; Kendall et al., 2007).~~

~~This two-fold information the isotope composition of nitrate ($\delta^{15}N$ and $\delta^{18}O$) provides, 1) the origin of nitrate and 2) the occurrence (and extension) of natural attenuation and other processes affecting nitrogen compounds, reveals the importance of using isotopic tools in assessing nitrate pollution in groundwater (Aravena et al., 1993; Aravena and Mayer, 2010; Clark and Fritz, 1997; Kendall, 1998; Kendall et al. 2007; Panno et al., 2001).~~

However, in areas characterized by ~~a~~ complex groundwater flow systems and exposed to multiple ~~potential~~ sources of nitrogen, the use of the sole $\delta^{15}N$ and $\delta^{18}O$ of NO_3^- and nitrate concentrations may result in not ~~it is usually difficult to cc~~conclusive~~ly~~ results. ~~identify the main origin and processes controlling the nitrogen budget based on the sole study of $\delta^{15}N$ and $\delta^{18}O$ of NO_3^-.~~

To overcome this difficulty, as the redox transformations affecting nitrate also affect the electron donor, some authors have coupled $\delta^{15}N$ and $\delta^{18}O$ of NO_3^- data with the isotope composition of the electron donors or with other types of hydrochemical data, such as conservative elements (Xu et al., 2016). Some authors combined chloride concentration (a conservative element) with $\delta^{15}N$ and $\delta^{18}O$ of NO_3^- to identify nitrate sources and transformation processes (Silva et al. 2002, Vitòria et al. 2008). Some others used the $\delta^{34}S$ and $\delta^{18}O$ of sulphate or $\delta^{13}C_{HCO3}$ to evaluate if sulphide or organic matter oxidation processes could be linked to denitrification processes (Aravena and Robertson, 1998; Otero et al., 2009; Rock and Mayer, 2002; Saccon et al., 2013; Vitòria et al. 2005, 2008).

~~several studies proposed a multi-isotope approach coupling hydrochemical data and $\delta^{15}N$ and $\delta^{18}O$ of NO_3^- with the isotope compositions of ions involved in the denitrification reactions (eq. 1 and 2): $\delta^{34}S$, $\delta^{18}O_{SO4}$ and $\delta^{13}C_{HCO3}$ (Aravena and Robertson, 1998; Cravotta, 1997; Otero et al., 2009; Rock and Mayer, 2002; Saccon et al., 2013; Vitòria, 2004; Vitòria et al., 2005, 2008), obtaining satisfactorily results.~~

Moreover, in the last decade, some studies have also used the isotope composition of boron ($\delta^{11}B$) in combination with the $\delta^{15}N$ and $\delta^{18}O$ of NO_3^- to trace the origin of NO_3^- in water (Delconte et al., 2014; Komor, 1997; Saccon et al., 2013; Seiler, 2005; Widory et al., 2004, 2005, ~~and~~ 2013). B is usually found in natural ground- and surface water as a minor constituent (<0.05 mg B L^{-1}) whereas contaminant sources are

enriched in B (>0.1 mg B L^{-1}; Tirez et al., 2010). Besides the fact that groundwater affected by anthropogenic activities may present elevated B contents (Vengosh et al., 1994), $\delta^{11}B$ values are significantly discriminated between manure and wastewater. As for nitrate isotopic composition, $\delta^{11}B$ of dissolved B can be modified by different processes. However, the processes that can shift B isotopic composition are aquifer matrix interaction (dissolution of B-bearing silicates) and adsorption-desorption interactions with clay minerals, iron and aluminium oxide surfaces, and/or organic matter (Yingkai and Lan, 2001). No effects on $\delta^{11}B$ composition are caused by volatilization and oxidation-reduction reactions (Bassett et al., 1995). Thus, the incorporation of $\delta^{11}B$ in the multi-isotope approach of nitrate polluted areas may be useful for a better identification of NO_3^- sources (manure or sewage), especially in semirural zones where agricultural and farming practices cohabitate with industrial and urban activities.

However, to our knowledge no study trying to combine these chemical/isotope approaches has ever been reported so far. Here, we aim at assessing the ~~added value~~ validity of a multi-~~isotope~~parameter approach in which, besides the classical $\delta^{15}N$ and $\delta^{18}O$ of NO_3^-, ~~combined with~~ hydrochemical ~~and hydrodynamic~~ data (e.g. Cl^- concentration), $\delta^{2}H$ and $\delta^{18}O$ of water, $\delta^{34}S$ and $\delta^{18}O$ of dissolved sulphate, $\delta^{13}C$ of HCO_3^- and $\delta^{11}B$ of dissolved B are used simultaneously to both identify ~~both~~ the sources ~~and the natural attenuation processes~~ of ~~nitrate pollution from samples from exploitation wells in an alluvial aquifer system~~ contamination and to characterise processes affecting the nitrate budget of a given watershed. ~~The proposed multi-isotope approach includes the simultaneous study of eight isotopes systematics: $\delta^{2}H$ and $\delta^{18}O$ of water, $\delta^{15}N$ and $\delta^{18}O$ of dissolved NO_3^-, $\delta^{34}S$ and $\delta^{18}O$ of dissolved sulphate, $\delta^{13}C$ of HCO_3^- and $\delta^{11}B$ of dissolved B.~~ This study was undertaken in the Baix Ter aquifer (NE

Spain), declared vulnerable to NO_3^- pollution in 1998 by the local government following the 91/676/EC European Nitrate Directive (EC, 1991). NO_3^- contents in groundwater exceeds the 50 mg NO_3^- L^{-1} threshold (ACA, 2007) due to the large amount of fertilizers used by local agriculture (Mas-Pla et al., 1998; Montaner et al. 2010) and pig raising practices that started in the 80's and intensified during the last decades (ACA, 2007; EEA, 1999). This aquifer is subjected to several anthropogenic pressures such as additional nitrate sources or groundwater exploitation that increases the complexity of the aquifer behaviour.

~~The assessment of the impact and occurrence of natural attenuation processes is of the utmost importance in the design of management strategies for groundwater quality policies.~~

2. Study area

The Baix Ter basin is located in the Baix Empordà tectonic basin (NE Catalonia, Spain) (Fig. 1). The study zone encompasses a 200 km^2 area characterized by the Ter River alluvial plain delimited by the Montgrí Range to the north (Mesozoic limestone formations) and by the Gavarres Range to the south (Paleozoic igneous and metamorphic rocks) that turns into a fluvio-deltaic environment in its eastern margin. The foothills of the Gavarres Range, as well as the basin basement present Paleogene sedimentary materials (sandstone and limestone formations) that are severely affected by fractures (Mas-Pla and Vilanova, 2001).

The Baix Empordà basin was formed during the distensive period of the Alpine orogenesis. Detritic, fine-grained and silty formations were sedimented during the Neogene. The Quaternary fluvio-deltaic deposits originated from the Ter River as well as from some minor tributaries from the Gavarres Range (i.e., Daró River, Fig. 1). They constitute the main aquifers of the area, and lay on the Neogene sediments in the

western area, and on the Paleogene in the eastern part of the basin. Fluvial deposits reach a maximum depth of 50-60 m in the central part of the basin and are constituted by three main distinguishable units according to the Holocene sedimentary sequence (Montaner et al. 2010): a deep level formed by alluvial coarse detritic material, gravel and sand; an intermediate level, formed by sandy lenticular bodies in a silty-sandy level; and a shallow level, mainly sandy formed by the present prograding alluvial deposits that transform into marsh and coastal deposits near the coast line.

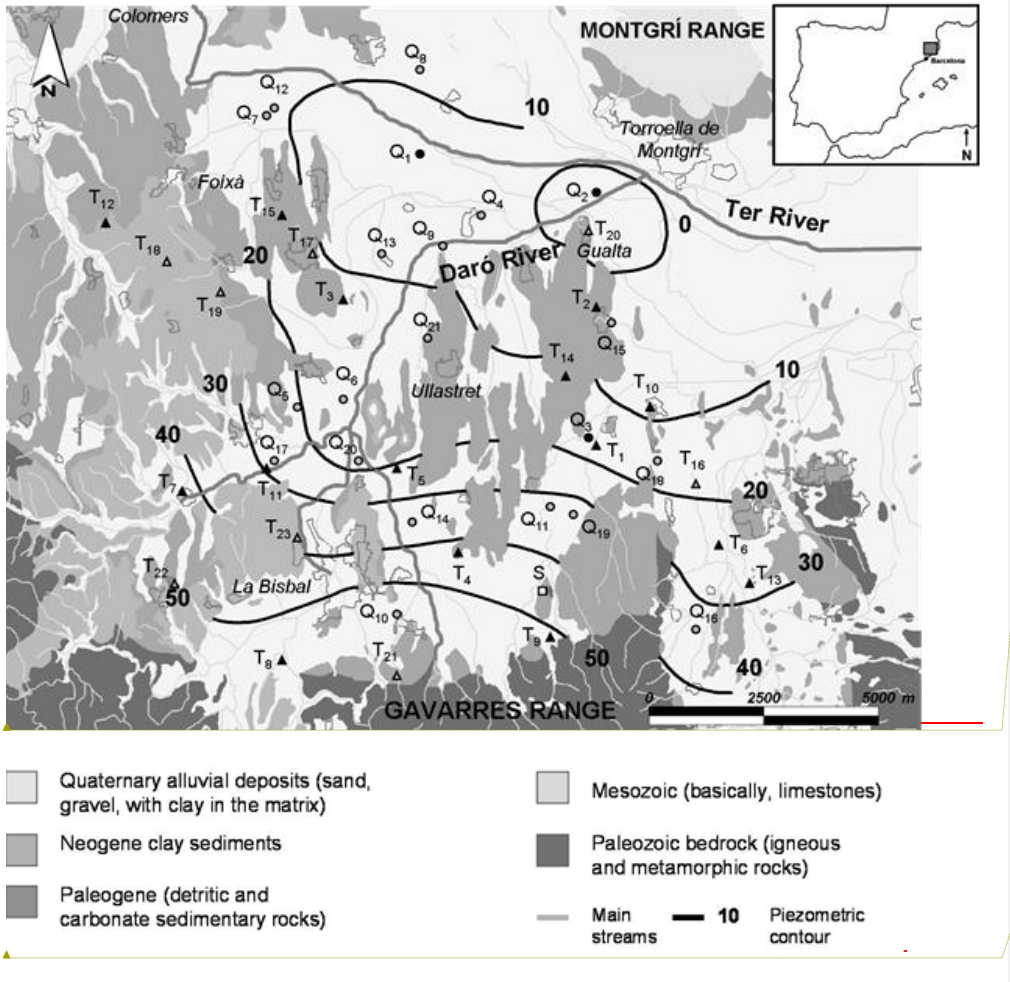

Formatted: Font: 12 pt

Formatted: Font: 12 pt

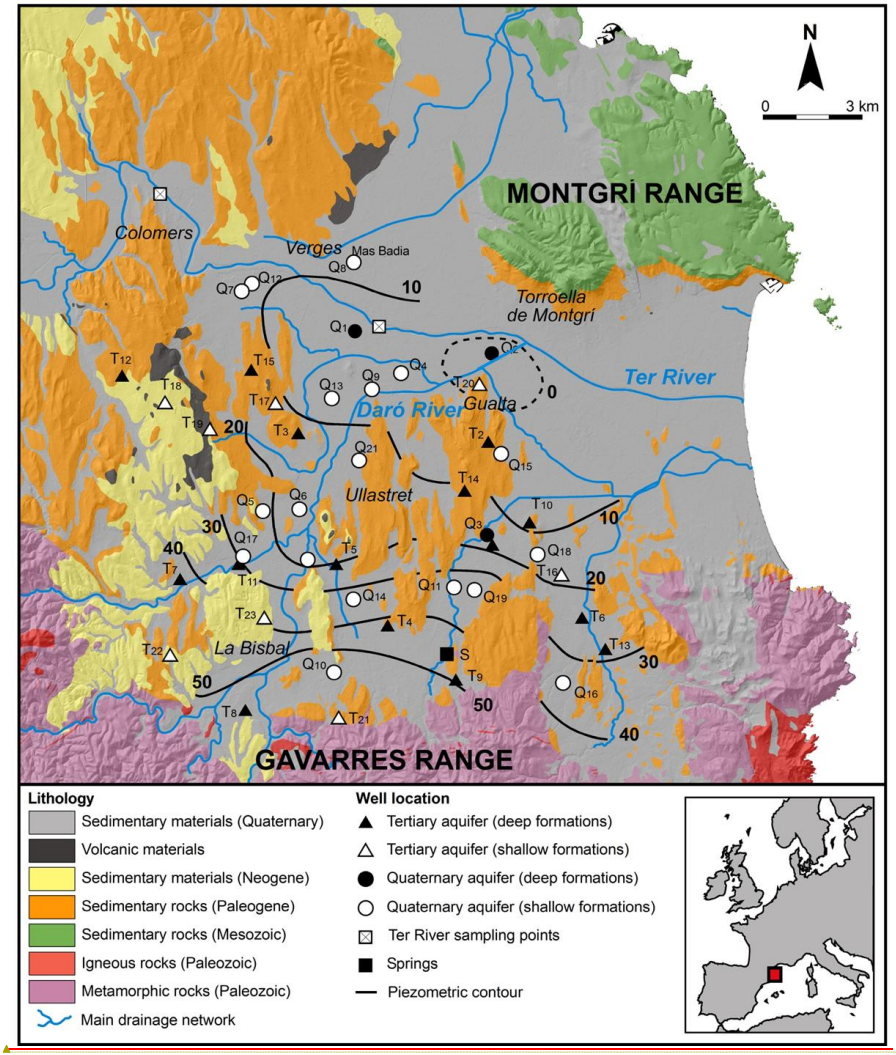

Figure 1. Geological map of the Baix Ter basin, sampling point locations labelled according to the hydrogeological formation where they are located. Potentiometric contour lines of the unconfined aquifer, mainly in the shallow Quaternary formations, correspond to the August 2004 survey. Dashed line represents the zero elevation potentiometric level in the deep quaternary formations (mainly leaky aquifers) affected by intensive withdrawal rates in the central area of the basin. Geology from ICGC (http:// www.icgc.cat).~~Figure 1. Baix Ter basin map showing the geology and sampling points, labelled according to their hydrogeological formation (round and triangle shapes~~

Formatted: Font: 12 pt

~~distinguish between Quaternary and Tertiary aquifers, respectively, and light and bold points, between shallow and deep formations, respectively; square refers to the sampled spring). Potentiometric contour lines correspond to the water table measurements of the Quaternary unit (August 2004).~~

Because of this lithological diversity, three distinct aquifer units are differentiated, from bottom to top: a leaky aquifer formed by the deeper coarse sediment layer, a leaky aquifer formed by the intermediate sandy layer, and an upper unconfined aquifer formed by the prograding deposits. All of them present significant lateral variations, especially the upper aquifer that reflects the fluvio-deltaic, marsh and coastal areas presently occurring in the plain. These aquifer units are separated by loamy layers that constitute low permeability units that act as aquitards. Nevertheless, all three aquifer layers overlap in the westernmost part of the area, between Colomers and Verges.

According to Montaner et al. (2010) these aquifers are mainly recharged by local precipitation, seasonal contribution from the Ter and Daró rivers (whether natural or induced by pumping), and by irrigation returns. Moreover, igneous and metamorphic rocks at the Gavarres Range act as regional recharge areas that discharge into the fluvio-deltaic Quaternary aquifers through the preferential upward vertical flow paths of the limestone and carbonate Paleogene aquifers and, more importantly, through the fractures that affect them ~~(Vilanova and Mas-Pla, 2004; Vilanova et al., 2008)~~. Potentiometric, hydrochemical and isotope data indicate that these different aquifers are hydraulically connected (~~Vilanova, 2004~~Vilanova et al., 2008).

Potentiometric maps reveal an influent (losing stream) behaviour of the Ter River in its western reach, between Colomers and Verges, and an effluent (gaining stream) behaviour of the Ter and Daró rivers downstream of Verges down to the coast line.

However, intense groundwater withdrawal from these aquifers started in the 60's with the agricultural and touristic development of the area that modified the natural flow field causing a noticeable depression cone in the centre of the formation, between the villages of Gualta and Torroella de Montgrí (Fig. 1). This cone creates a downward flow from the upper unconfined aquifer, also capturing the Ter River discharge, which recharges the supply wells located in the lower aquifer levels. The total groundwater abstraction is around 21 hm^3/yr, from which 62% are for domestic use (including the touristic season), 36% for agriculture activities and 2% for the industry (ACA, 2007).

The Baix Ter basin area supports rural agriculture and livestock activities, industrial activities and several small to medium-sized urban areas that drastically increase their population during summer due to their intense touristic activity. About 60% of the surface is covered by herbaceous dry-farmed and irrigated crops (mainly maize, sunflower and rice), 20% by forest and pasture and 7% by fruit growing (ACA, 2007).

The total nitrogen produced by livestock in the study zone is around 500 tons of N $year^{-1}$. 60% of this amount are from intensive pig rising (460 pigs/km^2; 50 m^3 ha^{-1} $year^{-1}$ of pig manure are applied onto maize crops; ACA, 2007). However, leakage from manure ponds or inappropriate spillages may also contribute to the increase of nitrogen, which is unassimilated by crops and incorporated into the saturated zone, ultimately raising NO_3^- concentrations in the groundwater. The "La Bisbal" water treatment plant discharges downstream of Daró River and produces mud that is eventually applied onto the fields, although some corrective measures were adopted to avoid wastewater spills.

3. Methodology

3.1. Sampling

Two sampling campaigns were conducted in the right bank alluvial plain of the Baix Ter basin in January 2004 (24 wells) and in August 2004 (40 wells) to cover both

284 the wet season with fertilization and growing of dry land cereals and the dry season with
285 cultivation of spring cereals, respectively.

286 All samples were taken from private wells supplied by the shallow Quaternary
287 hydrogeological formation and the upper unconfined aquifer (Q_S), in the deep
288 Quaternary formation and the lower unconfined aquifers (Q_D), and in the shallow (T_S)
289 and deep (T_D) Tertiary formations located in the Paleogene materials (Fig.1). Most of
290 the locations were sampled during both campaigns.

291 After measuring groundwater hydraulic head, wells were pumped until the water Eh
292 stabilized. Then, temperature, pH and electrical conductivity (EC) were measured in situ
293 and groundwater samples were collected in bottles that were previously rinsed several
294 times with groundwater. Samples were stored at 4ºC in a dark environment before
295 analysis.

296 **3.2. Analytical techniques**

297 Temperature, pH, EC and Eh were measured using a flow cell to avoid contact with
298 the atmosphere. Aqueous concentrations of chloride, nitrite, nitrate and sulphate were
299 determined by high-performance liquid chromatography (HPLC), HCO_3^- aqueous
300 concentration by volumetric titration, and total aqueous concentration of Na, K, Ca, Mg,
301 Fe, Mn and B by inductive-coupled plasma optical emission spectrometry (ICP-OES).
302 Ammonia aqueous concentration was determined by colorimetry (flow injection
303 analysis), and total organic C (TOC) concentration by the organic matter combustion
304 method. All these analyses were done at the Centres Científics i Tecnològics of the
305 Universitat de Barcelona (CCiT-UB).

306 δ^2H and $\delta^{18}O$ of water were measured using the H_2 and CO_2 equilibration
307 techniques respectively. H and O isotope compositions were measured by DI-IRMS on
308 a Delta S Finnigan Mat. $\delta^{15}N$ and $\delta^{18}O$ of dissolved NO_3^- were measured using the

309 $AgNO_3$ method (modified from Silva et al. (2000)) with an Elemental Analyser (Carlo
310 Erba 1108) coupled with an Isochrom Continuous Flow IRMS in the case of $\delta^{15}N$ and
311 with a Thermo-Chemical Elemental Analyser (TC/EA Thermo-Quest Finnigan) coupled
312 with a Delta C Finnigan Mat IRMS in the case of $\delta^{18}O$ (duplicate analyses). To measure
313 $\delta^{34}S$ and $\delta^{18}O$ of SO_4^{2-}, aqueous sulphate was precipitated as $BaSO_4$ by acidifying the
314 sample with HCl, boiling it, and adding an excess of $BaCl_2 \cdot 2H_2O$. $\delta^{34}S$ was measured
315 using an Elemental Analyser (Carlo Erba 1108) coupled with a Delta C Finnigan Mat,
316 while $\delta^{18}O$ was measured with the same methodology (TC/EA-IRMS) as $\delta^{18}O$ of
317 nitrate. In order to measure $\delta^{11}B$, sample volume was determined to ultimately yield 6 to
318 10 µg of B. Samples then underwent a two-step chemical purification using Amberlite
319 IRA-743 selective resin (method adapted from Gaillardet and Allègre (1995)). First, the
320 sample (pH~7) was loaded on a Teflon PFA® column filled with a 1 ml resin,
321 previously cleaned with ultrapure water and 2N ultrapure NaOH. After cleaning again
322 the resin with water and NaOH, the purified B was collected with 15 ml of sub-boiled
323 HCl 2N. After neutralisation of the HCl by Superpur NH_4OH (20%), the purified B was
324 loaded again on a small 100 ml resin Teflon PFA® column. B was collected with 2 ml
325 of HCl 2N. An aliquot corresponding to 2 mg of B was then evaporated below 70°C
326 with mannitol ($C_6H_8(OH)_6$) in order to avoid B loss during evaporation (Ishikawa and
327 Nakamura,1990). The dry sample was loaded onto a tantalum (Ta) single filament with
328 graphite (C), mannitol and caesium (Cs). $\delta^{11}B$ was determined on the Cs_2BO^{2+} ion
329 (Spivack and Edmond, 1986) by negative-ion Thermal-Ionization Mass Spectrometry
330 (TIMS). The analysis was run in dynamic mode by switching between masses 308 and
331 309. Each analysis corresponded to 10 blocks of 10 ratios. Samples were always run
332 twice. Total B blank was less than 10 ng corresponding to a maximum contribution of
333 0.2%, which was negligible. Seawater (IAEA-B1) was purified regularly in the same

334 way, in order to check for a possible chemical fractionation due to an uncompleted
335 recovery of B, and to evaluate the accuracy and reproducibility of the overall procedure.
336 Reproducibility was obtained by repeated measurements of the NBS951 and the
337 accuracy was controlled with the analysis of the IAEA-B1 seawater standard ($\delta^{11}B$ =
338 38.6±1.7‰). The $^{11}B/^{10}B$ ratio of replicate analyses of the NBS951 boric acid standard
339 (after oxygen correction) was 4.05045±0.00130 (2σ, n=183). The reproducibility of the
340 $\delta^{11}B$ was ±0.32‰ (2σ). The mean value obtained on $\delta^{11}B$ of seawater was
341 39.21±0.31‰ (2σ; n=20). In order to analyse the $\delta^{13}C$ of inorganic carbon, water
342 samples were acidified with ortho-phosphoric acid and shaken for at least two hours to
343 convert all bicarbonate into CO_2 and to reach equilibrium between the dissolved and
344 gaseous phases. Gas samples were then diluted with helium to facilitate the analysis.
345 $\delta^{13}C$ was measured on a Gas Chromatograph-Combustion-Isotopic Ratio Mass
346 Spectrometer (GC-C-IRMS). All isotope notations are expressed as δ per mil relative to
347 their respective international standards: Vienna Standard Mean Ocean Water (V-
348 SMOW), atmospheric N_2 (AIR), Vienna Canyon Diablo Troilite (V-CDT), NBS951 and
349 Vienna Pee Dee Belemnite (V-PDB) standards. Reproducibility is ±1.5‰ for $\delta^{2}H$,
350 ±0.2‰ for $\delta^{18}O_{H2O}$, ±0.3‰ for $\delta^{15}N$, ±0.2‰ for $\delta^{34}S$, ±0.5‰ for both $\delta^{18}O_{NO3}$ and
351 $\delta^{18}O_{SO4}$, ±0.3‰ for $\delta^{11}B$, and ±0.3‰ for $\delta^{13}C_{HCO3}$.

352 For isotope analyses, samples were prepared at the laboratory of the Mineralogia
353 Aplicada i Geoquimica de Fluids research group of the Universitat de Barcelona and the
354 analyses were performed at the Centres Científics i Tecnològics of the Universitat de
355 Barcelona (CCiT-UB), except those of $\delta^{11}B$ that were analysed at the BRGM (France)
356 and those of $\delta^{13}C$ that were analysed at the Environmental Isotope Laboratory (EIL) of
357 the University of Waterloo (Canada).

358 **4. Results and discussion**

Groundwater hydraulic head, hydrochemical and isotope data of the two campaigns are reported in Tables 1, 2 and 3.

Table 1. Hydrogeological formation, X and Y UTM coordinates, depth (m), hydraulic head (m.a.s.l.), and physico-chemical parameters measured in situ for the sampled points of each field campaign. See Fig. 1 for sampling locations in the Baix Ter basin. R_1 and R_2 Ter River samples are from the Colomers station, NW of the study zone (Fig. 1). (*n.d.*: Not determined).

Sample	Field campaign	Hydrogeological formation	X (UTM)	Y (UTM)	Depth (m)	Hydraulic head (m.a.s.l.)	T (ºC)	EC (25 ºC) (µS/cm)	pH	Eh (mV)
Q_1	1	Q_D	504970	4654520	28	13.1	14.0	787	7.9	89
Q_2	1	Q_D	508910	4653880	46	-1.4	14.4	596	8.0	46
Q_3	1	Q_D	508790	4648620	72	16.9	16.7	955	7.7	397
Q_2	2	Q_D	508910	4653880	46	-3.0	18.3	812	7.8	188
Q_3	2	Q_D	508790	4648620	72	15.6	18.2	1225	7.7	393
Q_4	1	Q_S	506280	4653300	7	10.8	15.0	1594	7.4	276
Q_5	1	Q_S	502300	4649320	10	27.4	16.0	1640	7.6	376
Q_6	1	Q_S	503340	4649390	10	22.4	14.6	899	7.6	332
Q_7	1	Q_S	501670	4655680	21	13.4	17.0	843	7.7	368
Q_8	1	Q_S	504920	4656490	20	10.9	16.9	862	7.9	366
Q_9	1	Q_S	505460	4652860	10	12.6	14.0	772	7.9	267
Q_{10}	1	Q_S	504340	4644620	8	60.3	16.3	1180	7.7	425
Q_{11}	1	Q_S	507820	4647100	6	32.0	13.3	722	8.2	361
Q_{12}	1	Q_S	501970	4655900	20	12.3	16.1	773	7.9	340
Q_{13}	1	Q_S	504290	4652570	16	13.1	14.9	836	7.8	449
Q_{14}	1	Q_S	504920	4646740	6	37.7	13.2	886	8.2	378
Q_{15}	1	Q_S	509180	4650980	6	5.2	15.3	2523	7.6	409
Q_{16}	1	Q_S	510970	4644350	6	36.4	14.7	1004	7.8	392
Q_5	2	Q_S	502300	4649320	10	24.8	16.8	2359	7.6	386
Q_6	2	Q_S	503340	4649390	10	*n.d.*	17.3	1125	7.8	318
Q_7	2	Q_S	501670	4655680	21	10.2	17.1	1164	7.5	413
Q_8	2	Q_S	504920	4656490	20	10.7	17.7	1383	7.8	332
Q_9	2	Q_S	505460	4652860	10	*n.d.*	16.2	1070	7.7	395
Q_{10}	2	Q_S	504340	4644620	8	60.4	16.2	1320	7.4	428
Q_{13}	2	Q_S	504290	4652570	16	8.7	16.2	1219	7.4	395
Q_{14}	2	Q_S	504920	4646740	12	36.1	17.6	949	7.5	365
Q_{15}	2	Q_S	509180	4650980	6	3.8	17.3	2993	8.0	388
Q_{16}	2	Q_S	510970	4644350	6	35.7	22.9	1007	7.8	443
Q_{17}	2	Q_S	501720	4647990	*n.d.*	29.5	17.6	809	7.9	386
Q_{18}	2	Q_S	510230	4648070	6	14.2	17.9	875	7.7	408
Q_{19}	2	Q_S	508410	4647030	12	32.8	16.4	999	7.6	348
Q_{20}	2	Q_S	503580	4647920	17	19.0	15.8	661	7.8	727
Q_{21}	2	Q_S	505090	4650800	17	15.0	16.2	980	7.5	445
S	1	spring	507650	4645200	0	55.0	15.0	629	7.7	319
S	2	spring	507650	4645200	0	55.0	15.4	748	7.9	334
T_1	1	T_D	508930	4648350	90	21.6	19.5	552	8.0	348
T_2	1	T_D	508830	4651340	100	7.2	14.9	908	8.0	369
T_3	1	T_D	503340	4651590	100	27.7	17.5	1176	7.8	378
T_4	1	T_D	505912	4646025	110	27.4	16.6	725	8.1	*n.d.*
T_5	1	T_D	504420	4647820	125	27.1	16.5	1325	7.8	343
T_6	1	T_D	511510	4646260	110	-4.5	18.5	736	7.8	362
T_1	2	T_D	508930	4648350	90	21.6	20.0	935	7.7	366
T_2	2	T_D	508830	4651340	100	11.4	19.8	1095	7.7	426
T_3	2	T_D	503340	4651590	100	22.1	17.2	1500	7.7	370
T_5	2	T_D	504420	4647820	125	24.4	19.1	1330	7.9	301
T_6	2	T_D	511510	4646260	110	-4.5	19.0	600	8.2	326
T_7	2	T_D	499910	4647360	70	42.0	21.2	1164	7.7	425
T_8	2	T_D	501790	4643590	156	*n.d.*	18.1	1374	8.0	357
T_9	2	T_D	507880	4644460	85	53.9	18.4	971	7.9	157
T_{10}	2	T_D	510025	4649000	125	*n.d.*	20.7	1053	7.9	183
T_{11}	2	T_D	501590	4647810	130	23.8	19.4	824	8.0	916
T_{12}	2	T_D	498230	4653260	110	*n.d.*	19.3	994	7.8	456
T_{13}	2	T_D	512180	4645340	175	*n.d.*	17.1	1137	7.6	393
T_{14}	2	T_D	508150	4649930	60	19.3	17.0	1449	7.6	159
T_{15}	2	T_D	501970	4653420	80	*n.d.*	19.1	1389	7.8	331
T_{16}	1	T_S	510930	4647500	22	-6.5	16.1	1006	7.9	363
T_{16}	2	T_S	510930	4647500	22	-5.8	16.8	1219	7.5	408
T_{17}	2	T_S	502650	4652480	40	23.7	19.2	2414	7.6	321
T_{18}	2	T_S	499460	4652480	34	126.0	18.0	837	8.0	357
T_{19}	2	T_S	500770	4651700	10	106.3	17.8	944	8.0	352
T_{20}	2	T_S	508550	4653010	9	9.0	17.7	1528	7.7	357
T_{21}	2	T_S	504505	4643350	5	102.5	22.2	649	7.7	385
T_{22}	2	T_S	499640	4645180	*n.d.*	*n.d.*	17.9	1055	7.6	327
T_{23}	2	T_S	502340	4646230	40	35.0	17.5	1438	7.5	372
R_1	-	Ter River	505699	4654685	-	-	*n.d.*	636	7.8	*n.d.*
R_2	-	Ter River	499361	4658519	-	-	*n.d.*	664	7.8	*n.d.*

Sample	Field campaign	Hydrogeological formation	Depth (m)	Hydraulic head (m.a.s.l.)	T (ºC)	EC (25 ºC) (µS/cm)	pH	Eh (mV)
Q_1	1	Q_D	28	13.1	14.0	787	7.9	89
Q_2	1	Q_D	46	-1.4	14.4	596	8.0	46
Q_3	1	Q_D	72	16.9	16.7	955	7.7	397
Q_2	2	Q_D	46	-3.0	18.3	812	7.8	188
Q_3	2	Q_D	72	15.6	18.2	1225	7.7	393
Q_4	1	Q_S	7	10.8	15.0	1594	7.4	276
Q_5	1	Q_S	10	27.4	16.0	1640	7.6	376
Q_6	1	Q_S	10	22.4	14.6	899	7.6	332
Q_7	1	Q_S	21	13.4	17.0	843	7.7	368
Q_8	1	Q_S	20	10.9	16.9	862	7.9	366
Q_9	1	Q_S	10	12.6	14.0	772	7.9	267
Q_{10}	1	Q_S	8	60.3	16.3	1180	7.7	425
Q_{11}	1	Q_S	6	32.0	13.3	722	8.2	361
Q_{12}	1	Q_S	20	12.3	16.1	773	7.9	340
Q_{13}	1	Q_S	16	13.1	14.9	836	7.8	449
Q_{14}	1	Q_S	6	37.7	13.2	886	8.2	378
Q_{15}	1	Q_S	6	5.2	15.3	2523	7.6	409
Q_{16}	1	Q_S	6	36.4	14.7	1004	7.8	392
Q_5	2	Q_S	10	24.8	16.8	2359	7.6	386
Q_6	2	Q_S	10	*n.d.*	17.3	1125	7.8	318
Q_7	2	Q_S	21	10.2	17.1	1164	7.5	413
Q_8	2	Q_S	20	10.7	17.7	1383	7.8	332
Q_9	2	Q_S	10	*n.d.*	16.2	1070	7.7	395
Q_{10}	2	Q_S	8	60.4	16.2	1320	7.4	428
Q_{13}	2	Q_S	16	8.7	16.2	1219	7.4	395
Q_{14}	2	Q_S	12	36.1	17.6	949	7.5	365
Q_{15}	2	Q_S	6	3.8	17.3	2993	8.0	388
Q_{16}	2	Q_S	6	35.7	22.9	1007	7.8	443
Q_{17}	2	Q_S	*n.d.*	29.5	17.6	809	7.9	386
Q_{18}	2	Q_S	6	14.2	17.9	875	7.7	408
Q_{19}	2	Q_S	12	32.8	16.4	999	7.6	348
Q_{20}	2	Q_S	17	19.0	15.8	661	7.8	727
Q_{21}	2	Q_S	17	15.0	16.2	980	7.5	445
S	1	spring	0	55.0	15.0	629	7.7	319
S	2	spring	0	55.0	15.4	748	7.9	334
T_1	1	T_D	90	21.6	19.5	552	8.0	348
T_2	1	T_D	100	7.2	14.9	908	8.0	369
T_3	1	T_D	100	27.7	17.5	1176	7.8	378
T_4	1	T_D	110	27.4	16.6	725	8.1	*n.d.*
T_5	1	T_D	125	27.1	16.5	1325	7.8	343
T_6	1	T_D	110	-4.5	18.5	736	7.8	362
T_1	2	T_D	90	21.6	20.0	935	7.7	366
T_2	2	T_D	100	11.4	19.8	1095	7.7	426
T_3	2	T_D	100	22.1	17.2	1500	7.7	370
T_5	2	T_D	125	24.4	19.1	1330	7.9	301
T_6	2	T_D	110	-4.5	19.0	600	8.2	326
T_7	2	T_D	70	42.0	21.2	1164	7.7	425
T_8	2	T_D	156	*n.d.*	18.1	1374	8.0	357
T_9	2	T_D	85	53.9	18.4	971	7.9	157
T_{10}	2	T_D	125	*n.d.*	20.7	1053	7.9	183
T_{11}	2	T_D	130	23.8	19.4	824	8.0	916
T_{12}	2	T_D	110	*n.d.*	19.3	994	7.8	456
T_{13}	2	T_D	175	*n.d.*	17.1	1137	7.6	393
T_{14}	2	T_D	60	19.3	17.0	1449	7.6	159
T_{15}	2	T_D	80	*n.d.*	19.1	1389	7.8	331
T_{16}	1	T_S	22	-6.5	16.1	1006	7.9	363
T_{16}	2	T_S	22	-5.8	16.8	1219	7.5	408
T_{17}	2	T_S	40	23.7	19.2	2414	7.6	321
T_{18}	2	T_S	34	126.0	18.0	837	8.0	357
T_{19}	2	T_S	10	106.3	17.8	944	8.0	352
T_{20}	2	T_S	9	9.0	17.7	1528	7.7	357
T_{21}	2	T_S	5	102.5	22.2	649	7.7	385
T_{22}	2	T_S	*n.d.*	*n.d.*	17.9	1055	7.6	327
T_{23}	2	T_S	40	35.0	17.5	1438	7.5	372
R_1	-	Ter River	-	-	*n.d.*	636	7.8	*n.d.*
R_2	-	Ter River	-	-	*n.d.*	664	7.8	*n.d.*

Table 2. Hydrochemical data for the January and August 2004 field campaigns ("*" = DOC concentrations instead of TOC concentrations). R_1 and R_2 Ter River samples are from the Colomers station, NW of the study zone (Fig. 1). (*n.d.*: Not determined; *u.d.l.*: under detection limit).

Sample	Field campaign	Hydrogeological formation	HCO_3^- (mg/L)	SO_4^{2-} (mg/L)	Cl^- (mg/L)	NO_3^- (mg/L)	Na^+ (mg/L)	K^+ (mg/L)	Ca^{2+} (mg/L)	Mg^{2+} (mg/L)	NH_4^+ (mg/L)	TOC (mg/L)	Mn (mg/L)	Fe (mg/L)	B (mg/L)
Q_1	1	Q_D	413	66	138	*u.d.l.*	43	*u.d.l.*	157	23	0.15	1.2	0.056	0.015	*u.d.l.*
Q_2	1	Q_D	349	48	51	*u.d.l.*	44	3	90	19	0.47	1.0	0.289	0.020	*u.d.l.*
Q_3	1	Q_D	361	117	79	115	37	*u.d.l.*	181	18	0.15	1.2	0.002	0.010	*u.d.l.*
Q_2	2	Q_D	341	41	61	*u.d.l.*	45	3	99	19	0.41	0.6	0.335	0.016	*u.d.l.*
Q_3	2	Q_D	335	129	79	144	36	*u.d.l.*	184	17	0.14	0.9	0.002	*u.d.l.*	*u.d.l.*
Q_4	1	Q_S	473	227	269	6	92	4	239	40	0.25	2.3	4.380	0.019	0.127
Q_5	1	Q_S	463	223	200	215	88	*u.d.l.*	291	28	0.13	2.1	0.002	0.019	*u.d.l.*
Q_6	1	Q_S	388	71	62	88	31	2	153	18	0.15	1.6	0.003	0.015	*u.d.l.*
Q_7	1	Q_S	353	111	76	48	30	*u.d.l.*	159	22	0.13	1.0	0.001	0.013	*u.d.l.*
Q_8	1	Q_S	347	136	99	13	60	3	128	25	0.12	1.4	0.783	0.016	*u.d.l.*
Q_9	1	Q_S	372	86	84	25	63	4	122	17	0.16	1.2	0.002	0.012	0.217
Q_{10}	1	Q_S	384	114	60	325	41	*u.d.l.*	245	15	0.18	1.3	0.001	0.014	0.113
Q_{11}	1	Q_S	253	60	52	31	31	3	94	13	0.17	3.3	0.003	0.018	*u.d.l.*
Q_{12}	1	Q_S	324	134	81	12	43	2	141	20	0.18	1.1	0.001	0.011	0.055
Q_{13}	1	Q_S	401	89	106	51	44	*u.d.l.*	167	20	0.15	1.9	0.001	0.017	0.089
Q_{14}	1	Q_S	210	77	52	147	29	*u.d.l.*	128	12	0.15	1.7	0.002	*u.d.l.*	*u.d.l.*
Q_{15}	1	Q_S	427	277	294	387	94	72	283	76	0.14	3.2	0.001	0.011	0.168
Q_{16}	1	Q_S	351	124	76	168	57	*u.d.l.*	183	19	0.17	1.9	0.001	*u.d.l.*	*u.d.l.*
Q_5	2	Q_S	483	321	226	328	123	*u.d.l.*	331	30	0.14	1.6	0.001	*u.d.l.*	*u.d.l.*
Q_6	2	Q_S	366	88	59	129	28	2	165	18	0.16	0.6	0.006	*u.d.l.*	*u.d.l.*
Q_7	2	Q_S	399	112	79	122	30	*u.d.l.*	201	26	0.11	0.5	0.001	0.011	*u.d.l.*
Q_8	2	Q_S	337	204	139	51	71	3	174	31	0.08	1.1	0.971	*u.d.l.*	*u.d.l.*
Q_9	2	Q_S	358	86	84	26	58	4	130	17	0.11	0.6	0.002	*u.d.l.*	0.209
Q_{10}	2	Q_S	440	76	50	241	45	*u.d.l.*	225	13	0.12	0.9	0.002	0.012	0.189
Q_{13}	2	Q_S	405	120	86	66	44	2	178	21	0.08	1.2	0.001	*u.d.l.*	0.123
Q_{14}	2	Q_S	195	66	55	201	29	*u.d.l.*	140	13	0.08	0.5	0.002	0.011	*u.d.l.*
Q_{15}	2	Q_S	413	371	362	480	111	68	345	85	0.14	3.4	0.001	*u.d.l.*	0.150
Q_{16}	2	Q_S	356	93	55	65	47	*u.d.l.*	143	14	0.14	0.6	0.001	*u.d.l.*	*u.d.l.*
Q_{17}	2	Q_S	301	29	28	60	18	*u.d.l.*	116	12	0.13	0.4	0.001	*u.d.l.*	*u.d.l.*
Q_{18}	2	Q_S	390	102	47	83	38	6	163	14	0.13	0.6	0.001	*u.d.l.*	*u.d.l.*
Q_{19}	2	Q_S	304	55	52	205	24	*u.d.l.*	166	14	0.15	0.7	0.001	0.022	*u.d.l.*
Q_{20}	2	Q_S	177	52	52	50	29	5	83	11	0.12	0.9	0.001	0.012	0.082
Q_{21}	2	Q_S	313	95	71	45	55	4	124	16	0.21	0.6	0.002	0.011	0.232
S	1	spring	298	64	47	37	29	*u.d.l.*	110	12	0.18	1.4	0.001	0.011	*u.d.l.*
S	2	spring	268	58	50	68	31	*u.d.l.*	117	13	0.15	1.0	0.001	0.013	*u.d.l.*
T_1	1	T_D	417	68	43	10	42	3	131	13	0.13	0.8	0.001	0.012	*u.d.l.*
T_2	1	T_D	470	156	87	9	51	3	129	54	0.13	1.3	0.018	0.019	*u.d.l.*
T_3	1	T_D	276	116	123	222	55	*u.d.l.*	185	22	0.15	1.9	0.001	0.014	*u.d.l.*
T_4	1	T_D	383	110	60	15	33	49	118	24	0.16	1.2	0.025	0.016	0.071
T_5	1	T_D	430	152	119	222	105	12	178	36	0.20	2.8	0.007	0.012	0.066
T_6	1	T_D	382	59	76	46	57	3	118	20	0.14	1.2	0.007	0.014	*u.d.l.*
T_1	2	T_D	402	55	41	23	35	3	136	12	0.16	0.4	0.001	*u.d.l.*	*u.d.l.*
T_2	2	T_D	435	157	74	11	44	3	127	51	0.12	0.7	0.026	*u.d.l.*	0.081
T_3	2	T_D	376	91	180	221	68	4	214	30	0.12	1.7	0.001	*u.d.l.*	0.065
T_5	2	T_D	514	118	99	61	162	11	94	23	0.18	0.6	0.010	*u.d.l.*	0.104
T_6	2	T_D	354	34	70	3	54	3	100	18	0.14	0.3	0.007	*u.d.l.*	0.051
T_7	2	T_D	368	83	66	139	32	*u.d.l.*	183	14	0.14	0.9	0.001	*u.d.l.*	*u.d.l.*
T_8	2	T_D	222	107	135	265	58	9	181	24	0.12	1.1	0.007	0.016	*u.d.l.*
T_9	2	T_D	384	31	118	*u.d.l.*	75	5	81	39	0.16	0.9	0.197	0.013	0.055
T_{10}	2	T_D	533	74	52	*u.d.l.*	63	2	168	16	0.10	0.4	0.064	0.013	0.053
T_{11}	2	T_D	323	32	46	69	41	3	106	16	0.11	0.8	0.001	0.013	*u.d.l.*
T_{12}	2	T_D	379	52	62	71	33	3	104	45	0.12	0.4	0.002	0.013	*u.d.l.*
T_{13}	2	T_D	392	86	96	46	55	2	146	28	0.12	0.7	0.001	0.010	0.051
T_{14}	2	T_D	619	87	126	*u.d.l.*	74	4	102	94	0.33	0.5	0.042	0.016	0.061
T_{15}	2	T_D	401	95	130	152	114	3	110	42	0.21	1.2	0.002	0.014	0.095
T_{16}	1	T_S	388	149	93	63	55	2	162	37	0.12	1.4	0.002	0.014	*u.d.l.*
T_{16}	2	T_S	371	146	102	71	49	*u.d.l.*	169	32	0.23	0.9	0.002	0.012	*u.d.l.*
T_{17}	2	T_S	372	245	231	419	122	59	223	70	0.11	2.6	0.003	*u.d.l.*	0.084
T_{18}	2	T_S	249	30	31	147	15	*u.d.l.*	121	19	0.14	0.6	0.001	*u.d.l.*	*u.d.l.*
T_{19}	2	T_S	348	56	39	89	33	7	137	13	0.14	1.2	0.003	*u.d.l.*	*u.d.l.*
T_{20}	2	T_S	350	210	108	212	56	6	200	38	0.17	2.2	0.001	*u.d.l.*	0.123
T_{21}	2	T_S	300	30	36	6	22	*u.d.l.*	104	9	0.14	1.0	0.002	0.012	*u.d.l.*
T_{22}	2	T_S	371	81	49	153	29	*u.d.l.*	193	8	0.16	1.1	0.002	0.012	*u.d.l.*
T_{23}	2	T_S	355	66	181	190	75	*u.d.l.*	216	24	0.26	0.7	0.004	0.010	*u.d.l.*
R_1	-	Ter River	194	73	50	7	38	5	75	11	*n.d.*	4.3*	0.029	0.010	0.075
R_2	-	Ter River	204	74	50	9	40	5	78	12	*n.d.*	4.5*	0.025	0.012	0.090

Table 3. Isotope data for the January and August 2004 field campaigns. R_1 and R_2 Ter River samples are from the Colomers station, NW of the study zone (Fig. 1). (*n.d.*: Not determined).

Sample	Field campaign	Hydrogeological formation	$\delta^{18}O\text{-}H_2O$ (‰)	$\delta^{2}H$ (‰)	$\delta^{15}N$ (‰)	$\delta^{18}O\text{-}NO_3$ (‰)	$\delta^{34}S$ (‰)	$\delta^{18}O\text{-}SO_4$ (‰)	$\delta^{13}C\text{-}DIC$ (‰)	$\delta^{11}B$ (‰)
Q_1	1	Q_D	-5.2	-35.8	*n.d.*	*n.d.*	14.7	16.1	-14.9	*n.d.*
Q_2	1	Q_D	-5.5	-37.8	*n.d.*	*n.d.*	13.9	13.6	-13.7	*n.d.*
Q_3	1	Q_D	-5.4	-35.4	11.6	8.3	0.4	5.6	-13.6	*n.d.*
Q_2	2	Q_D	-5.9	-37.6	*n.d.*	*n.d.*	10.3	12.4	-13.8	*n.d.*
Q_3	2	Q_D	-5.5	-34.9	12.3	8.4	0.9	5.5	-13.7	*n.d.*
Q_4	1	Q_S	-5.1	-33.6	32.5	18.1	8.2	13.0	-13.2	34.5
Q_5	1	Q_S	-5.3	-34.6	15.9	8.9	12.2	10.1	-12.9	*n.d.*
Q_6	1	Q_S	-5.3	-33.9	11.3	6.8	6.2	6.8	-13.2	*n.d.*
Q_7	1	Q_S	-6.0	-40.8	12.2	7.7	6.3	7.8	-11.3	*n.d.*
Q_8	1	Q_S	-6.5	-44.1	20.5	13.7	9.1	10.1	-12.7	*n.d.*
Q_9	1	Q_S	-5.4	-35.3	19.1	10.1	6.8	8.9	-14.0	23.3
Q_{10}	1	Q_S	-5.8	-39.5	10.4	4.4	5.9	4.8	-12.5	25.7
Q_{11}	1	Q_S	-6.3	-39.6	13.6	8.7	5.1	7.8	-16.0	*n.d.*
Q_{12}	1	Q_S	-6.3	-41.9	13.3	8.1	8.2	8.9	-12.4	26.0
Q_{13}	1	Q_S	-5.3	-35.9	14.7	9.2	6.3	8.2	-13.9	28.3
Q_{14}	1	Q_S	-5.6	-36.8	7.7	5.5	4.0	5.4	-11.3	*n.d.*
Q_{15}	1	Q_S	-4.8	-31.8	13.5	7.5	2.6	5.8	-14.6	30.4
Q_{16}	1	Q_S	-5.5	-36.9	8.7	4.2	5.3	5.3	-14.0	*n.d.*
Q_5	2	Q_S	-5.3	-33.5	18.9	5.3	12.7	10.2	-15.5	*n.d.*
Q_6	2	Q_S	-5.3	-33.8	12.3	7.2	6.1	7.0	-13.6	*n.d.*
Q_7	2	Q_S	-5.3	-36.3	12.3	6.5	3.0	6.0	-12.0	*n.d.*
Q_8	2	Q_S	-6.6	-43.9	16.3	9.5	8.0	7.8	-11.8	*n.d.*
Q_9	2	Q_S	-5.5	-34.8	21.6	10.6	7.7	9.9	-14.1	*n.d.*
Q_{10}	2	Q_S	-6.0	-40.6	13.4	4.6	6.4	5.1	-16.0	*n.d.*
Q_{13}	2	Q_S	-5.3	-33.8	15.7	9.1	5.9	8.5	-13.6	*n.d.*
Q_{14}	2	Q_S	-5.2	-34.8	9.9	4.4	4.6	5.0	-14.7	*n.d.*
Q_{15}	2	Q_S	-4.9	-31.8	16.2	4.6	3.3	5.3	-14.1	*n.d.*
Q_{16}	2	Q_S	-5.8	-37.3	7.2	4.3	4.7	6.1	-14.1	*n.d.*
Q_{17}	2	Q_S	-5.4	-35.6	8.4	4.8	7.2	6.6	-15.0	*n.d.*
Q_{18}	2	Q_S	-5.6	-38.0	8.2	4.5	-1.4	6.3	-12.2	*n.d.*
Q_{19}	2	Q_S	-5.5	-38.2	10.5	5.5	3.1	4.9	-13.4	*n.d.*
Q_{20}	2	Q_S	-5.6	-36.2	13.6	7.4	5.6	6.6	-14.9	9.0
Q_{21}	2	Q_S	-5.6	-36.9	16.6	9.9	5.4	7.5	-14.7	1.4
S	1	spring	-5.8	-37.4	8.6	5.0	5.3	7.3	-14.3	*n.d.*
S	2	spring	-5.9	-37.7	9.6	6.8	5.4	7.2	-13.5	*n.d.*
T_1	1	T_D	-5.6	-37.8	8.9	6.8	1.6	8.2	-10.2	*n.d.*
T_2	1	T_D	-5.2	-35.1	16.0	8.0	-13.5	3.8	-9.0	*n.d.*
T_3	1	T_D	-5.1	-33.1	7.6	4.7	4.9	6.0	-13.7	*n.d.*
T_4	1	T_D	-5.5	-36.3	14.9	10.1	4.9	10.1	-13.3	31.7
T_5	1	T_D	-5.3	-34.7	11.1	5.3	4.2	4.8	-12.5	23.9
T_6	1	T_D	-5.6	-35.7	12.8	6.9	2.3	8.0	-12.0	*n.d.*
T_1	2	T_D	-5.8	-36.4	10.8	6.8	1.5	7.6	-11.2	*n.d.*
T_2	2	T_D	-5.3	-35.3	22.6	10.9	-13.4	4.2	-9.1	*n.d.*
T_3	2	T_D	-5.2	-36.1	11.0	7.0	5.5	6.2	-13.9	*n.d.*
T_5	2	T_D	-5.9	-37.5	13.7	6.5	5.8	7.9	-8.5	*n.d.*
T_6	2	T_D	-5.9	-37.1	12.1	9.1	-2.6	11.1	-11.9	*n.d.*
T_7	2	T_D	-5.5	-36.3	10.8	5.2	5.2	6.6	-13.4	*n.d.*
T_8	2	T_D	-5.6	-35.7	13.8	6.1	5.3	4.6	-15.4	*n.d.*
T_9	2	T_D	-6.1	-39.0	*n.d.*	*n.d.*	14.2	12.0	-11.5	*n.d.*
T_{10}	2	T_D	-5.7	-37.6	*n.d.*	*n.d.*	10.0	10.6	-10.2	*n.d.*
T_{11}	2	T_D	-5.4	-39.7	11.6	6.6	6.3	6.2	-13.0	*n.d.*
T_{12}	2	T_D	-5.2	-37.5	13.8	7.1	-1.8	4.5	-12.1	*n.d.*
T_{13}	2	T_D	-5.7	-37.6	11.9	5.6	1.7	5.8	-12.5	*n.d.*
T_{14}	2	T_D	-5.4	-36.4	*n.d.*	*n.d.*	-16.0	4.9	-6.5	*n.d.*
T_{15}	2	T_D	-5.4	-36.6	12.2	5.0	6.2	5.2	-13.1	*n.d.*
T_{16}	1	T_S	-5.4	-34.8	10.7	8.5	-4.1	5.8	-11.3	*n.d.*
T_{16}	2	T_S	-5.0	-35.1	13.3	9.4	-1.7	5.5	-11.9	*n.d.*
T_{17}	2	T_S	-5.1	-34.3	16.1	1.8	5.9	6.3	-14.5	29.5
T_{18}	2	T_S	-5.0	-33.9	6.3	3.5	4.1	5.0	-13.5	*n.d.*
T_{19}	2	T_S	-5.9	-38.1	9.3	6.2	7.3	9.2	-16.2	*n.d.*
T_{20}	2	T_S	-5.4	-36.0	12.2	5.1	3.3	5.6	-13.2	25.5
T_{21}	2	T_S	-6.2	-36.8	5.0	6.3	6.9	5.1	-14.9	*n.d.*
T_{22}	2	T_S	-5.7	-36.2	11.5	6.2	6.6	4.9	-15.6	*n.d.*
T_{23}	2	T_S	-5.6	-38.2	16.1	6.1	9.4	4.3	-14.8	*n.d.*
R_1	-	Ter River	*n.d.*	*n.d.*	13.2	4.2	11.3	9.5	*n.d.*	*n.d.*
R_2	-	Ter River	*n.d.*	*n.d.*	*n.d.*	*n.d.*	*n.d.*	*n.d.*	*n.d.*	*n.d.*

382
383

384 4.1. Hydrodynamic data and potentiometric map

385 Hydraulic head measurements in the Quaternary aquifer conducted during the August
386 campaign were used to draw the potentiometric contour lines shown in Fig.1, as this

represents the largest pressure in the groundwater system resources. The generated potentiometric map shows that groundwater flow lines were mainly oriented along a south to north trend (from the Gavarres massif to the Ter River) (Fig. 1) although close to the Ter River, groundwater flow changed to a west-to-east direction towards the sea. ~~This is in agreement with the conceptual flow model described in previous studies (e.g., Vilanova and Mas-Pla, 2004).~~ The potentiometric map also reflects the depression cone of the Gualta village resulting from the intense groundwater withdrawal activity of its supply wells. However, it was not possible to draw a consistent potentiometric plot of the Tertiary aquifer ~~that was~~ able to corroborate the upward vertical flow line connecting the underlying confined fractured Tertiary unit to the shallow Quaternary aquifer that was suggested by Vilanova ~~and Mas-Pla (2004~~et al. (2008). Potentiometric levels in the Tertiary aquifer may vary seasonally due to groundwater pumping, controlling the recharge relation with the Ter River alluvial aquifer.

4.2. $\delta^{2}H$ and $\delta^{18}O$ data. Sources of recharge

Fig. 2 shows th~~at~~ $\delta^{2}H$ and $\delta^{18}O$ of groundwater samples from both campaigns mostly plot~~ted~~ under ~~against the~~ the annual ~~local~~ Local M~~m~~eteoric W~~w~~ater L~~l~~ine (~~(~~LMWL~~,~~ (Vilanova~~,~~ et al., 2008~~4~~). ~~Samples mostly plot under the LMWL.~~

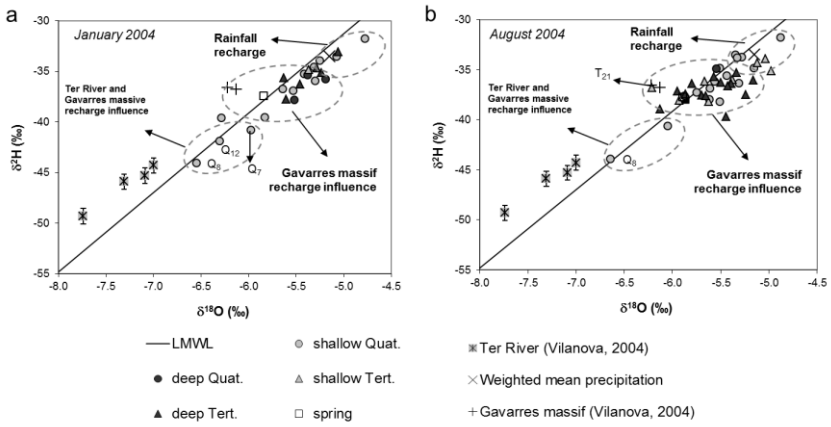

404

405 Figure 2. $\delta^{18}O_{H2O}$ and $\delta^{2}H$ of the Baix Ter groundwater samples collected in January
406 2004 (a) and August 2004 (b). The annual -Local Meteoric Water Line (LMWL)
407 follows the equation $\delta^{2}H = 7.98(\pm2.71)\ \delta^{18}O + 7.85(\pm0.47)$ (r^2=0.924, n=23) (Vilanova
408 et al., 2008~~4~~), whose slope is equal to that of the neighbouring areas ($\delta^{2}H = 7.9\ \delta^{18}O +$
409 9.8; Neal et al., 1992).

410 However, the wide range of $\delta^{2}H$ and $\delta^{18}O$ values from the Quaternary aquifer
411 indicates the implication of several recharge flow systems affecting the aquifer~~, with~~
412 ~~distinct hydrogeological characteristics, affecting the aquifer.~~. Some of the samples fall
413 very close to the weighted mean precipitation ($\delta^{2}H$ = -33.5‰, $\delta^{18}O$ = -5.2‰) calculated
414 from the Mas Badia station data (located in the Baix Ter basin; Fig. 2) showing the
415 influence of the infiltration of rainfall into the basin.

416 ~~Three~~ S~~s~~amples located at the NW of the shallow Quaternary aquifer (Q_7, Q_8 and
417 Q_{12}) yielded lighter isotope compositions with values similar to those of the Ter River
418 reported by Vilanova (2004; $\delta^{2}H$ from -50 to -45‰, $\delta^{18}O$ from -8 to -7‰), indicating a
419 contribution from the Ter River to the alluvial aquifer groundwater.~~. These $\delta^{2}H$ and~~
420 ~~$\delta^{18}O$ from the Ter River waters are the lightest observed in the area, explained by the~~
421 ~~fact that the Ter River discharge originates at a higher recharge altitude in the Pyrenees~~

~~Mountains. Thus, the isotope compositions of the water molecule identify a contribution from the Ter River to the alluvial aquifer groundwater in the NW part of the study zone.~~

Finally, ~~some~~ other samples from the Quaternary aquifer present δ^2H and $\delta^{18}O$ compositions intermediate between those influenced by the rainfall and those influenced by the Ter river water (Fig. 2) but also close to ~~. H and O Isotope compositions of these samples, however, are very close to~~ those of sample T_{21}, located in the Gavarres massif foothill (south of the study area, Fig. 1). Thus, ~~T~~these samples can be geochemically and isotopically considered as representative of the recharge from the Gavarres massif, given its very low mineralization and its isotope composition (Fig.2). As irrigation demand is fully covered by groundwater in the sampled area, the potential effects of irrigation returns on groundwater isotopic composition would not in any case modify the recharge model herein proposed.~~that is very similar to the groundwater from the Paleozoic materials in the Gavarres massif (Vilanova, 2004; Fig. 2).~~

In Tertiary aquifers, ~~M~~most of the groundwater samples ~~from the Tertiary aquifers~~ fell between the weighted mean precipitation signature and the isotope composition of groundwater from the Gavarres massif (Fig. 2). They present a narrower range of δ^2H and $\delta^{18}O$ compositions, although they overlap with the intermediate isotopic composition of the Quaternary aquifer groundwater samples (Fig. 2). This overlap suggests that both aquifers share a common source of recharge or are somehow connected. This is consistent with the conceptual model described by Vilanova ~~and Mas-Pla~~et al. (200~~8~~4) in which an upward groundwater flow was proposed connecting the Tertiary aquifer to the deep Quaternary aquifer in the northern part of the area. Therefore, the contribution from the Tertiary units towards the Quaternary aquifer cannot be discarded despite the fact that this could not be supported by the potentiometric map.

4.3. Hydrochemical data

Chemical data for groundwater samples collected in the Baix Ter basin (Tables 1 and 2) showed a HCO_3^--Ca^{2+}-Mg^{2+} facies, in accordance with the hydrochemistry being controlled by carbonate dissolution reactions that occur throughout the Tertiary materials and alluvial formations. The rapid kinetic of carbonate dissolution hides the hydrochemical characteristics acquired from the igneous and metamorphic rocks of the Gavarres massif (Vilanova et al., 2008). Groundwater pH values were all above 7.4, HCO_3^- concentrations were between 177 and 619 mg L^{-1} and EC varied from 552 µS cm^{-1} to 2993 µS cm^{-1}.

In all the studied area, NO_3^- concentrations presented a wide range of values ~~in both the Quaternary and Tertiary aquifers,~~ from ~~samples with NO_3^-~~ below the detection limit (0.1 mg L^{-1}) to concentrations up to 480 mg L^{-1}. 60% of the studied samples had NO_3^- levels above the legal threshold of 50 mg L^{-1} for drinking water (EC, 1998). No NO_2^- was detected. Ammonium concentration ranged between 0.08 mg L^{-1} and 0.47 mg L^{-1}. It can be observed that ~~The~~ NO_3^- concentrations of the river samples presented values of 9 and 7 mg L^{-1}, consistent with surface water nitrate values and lower than the monthly NO_3^- average for the Ter River (15 mg L^{-1}; σ = 5.1, n = 37) between 2003 and 2006 (ACA, 2015). However, nitrate concentration in aquifers showed a diffuse spatial distribution.

~~Nitrate spatial distribution shows a diffuse regional pattern: i~~In shallow aquifers (Q_S and T_S), nitrate concentrations ranged from 6 to 480 mg L^{-1}, while in deeper aquifers they went from values below detection limit up to 265 mg L^{-1}. This distribution does not seem to be linked to any specific groundwater flow direction nor limit of the aquifer units. It can be explained by the highly complex hydrogeology of the study zone and its distinct recharge areas, and by the mixing of waters from distinct origins and qualities

within the well borehole. Several factors such as the intended exploitation of different levels to increase the well efficiency, the possible lack of well casing derived from an incomplete borehole construction, and/or the presence of preferential flow paths through fractures or fault zones that connect local and regional flow systems, i.e. Quaternary and Tertiary aquifers could account for the mixing of waters. Moreover, the intensive pumping during irrigation and low rainfall periods can also enhance re-circulation between aquifer levels, mainly from the shallow to deeper ones, resulting in a decrease of the quality of the water resources stored in the deeper aquifer layers. ~~It should then be noticed that nitrate concentrations are more representative of the unknown well characteristics than of the hydrogeological layer where the borehole is drilled.~~

The lowest NO_3^- contents in the Quaternary aquifer were observed near the Ter River suggesting some influence from induced stream recharge; and in the SE area, near the Gavarres Range, in the Tertiary aquifer.

During the first sampling campaign, two samples from the shallow Quaternary aquifer (Q_4 and Q_8, Table 2) presented NO_3^- concentrations of 6 mg L^{-1} and 13 mg L^{-1}, respectively, coupled with high levels of Mn (4.4 and 0.8 mg Mn L^{-1}) and around 2 mg L^{-1} of total organic carbon. Two samples in the Q_D (Q_1 and Q_2) and three samples in T_D aquifers (T_9, T_{10} and T_{14}) had NO_3^- below detection limit, an Eh value below 200 mV and showed the highest ammonium and manganese concentrations (Tables 1 and 2, Fig.3). Moreover, NO_3^- in Q_2 has been monitored through time and has always been below detection limit. ~~In our study, the ammonium content in Q_2 displayed the highest value (0.47 mg L^{-1}).~~ These characteristics are typical of groundwater under reducing conditions, and would suggest that they are undergoing denitrification processes. However, measured TOC concentrations for Q_1, Q_2, T_9, T_{10} and T_{14} (between 0.4 and 1.2 mg L^{-1}) are not high enough to stoichiometrically allow the reduction of NO_3^- by

oxidation of organic matter in anaerobic conditions (Rivett et al., 2008), but they may indicate the presence of organic matter that could represent a residual content after previous consumption by heterotrophic denitrifying bacteria.

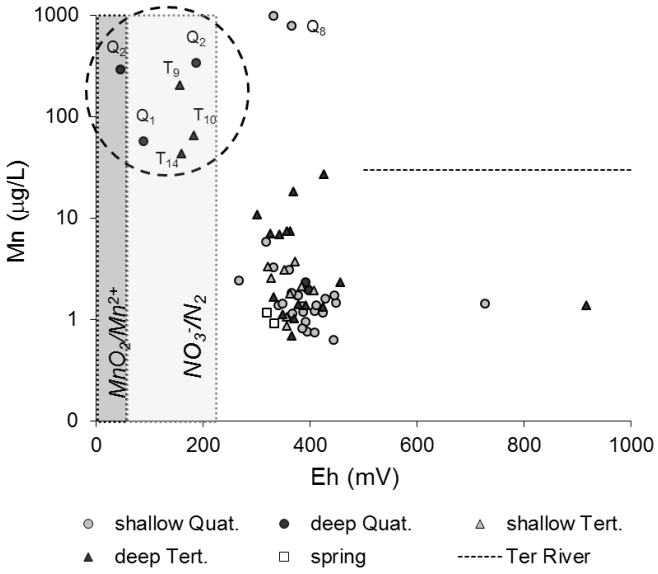

Figure 3. Mn concentrations plotted against the Eh values of the groundwater samples. Eh ranges of MnO_2/Mn^{2+} and $NO_3^-/N_{2(g)}$ redox pairs are taken from Rivett et al. (2008).

Some ~~of the~~ samples with high NO_3^- concentration (Q_5, Q_{10}, Q_{15} and Q_{16} from Q_S, T_{17} and T_{20} from T_S, and T_3, T_5 and T_8 from T_D) also presented high sulphate and chloride concentrations (up to 371 and 362 mg L^{-1}, respectively) (Fig. 4a, b). Considering that Cl^- is a conservative element largely unaffected by physical, chemical and microbiological processes occurring in the groundwater (Altman and Parizek, 1995), the $[NO_3^-]/[Cl^-]$ ratio can be used to eliminate the potential effect of dilution. In Fig. 4c, sulphate concentration is plotted against the $[NO_3^-]/[Cl^-]$ ratio. Groundwater SO_4^{2-} varied between 29 and 371 mg L^{-1}, with an average value of 108 mg L^{-1} (n = 64). But a set of samples, with $1<[NO_3^-]/[Cl^-]<2$, present moderate SO_4^{2-} concentrations but

514 also high NO_3^- and consequently high Cl^- concentrations. Samples with $[NO_3^-]/[Cl^-]>2$

515 had high NO_3^- but lower SO_4^{2-} concentrations (Fig. 4c).

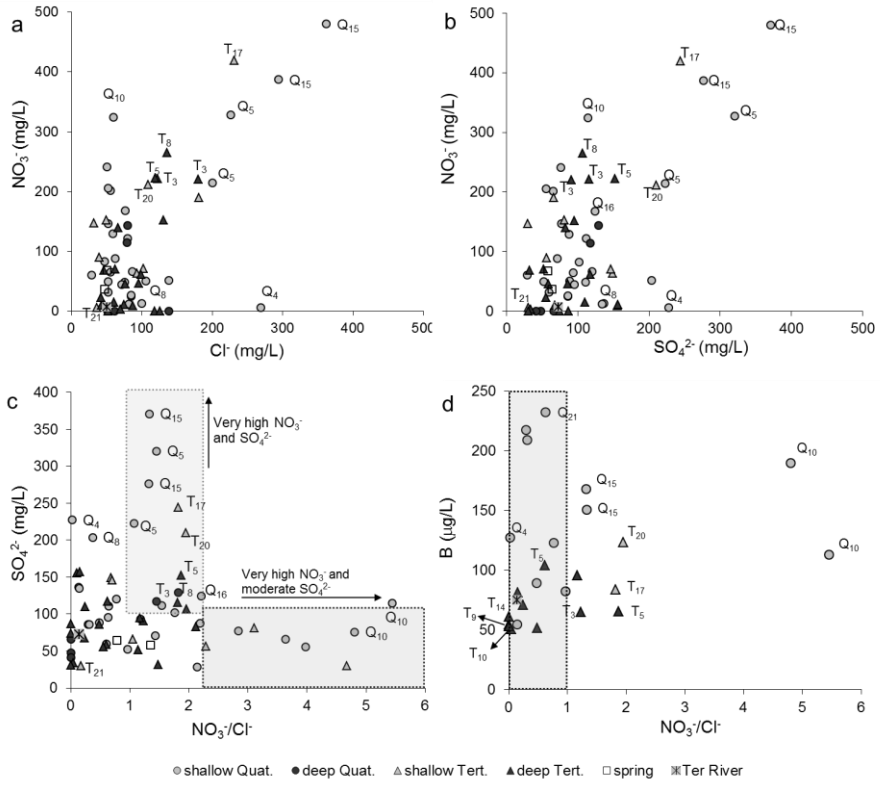

516

517 Figure 4. a) NO_3^- concentration versus Cl^- concentration, b) NO_3^- concentration versus

518 SO_4^{2-} concentration, c) SO_4^{2-} concentration versus (NO_3^-/Cl^-) ratio, and d) B

519 concentration versus (NO_3^-/Cl^-) ratio.

520

521 Since no evaporitic or gypsum outcrops nor disseminated pyrite exist in the study

522 area, these SO_4^{2-} concentrations must originate from anthropogenic sources such as

523 manure, synthetic fertilizers or sewage. High Cl^- concentrations can be caused by the

524 input of organic fertilizers since they generally show elevated chloride concentrations

525 (Karr et al., 2001; Menció et al. 2016). All these observations suggest that both the

526 mineral and the organic fertilizers are the major vectors of contamination.

In most of samples, B concentration was below the detection limit. However, B concentrations around 0.1-0.2 mg L^{-1} have been measured in samples with high nitrate, sulphate and chloride concentrations (e.g. Q10 and Q15, Fig. 4d) suggesting sewage and manure as other potential contamination sources. However, as seen in Fig. 4d, samples with the highest B concentration (up to 232 μg/L) presented intermediate nitrate concentrations (25-45 mg NO_3^- L^{-1}), showing that the presence of B in groundwater is not necessarily linked to high NO_3^- concentrations.

Thus, our results show that groundwater is probably affected by more than one source of contamination and that natural denitrification may be acting in some areas. However, ~~, but an~~ the unambiguous identification of these sources and processes based on the sole hydrochemical data is somewhat difficult as the signal may be hindered by the mixing of groundwaters from different layers and recharge flow systems.

4.4. Isotope data. Pollution sources and attenuation processes

4.4.1. $\delta^{15}N$ and $\delta^{18}O$ of NO_3^-

NO_3^- isotope composition in groundwater ranged between +5.0 and +32.5‰ for $\delta^{15}N$, with an average value of +13.0‰ (n = 58), and between +1.8 and +18.1‰ for $\delta^{18}O$, with an average value of +7.1‰ (n = 58) (Table 3).

As seen in Fig. 5a, five groundwater samples (Q_{14} and Q_{16} from Q_S, T_3 from T_D, and T_{18} and T_{21} from T_S) presented $\delta^{15}N$ values compatible with ~~comparable to those of~~ soil organic nitrogen (from +3 to +8‰~~, Table 4~~), fertilizers (-4 to +8‰) and sewage (+5 to +20‰)~~.~~ (Table 4). Within these samples, only sample T_{21} presented low nitrate, sulphate and chloride concentration (6 mg L^{-1} NO_3^-, 36 mg L^{-1} Cl^- and 30 mg L^{-1} SO_4^{2-}). The low $\delta^{15}N$ (+5.0‰) measured in sample T_{21}, coupled with its δ^2H and $\delta^{18}O$, that are similar to those of the Gavarres massif (Fig. 2), indicate that the NO_3^- for ~~this~~ these samples is consistent with a natural soil origin. T_{21} represents thus the local NO_3^-

background. However, as ~~in~~for samples Q_{14}, Q_{16}, T_3, and T_{18}~~-~~, nitrate contents range from 65 to 222 mg L^{-1}. ~~-T~~the origin of ~~the~~ NO_3^- for these samples cannot be solely attributed to the mineralization of soil nitrogen (as in T_{21}) ~~as~~which ~~it~~ cannot explain such high concentrations.

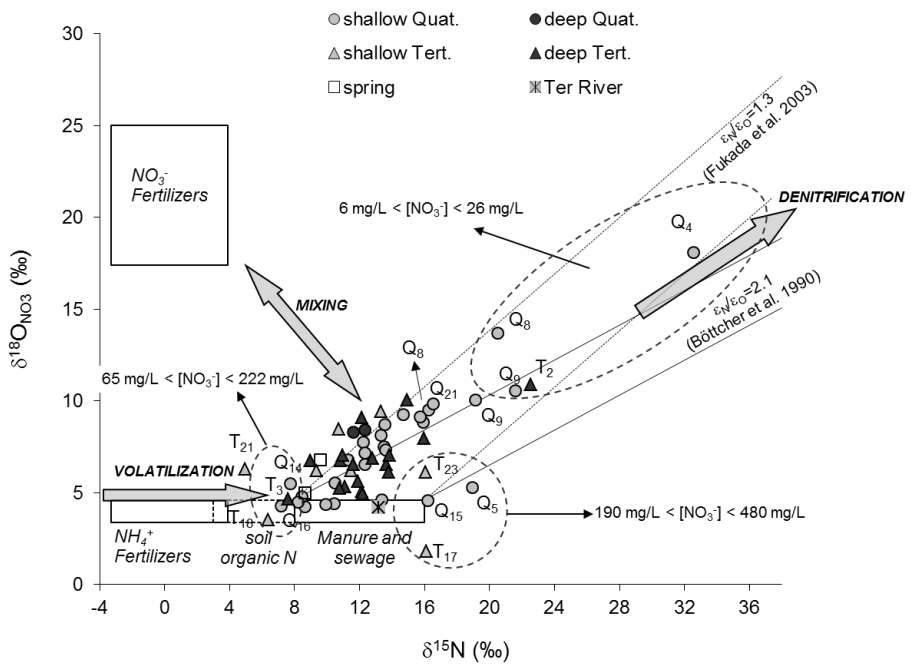

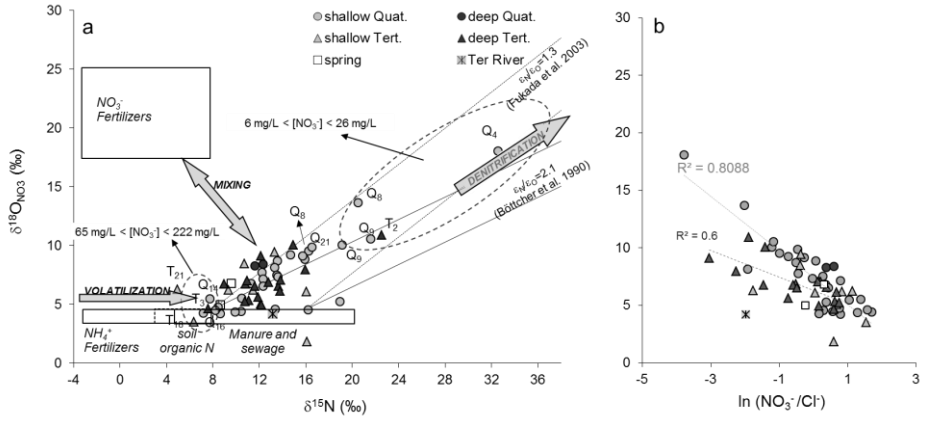

Formatted: Font: 12 pt

Figure 5. a) Variations of the $\delta^{15}N$ and $\delta^{18}O$ of dissolved NO_3^- in groundwater according to their hydrogeological unit. Isotope ranges of the main NO_3^- sources listed in Table 4 are also represented. The extreme isotopic fractionation ratios from the literature are $\varepsilon_N/\varepsilon_O = 2.1$ (Böttcher et al., 1990) and $\varepsilon_N/\varepsilon_O = 1.3$ (Fukada et al., 2003). b) $\delta^{18}O_{NO3}$ values plotted against $\ln(NO_3^-/Cl^-)$ according to their hydrogeological unit. R^2 values corresponding to the linear regressions for shallow Quat. and deep Tert. Units are also reported.

~~However, as in samples Q_{14}, Q_{16}, T_3, and T_{18} nitrate contents range from 65 to 222 mg L^{-1} the origin of the NO_3^- for these samples cannot be solely attributed to the mineralization of soil nitrogen (as in T_{21}) as it cannot explain such high concentrations.~~

~~Thus, other sources of NO_3^- must be considered though a small contribution of soil organic nitrogen is possible (Wassenaar, 1995). Nitrate derived from ammonium fertilizers present $\delta^{15}N$ values between -4 and +4‰ (Table 4). This value can be enriched in ^{15}N by volatilization processes leading to values in the range of soil nitrogen, as it was observed by Vitòria (2004) in the Maresme region (Catalonia, NE Spain), where mineral fertilizers were shown to be the only source of NO_3^-.~~

~~$\delta^{15}N$ value of NO_3^- produced after nitrification would be similar to that of the former ammonium affected by volatilization because of the large isotopic fractionation occurring when nitrification is stimulated by e.g. large amounts of available NH_4^+ (Kendall 2007 and references therein). This would explain the lack of nitrite in the area. Therefore, synthetic ammonium fertilizers could be the source of NO_3^- for Q_{14}, Q_{16}, T_3 and T_{18} samples. Nevertheless, as seen in Fig. 5, nitrate in these samples could also result from a mixing between NO_3^- derived from synthetic fertilizers and NO_3^- derived from manure or sewage (+8 to + 20‰, Table 4).~~ Therefore, although a small

contribution of soil organic nitrogen is possible (Wassenaar, 1995), measured isotope values may originate from synthetic fertilizers or sewage/manure sources or from a mixing of both (Fig. 5a).

~~However, the main group of samples presented $\delta^{15}N$ ranging between +8 and +16‰, indicating that NO_3^- may originate from ^{15}N-enriched anthropogenic organic matter (manure or sewage) (Fig. 5).~~

Table 4. Ranges of nitrate, sulphate, boron and dissolved inorganic carbon isotope compositions of the main potential sources of nitrate obtained from the literature.

NO_3^- source / Isotope ratio (‰)	Pig manure	Mineral fertilizers	Sewage	Soil
$\delta^{15}N$	+8 — +16	-4 — +4	+8 — +20	+3 — +8
	Vitòria (2004)	*Bateman and Kelly (2007), Kendall et al. (2007), Vitòria et al. (2004)*	*Aravena and Mayer (2010), Vane et al. (2010), Curt el al. (2004)*	*Aravena and Mayer (2010), Heaton (1986), Kendall et al. (2007)*
$\delta^{18}O_{NO3}$	+3.4 — +4.6	+17 — +25	+3.4 — +4.6	+3.4 — +4.6
	Estimated in this study according to eq.5	*Aravena and Mayer (2010), Vitòria et al. (2004), Xue et al. (2009)*	*Estimated in this study according to eq.5*	*Estimated in this study according to eq.5*
$\delta^{34}S$	-0.9 — +5.8	0 — +10	+7.6 — +11.7	0 — +6
	Cravotta (1997)	*Vitòria et al. (2004)*	*Otero et al. (2008)*	*Krouse and Mayer (2000)*
$\delta^{18}O_{SO4}$	+3.8 — +6	+9 — +15	+9 — +11.1	0 — +6
	Otero et al. (2007), Vitòria (2004)	*Vitòria et al. (2004)*	*Otero et al. (2008)*	*Krouse and Mayer (2000)*
$\delta^{11}B$	+19.5 — +42.4	-9 — +15	-7.7 — +12.9	-
	Widory et al. (2005)	*Komor (1997), Widory et al. (2005), (2013)*	*Bassett et al. (1995), Vengosh et al. (1994), Widory et al. (2013), Xue et al. (2009)*	-
$\delta^{13}C_{HCO3}$	-23.8 — -16.4	-35 — -24	-25 — -13	-23
	Cravotta (1997), Vitòria (2004)	*Vitòria et al. (2004)*	*Jurado et al. (2013), Li et al. (2010), Waldron et al. (2001)*	*Clark and Fritz (1997)*

NO_3^- source / Isotope ratio (‰)	Pig manure	Mineral fertilizers	Sewage	Soil
$\delta^{15}N$	+8 — +16	-4 — +8	+5 — +20	+3 — +8
	Vitòria (2004)	*Vitòria et al. (2004), Michalski et al. (2015)*	*Aravena and Mayer (2010), Vane et al. (2010), Curt el al. (2004)*	*Aravena and Mayer (2010), Heaton (1986), Kendall et al. (2007)*
$\delta^{18}O_{NO3}$	+3.4 — +4.6	+17 — +25	+3.4 — +4.6	+3.4 — +4.6
	Estimated in this study according to eq.5	*Aravena and Mayer (2010), Vitòria et al. (2004), Xue et al. (2009)*	*Estimated in this study according to eq.5*	*Estimated in this study according to eq.5*
$\delta^{34}S$	-0.9 — +5.8	0 — +10	+7.6 — +11.7	0 — +6
	Cravotta (1997)	*Vitòria et al. (2004)*	*Otero et al. (2008)*	*Krouse and Mayer (2000)*
$\delta^{18}O_{SO4}$	+3.8 — +6	+9 — +15	+9 — +11.1	0 — +6
	Otero et al. (2007), Vitòria (2004)	*Vitòria et al. (2004)*	*Otero et al. (2008)*	*Krouse and Mayer (2000)*
$\delta^{11}B$	+19.5 — +42.4	-9 — +15	-7.7 — +12.9	-
	Widory et al. (2005)	*Komor (1997), Widory et al. (2005), (2013)*	*Bassett et al. (1995), Vengosh et al. (1994), Widory et al. (2013), Xue et al. (2009)*	-
$\delta^{13}C_{HCO3}$	-23.8 — -16.4	-35 — -24	-25 — -13	-23
	Cravotta (1997), Vitòria (2004)	*Vitòria et al. (2004)*	*Jurado et al. (2013), Li et al. (2010), Waldron et al. (2001)*	*Clark and Fritz (1997)*

Most of the samples presented $\delta^{15}N$ ranging between +8 and +16‰, indicating that NO_3^- may originate from ^{15}N-enriched anthropogenic organic matter (manure or sewage) (Fig. 5a). ~~Finally, $\delta^{15}N$ values higher than +16‰ were observed in eleven samples. Four of these samples (Q_5 and Q_{15} from Q_S, and T_{17} and T_{23} from T_S) can be explained by volatilization processes as they showed high NO_3^- concentrations (between 190 and 480 mg L^{-1}) and $\delta^{18}O_{NO3}$ values up to +6‰. By contrast,~~Finally, some samples (Q_4, Q_8 and Q_9, from Q_S, and T_2 from T_D) presented ~~five other samples with~~ $\delta^{15}N$ values ~~also~~ higher than +16‰, coupled to low NO_3^- contents (between 6 and 26 mg L^{-1}, Table 2) and high $\delta^{18}O_{NO3}$ values (close to +10‰). ~~(Q_4, Q_8 and Q_9, from Q_S, and T_2 from T_D) have more likely been affected by denitrification since their NO_3^- contents were low (between 6 and 26 mg L^{-1}) and their $\delta^{18}O_{NO3}$ were close to +10‰.~~

The range of $\delta^{18}O$ of NO_3^- for NH_4^+ fertilizers, soil nitrogen and manure and sewage provided in Table 4 and plotted in Fig. 5a (+3.4‰ to +4.6‰), has been estimated according to eq. 5 (Anderson and Hooper, 1983; Hollocher, 1984; Kendall et al., 2007), where the $\delta^{18}O_{H2O}$ values are the highest and lowest groundwater $\delta^{18}O$ measured in the Baix Ter basin, and the $\delta^{18}O_{O2}$ is that of the atmospheric O_2 (+23.5‰; Horibe et al., 1973).

$$\delta^{18}O_{NO3} = 2/3(\delta^{18}O_{H2O}) + 1/3(\delta^{18}O_{O2}) \quad (5)$$

$\delta^{18}O_{NO3}$ values measured in the groundwater samples ranged from +1.8‰ to +18.1‰ (Fig.5b). While nitrate fertilizers are currently applied onto local crops their direct contribution to groundwater nitrate must be discarded as $\delta^{18}O$ and $\delta^{15}N$ of groundwater NO_3^- fall very far from nitrate fertilizers values (Fig. 5a). Moreover, most of samples had $\delta^{18}O_{NO3}$ higher than the calculated values for full equilibrium with the $\delta^{18}O$ of groundwater. Both results could be interpreted as a consequence of three

different processes: i) the mineralization-immobilization-turnover (MIT) process, ii) the higher consumption of NO_3^- from mineral fertilizers compared to that of ammonium in the root zone and iii) the reduction of NO_3^- via denitrifying bacteria. The MIT process consists of a microbial-mediated immobilization of nitrate N as organic nitrogen, the subsequent mineralization of this organic nitrogen to ammonium, and finally the nitrification of this ammonium back to NO_3^- (Mengis et al., 2001). This turnover process results in an important ^{18}O depletion of the initial $\delta^{18}O_{NO3}$ of the synthetic fertilizers (+17‰ to +20‰, Table 4). As synthetic fertilizers are currently used in the area, MIT process must be very active in order to explain why our results do not show the low $\delta^{15}N$ and high $\delta^{18}O$ values of nitrate from synthetic fertilizers. This indicates all NO_3^- from synthetic fertilizers that infiltrated underwent this process and that this source cannot be dismissed.

As pig manure is mainly liquid, the infiltration of ammonium from manure through the non-saturated zone to the saturated one is faster than that of nitrate from solid synthetic fertilizers, which need to be dissolved by rain or irrigation. Ammonium soil sorption capacity can be considered negligible as the soil is already saturated due to the long-standing fertilization practices affecting the area. Ammonium is also fast and completely nitrified into nitrate in the non-saturated zone. All these elements favour ammonium from pig manure to reach the saturated zone ~~and to be incorporated as nitrate into the~~ polluting groundwater. On the contrary, nitrate from ~~the slow release of~~ synthetic fertilizers remains ~~slightly longer~~ on the agricultural soil, ~~increasing the possibility of being absorbed by roots or of being~~ incorporated and stored in the soil organic matter pool ~~(~~by means of the MIT process~~)~~. It could then be slowly rereleased for either uptake by crops or export into the hydrosphere (Sebilo et al., 2013). Finally, the reduction of NO_3^- via denitrifying bacteria, which is characterized by a heavy-

isotope enrichment of both the $\delta^{15}N$ and $\delta^{18}O$ of the residual nitrate, can overprint the mixing of potential end-members and can significantly alter both the NO_3^- concentration (i.e. attenuation) and corresponding N and O isotope compositions.

$\delta^{15}N$ and $\delta^{18}O$ of NO_3 from the Ter River samples were in agreement with a wastewater origin.

Ten of the samples had $\delta^{18}O_{NO3}$ and $\delta^{15}N$ higher than +8‰ and +15‰, respectively. Fig. 5a shows that these samples roughly aligned following a $\varepsilon_N:\varepsilon_O$ ratio of 2, consistent with natural denitrification (Kendall et al., 2007). This means that the nitrate isotopic compositions but also the low nitrate concentration measured in those samples result from natural denitrification processes occurring in the aquifers. This is confirmed by Fig. 5b, in which a negative linear correlation between $\delta^{18}O_{NO3}$ and $\ln(NO_3^-/Cl^-)$ is observed for these samples, indicating that denitrification is taking place (Vitòria et al. 2008). The highest denitrified samples (i.e. with the higher coupled $\delta^{18}O_{NO3}$ and $\delta^{15}N$) were observed either in the shallow Quaternary levels near the Ter River (Q_4, Q_8, Q_9) or in the Tertiary aquifers (T_2). Moreover, the NO_3^- concentration measured below the detection limit in the samples Q_1, Q_2, T_9, T_{10} and T_{14} (Fig. 2) can also be interpreted as resulting of natural denitrification. Considering that no significant variations were identified in both the isotope and chemical compositions of our samples between both campaigns,

~~During the second sampling campaign, 19 samples from the previous campaign were resampled, and among those only 4 showed a significant decrease in their NO_3^- concentration. Among these only two showed corresponding significant shifts in their isotope and chemical compositions, in agreement with natural denitrification (Q_{10}, T_5).~~ ~~This suggests that~~ it can be inferred that natural denitrification had a moderate activity and/or that NO_3^- attenuation was balanced by the input of new NO_3^- into the aquifer.

4.4.2. $\delta^{34}S$ and $\delta^{18}O$ of SO_4

SO_4^{2-} isotope compositions ranged between -16.0 and +14.7‰ for $\delta^{34}S$, with an average value of +4.5‰ (n = 64), and between +3.8 and +16.1‰ for $\delta^{18}O_{SO4}$, with an average value of +7.2‰ (n = 64) (Table 3, Fig. 6). Most of the groundwater samples fall within the area defined by the isotope signatures of local anthropogenic sources (Table 4) showing that SO_4^{2-} in the Baix Ter groundwater can be explained by a ternary mixing between: 1) mineral fertilizers, 2) sewage and 3) pig manure (Fig. 6). This comforts the conclusions from the study of sulphate and nitrate groundwater concentrations.

Still, the $\delta^{34}S$ and a $\delta^{18}O_{SO4}$ values measured between 0 and +6‰ of samples Q_{17}, T_{11}, T_{18} and T_{21} could indicate a soil origin (Table 4), in agreement with their low SO_4^{2-} concentrations (around 30 mg SO_4^{2-} L^{-1}).

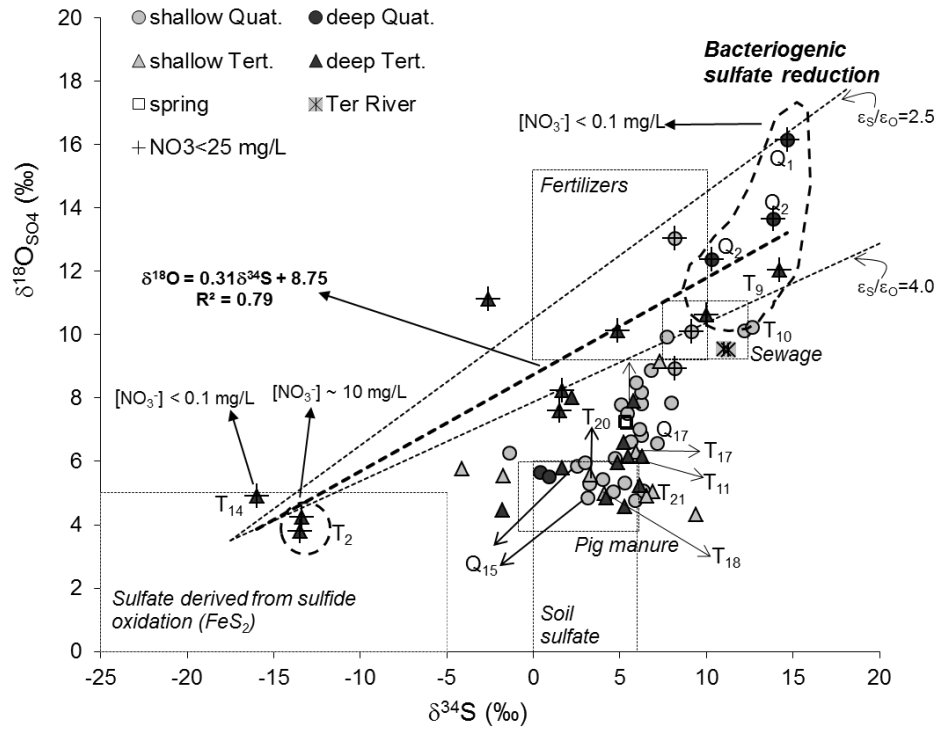

Figure 6. $\delta^{34}S$ and $\delta^{18}O$ of dissolved SO_4^{2-} in groundwater according to their hydrogeological unit. Isotope ranges of natural and anthropogenic SO_4 sources listed in Table 4 are also represented. The area of sulphates derived from sulphide oxidation is from Van Stempvoort and Krouse (1994). Dashed lines define the isotopic fractionation range ($\varepsilon^{34}S/\varepsilon^{18}O_{SO4}$) in SO_4 reduction reactions, varying between 2.5 and 4 (Mizutani and Rafter, 1973).

Two sampling sites (T_2 and T_{14}) yielded the lowest negative $\delta^{34}S$ values and had $\delta^{18}O_{SO4}$ around +5‰, revealing a SO_4^{2-} contribution from a ^{34}S-depleted source of reduced S (Fig. 6). Moreover, both T_2 and T_{14} showed very low (9 mg L^{-1}) or below detection limit (0.1 mg L^{-1}) nitrate concentrations, respectively. On the contrary, samples Q_1, Q_2, T_9 and T_{10}, with nitrate concentration below the detection limit (0.1 mg L^{-1}) exhibited the highest $\delta^{34}S$ and $\delta^{18}O_{SO4}$ values (+14.7‰ and +16.1‰ respectively).

All these samples in which nitrate concentration is below detection limit, together with other samples with very low nitrate aqueous concentration (NO_3^- < 25 mg L^{-1}) and $\delta^{18}O_{SO4}$ higher than +8‰ define a linear trend with $\varepsilon_S/\varepsilon_O$ = 1/0.31=3.2 compatible with a bacteriogenic reduction of SO_4^{2-} (Mizutani and Rafter, 1973) (Fig. 6). This is consistent with their corresponding low Eh values and high Mn concentrations (Fig. 3). However, as the presence of pyrite and gypsum in the area is scarce, autotrophic denitrification can be discarded as the main denitrifying process occurring in the study zone.

$\delta^{34}S$ and $\delta^{18}O_{SO4}$ of the Ter River samples also indicated, in agreement with their $\delta^{15}N$ and $\delta^{18}O_{NO3}$, that the dissolved SO_4^{2-} in surface waters originated from wastewater.

4.4.3. $\delta^{11}B$

Boron isotopes measurements were performed in 12 groundwater samples, selected considering both their NO_3^- and B contents and their location in the vicinity of pig farms or urban areas with the aim of discriminating between these two origins.

Pig manure present $\delta^{11}B$ values ranging from +19.5‰ to +42.4‰, significantly higher than urban wastewater values that range from -7.7‰ to +12.9‰ (Table 4). However, mineral fertilizers are characterized by a $\delta^{11}B$ range similar to sewage (-9‰ to +15‰, Table 4). Although mineral fertilizers can present a wide range of B concentrations they usually have lower B contents compared pig manure (Fig. 7a).

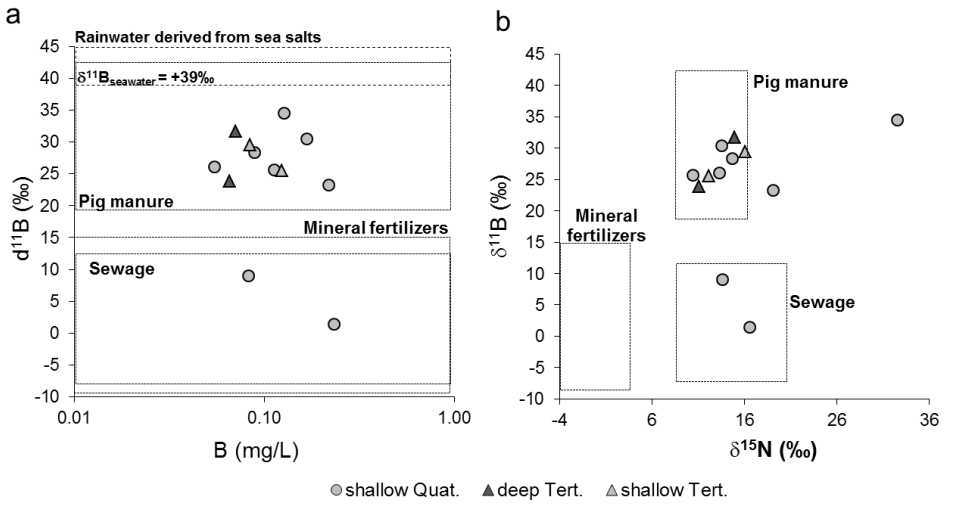

Formatted: Font: 12 pt

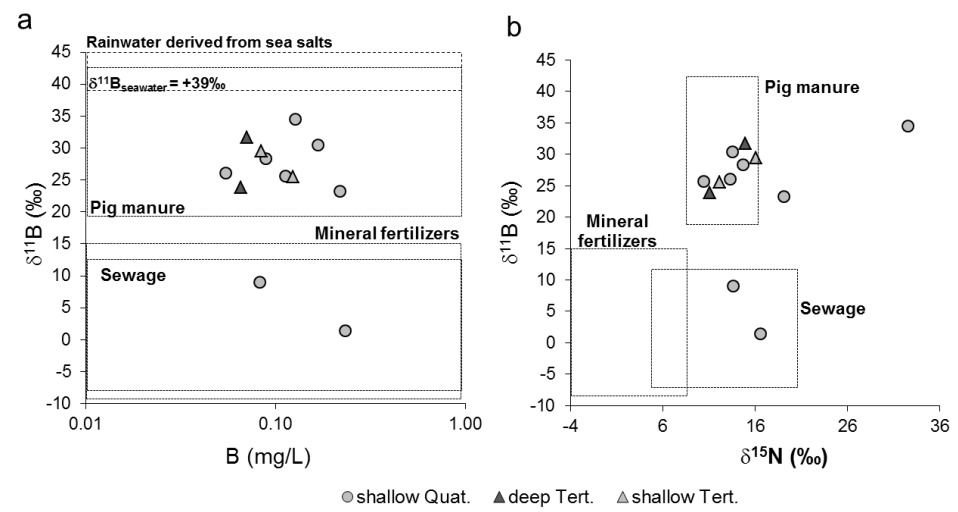

Figure 7. $\delta^{11}B$ values plotted against B concentration (a) and $\delta^{15}N$ values (b). Isotope ranges of the main NO_3^- sources listed in Table 4 are also represented. $\delta^{11}B_{seawater}$ is taken from Vengosh et al. (1994).

$\delta^{11}B$ composition of dissolved B in selected groundwater samples ranged between +1.4‰ and +34.5‰, with an average value of +24.1‰ (n = 12). B concentrations in these samples ranged between 0.055 and 0.232 mg L^{-1}. No trends or enrichment in $\delta^{11}B$ composition of dissolved B with decreasing B content were observed (Fig. 7a), indicating that B is not explained by binary mixing relationships and that no significant sorption/desorption processes of B onto/from clay minerals are occurring. Most samples fell in the isotope range of pig manure (Fig. 7a and 7b). This is in agreement with the conclusions drawn from the NO_3^- and SO_4^{2-} isotope data. Two of the samples showed $\delta^{11}B$ values consistent with a wastewater origin. They correspond to groundwater collected in La Bisbal (Q_{20}) and Ullastret (Q_{21}) water supply wells (Fig. 1), located downstream the discharge of the La Bisbal water treatment plant into the Daró River.

Formatted: Font: 12 pt

730 Boron analyses, thus, suggest that pig manure is the main source of contamination
731 and that the influence of sewage and mineral fertilizers is lower than the contribution
732 from organic residues.

733 **4.4.4. $\delta^{13}C$ of HCO_3^-**

734 Samples presented $\delta^{13}C_{HCO3}$ values between -6.5‰ and -16.2‰ (Table 3). $\delta^{13}C_{HCO3}$
735 values of marine marls in the study zone are $\delta^{13}C \sim 0$‰. Typical $\delta^{13}C$ values for CO_2
736 dissolved in the soil are between -14‰ and -16‰; for soil HCO_3^- $\delta^{13}C$ values are
737 around -23‰ and for pig manure, mineral fertilizers and sewage, $\delta^{13}C$ values range
738 from -23.8‰ to -16.4‰, from -35‰ to -24‰ and from -25‰ to -13‰, respectively
739 (Table 4).

740 Denitrification catalysed by organic matter oxidation induces a decrease in NO_3^-
741 and in total organic carbon concentrations coupled with an increase in dissolved
742 inorganic carbon concentration (eq.1), causing an increase of $\delta^{15}N$ and $\delta^{18}O_{NO3}$ and a
743 decrease in $\delta^{13}C_{HCO3}$ (Faure, 1977).

744 Fig. 8a shows the evolution of the $\delta^{18}O_{NO3}$ as a function of $\ln(NO_3^-/HCO_3^-)$. A slight
745 increase in $\delta^{18}O_{NO3}$ coupled to a decrease in $\ln(NO_3^-/HCO_3^-)$ can be observed that would
746 suggest that denitrification may occur. Nevertheless, we were not able to observe the
747 corresponding decrease in $\delta^{13}C_{HCO3}$ in our results (Fig. 8b). As already discussed
748 porewaters presented HCO_3^--Ca^{2+}-Mg^{2+} facies, with saturation indices for Ca-Mg-
749 carbonates between -1 and 1. This indicates that bicarbonate is in equilibrium with Ca-
750 Mg-carbonates whose dissolution and precipitation will contribute to the buffering of
751 the $\delta^{13}C_{HCO3}$ of our samples with a final isotope composition corresponding to
752 sedimentary rocks ($\delta^{13}C$ around 0 ‰ after Travé et al., 1997). Besides these
753 dissolution/precipitation reactions, $\delta^{13}C_{HCO3}$ can be also affected by other reactions such

754 as equilibrium with CO_2(g) and other sources such as manure or sewage (Clark and
755 Fritz, 1997).

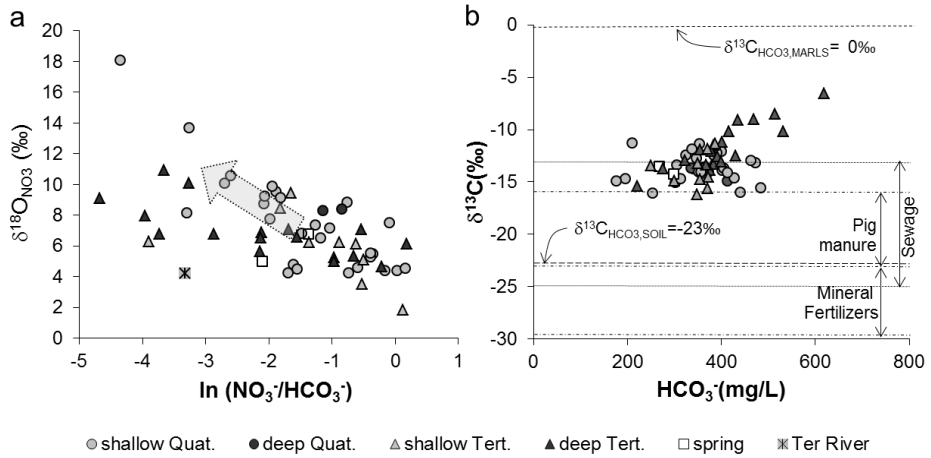

756

757 Figure 8. a) $\delta^{18}O_{NO3}$ values plotted against $\ln(NO_3^-/HCO_3^-)$. b) $\delta^{13}C_{HCO3}$ values plotted
758 against HCO_3^- concentration. Isotope ranges of the main NO_3^- sources listed in Table 4
759 are also represented. Value for $\delta^{13}C_{HCO3}$ for marls is from Travé et al. (1997).

760 **5. Conclusions**

761 Here we have ~~The~~ coupled the study of hydrochemical and multi-isotope data ~~in~~
762 ~~relation~~ with ~~the~~ hydrogeological framework information to identify ~~provides a valuable~~
763 ~~insight into~~ the sources and to characterise processes controlling the budget of dissolved
764 NO_3^- in ground- and surface water ~~, even~~ in a complex hydrogeological system (the
765 Baix Ter basin). ~~This approach has proved to be useful in providing both a better~~
766 ~~identification of the pollution sources and a better description of the natural attenuation~~
767 ~~processes taking place. This is a very valuable information for the design of water~~
768 ~~quality management policies.~~

769 ~~I~~When applied to the Baix Ter basin, isotope data have ~~been useful to further define~~
770 shown that the sources of recharge ~~of~~ for both the Tertiary and the Quaternary aquifers
771 are ~~, namely~~ the rainfall, the Ter River in the NW and a contribution from Les Gavarres

Massif. Moreover, ~~it~~ they showed that dissolved NO_3^- in groundwater in the study area mainly comes from pig manure application onto the fields, with minor contributions from sewage and mineral fertilizers. The study of $\delta^{11}B$ confirmed pig manure as the main vector of pollution but also identified an urban origin for two of the analysed wells. The dual-isotope ($\delta^{15}N$ and $\delta^{18}O$ of NO_3) approach indicated that mineralization-immobilization-turnover (MIT) and natural denitrification processes are occurring within the study area. The $\delta^{34}S$ and $\delta^{18}O$ of SO_4^{2-} showed that NO_3^- reduction is not controlled by the oxidation of pyrites but rather by the oxidation of organic matter. However, the role of organic matter in NO_3^- attenuation could neither be confirmed nor discarded by the study of the $\delta^{13}C_{HCO3}$ as other processes and sources ultimately buffered these isotope compositions. The consumption of organic matter in anaerobic environments is favoured by 1) the river-aquifer connection, 2) the existence of some organic layers in the Ter riversides, and 3) mixing between polluted groundwater and deep regional flows with reducing conditions.

Since the role of organic matter in the NO_3^- reduction is still an on-going research, further studies on the $\delta^{13}C$ of local contaminant sources and on the role of MnO_2 should be further investigated. Even if working with samples from exploitation wells, it has been proved that ~~M~~multi-isotope studies allow us to: i) describe groundwater dynamics, ii) discriminate between sources of pollution and determine their relative contribution, iii) characterise the processes affecting the overall nitrogen budget, such as natural attenuation, that in another way would go unnoticed. Still, these approaches highly depend on the knowledge of the isotopic signatures of the different potential sources of nitrate contamination of a given area, on the complexity of the aquifers complex and on the availability of a good infrastructure (e.g. multi-piezometers).

Acknowledgements

This research was funded by the ATENUATION (CGL2011-29975-C04-01) and REMEDIATION (CGL2014-57215-C4-1-R) projects from Spanish Ministry of Economy and Competitiveness (MINECO) and the AGAUR from the Catalan Government (grant 2014SGR-1456).~~and CGL2014-57215-C4-1-R from the Spanish Government and project 2014SGR-1456 from Catalan Government~~. We would like to thank the Centres Científics i Tecnològics of the Universitat de Barcelona for its laboratory help. Authors acknowledge the fruitful comments of the three anonymous reviewers.

References

ACA, 2007. Diagnosis de la causalidad de la contaminación por nitratos de algunos abastecimientos públicos en las zonas vulnerables de Cataluña, análisis de alternativas, medidas de prevención y corrección. Área vulnerable 1 Girona. Estudio 1: Llanura aluvial de los ríos Ter y Daró, provincia de Girona. ACA (Water Catalan Agency) Internal Report. 168 pp.

ACA, 2015. Agència Catalana de l'Aigua. Generalitat de Catalunya. Consulta de dades. Available at: http://aca-web.gencat.cat/aca/appmanager/aca/aca/ (June 2016).

Altman, S.J., Parizek, R.R., 1995. Dilution of non-point source nitrate in ground water. J. Environ. Qual. 24, 707-718.

Amiri, H., Zare, M., Widory. D., 2015. Assessing sources of nitrate contamination in the Shiraz urban aquifer (Iran) using the $\delta^{15}N$ and $\delta^{18}O$ dual-isotope approach. Isotopes in Environmental and Health Studies. DOI: 10.1080/10256016.2015.1032960.

Anderson, K. K., Hooper, A. B., 1983. O_2 and H_2O are each the source of one O in NO_2^- produced from NH_3 by Nitrosomas-^{15}N-NMR evidence. FEBS Letters, 64, 236–40.

Aravena, R., Evans, M.L., Cherry, J.A., 1993. Stable isotopes of oxygen and nitrogen in source identification of nitrate from septic tanks. Ground Water, 31, 180–186.

Aravena, R., Robertson, W.D., 1998. Use of Multiple Isotope Tracers to Evaluate Denitrification in Ground Water: Study of Nitrate from a Large-Flux Septic System Plume. Ground Water, 36, 975-982.

Aravena, R., Mayer, B., 2010. Isotopes and Processes in the Nitrogen and Sulfur Cycles. In: Aelion, C.M., Höhener, P., Hunkeler, D., Aravena, R. (Eds.),

Environmental Isotopes in Biodegradation and Bioremediation. CRC Press, pp. 203–246.

~~Archna, Surinder K. Sharma, Ranbir Chander Sobti, 2012. Nitrate Removal from Ground Water: A Review. E-Journal of Chemistry, 9, 4, 1667-1675. doi:10.1155/2012/154616.~~

Barroso, M.F., Ramalhosa, M.J., Olhero, A., Antão, M.C., Pina, M.F., Guimarães, L., Teixeira, J., Alfonso, M.J., Delerue-Matos, C., Chaminé, H.I., 2015. Assessment of groundwater contamination in an aricultural peri-urban area (NW Portugal): an integrated approach. Environ Earth Sci 73, 2881-2894.

Basset, R.L., Buszka, P.M., Davidson, G.R., Chong-Diaz, D., 1995. Identification of groundwater solute sources using boron isotopic composition. Environ. Sci. Technol. 29, 2915–2922.

~~Bateman, A.S., Kelly, S.D., 2007. Fertilizer nitrogen isotope signatures. Isotopes in Environmental and Health Studies, 43, 237-247.~~

Borch, T., Kretzschmar, R., Kappler, A., Van Cappellen, P., Ginder-Vogel, M., Voegelin, A., Campbell, K., 2010. Biogeochemical Redox Processes and their Impact on Contaminant Dynamics. Environmental Science and Technology, 44, 15–23.

Böttcher, J., Strebel, O., Voerkelius, S., Schmidt, H.L., 1990. Using isotope fractionation of nitrate-nitrogen and nitrate-oxygen for evaluation of microbial denitrification in sandy aquifer. Journal of Hydrology, 114, 413-424.

Bryan, N.S., Alexander, D.D., Coughlin, J.R., Milkowski, A.L., Boffetta, P., 2012. Ingested nitrate and nitrite and stomach cancer risk: An updated review. Food and Chemical Toxicology, 50, 3646–3665.

Clark, I.D., Fritz, P., 1997. Environmental Isotopes in Hydrogeology. Lewis Publishers, New York. 352 pp.

Cravotta, C.A., 1997. Use of Stable Isotopes of Carbon, Nitrogen and Sulphur to Identify Sources of Nitrogen in Surface Waters in the Lower Susquehanna River Basin, Pennsylvania. U.S. Geological Survey Water-Supply Paper 2497.

Curt, M.D., Aguado, P., Sánchez, G., Bigeriego, M., ~~and~~ Fernández, J., 2004. Nitrogen isotope ratios of synthetic and organic sources of nitrate water contamination in Spain. Water, Air and Soil Pollution, 151, 135-142.

Delconte. C.A., Sacchi, E., Racchetti, E., Bartoli, M., Mas-Pla, J., Re, V., 2014. Nitrogen inputs to a river course in a heavily impacted watershed: a combined hydrochemical and isotopic evaluation (Oglio River Basin, N Italy). Science of the Total Environment 466-467, 924-938, DOI: 10.1016/j.scitotenv.2013.07.092.

EC (European Communities), 1991. Council Directive 91/676/EC, of 12 December 1991, concerning the protection of waters against pollution caused by nitrates from agricultural sources.

EC (European Communities), 1998. Council Directive 98/83/EC, of 3 November 1998, on the quality of water intended for human consumption.

EC (European Communities), 2000. Directive 2000/60/EC of the European Parliament and of the Council establishing a framework for the Community action in the field of water policy (Water Framework Directive). Official Journal of the European Communities, OJ L 327.

EC (European Communities), 2006. Directive 2006/118/EC of the European Parliament and of the Council on the protection of groundwater against pollution and deterioration (Groundwater Directive). Official Journal of the European Communities, OJ L 372.

EEA (European Environment Agency), 1999. Nutrients in European Ecosystems. Environmental assessment report Nº 4.

EEA (European Environment Agency), 2012. European waters: assessment of status and pressures. EEA Report Nº 8. Published: Nov 13, 2012. Copenhagen, Denmark.

EEA (European Environment Agency), 2015. Nutrients in freshwater. Indicator assessment. Data and maps. IND-8-en. CSI 020, WAT 003. Published: Sep 4th, 2015. Copenhagen, Denmark. Available as a website at http://www.eea.europa.eu/data-and-maps/indicators/nutrients-infreshwater/nutrients-in-freshwater-assessment-published-6.

Faure, G. 1997. Principles of isotope geology, Wiley, 2nd Ed, 589 pp.

Fukada, T., Hiscock, K., Dennis, P.F., Grischek, T., 2003. A dual isotope approach to identify denitrification in groundwater at a river-bank infiltration site. Water Res. 37, 3070–3078.

Gaillardet, J., Allègre, C.J., 1995. Boron isotopic compositions of corals: Seawater or diagenesis record? Earth and Planetary Science Letters 136, 665-676.

Heaton, T.H.E., 1986. Isotopic studies of nitrogen pollution in the hydrosphere and atmosphere: a review. Chem. Geol. 59, 87–102.

Hollocher, T. C., 1984. Source of oxygen atoms in nitrate in the oxidation of nitrite by *Nitrobacter agilis* and evidence against a P-O-N anhydride mechanism in oxidative phosphorylation. Archives of Biochemistry and Biophysics, 233, 721–27.

Horibe, Y., Shigehara, K., Takakuwa, Y., 1973. Isotope separation factors of carbon dioxide-water system and isotopic composition of atmospheric oxygen. Journal of Geophysical Research, 78, 2625-2629.

905 Ishikawa, T., Nakamura, E., 1990. Suppression of boron volatilization from a
906 hydrofluoric acid solution using a boron-mannitol complex., Analytical
907 Chemistry 62, 2612–2616.
908 Jurado, A., Vàzquez-Suñé, E., Soler, A., Tubau, I., Carrera, J., Pujades, E., Anson, I.,
909 2013. Application of multi-isotope data (O, D, C and S) to quantify redox
910 processes in urban groundwater. Applied Geochemistry, 34, 114–125.
911 Karr, J.D., Showers, W.J., Wendell Gilliam, J., Scott Andres, A., 2001. Tracing nitrate
912 transport and environmental impact from intensive swine farming using delta
913 nitrogen-15. J. Environ. Qual. 30, 1163–1175.
914 ~~Kendall, C., 1998. Tracing Nitrogen Sources and Cycling in Catchments. In: Isotope~~
915 ~~Tracers in Catchment Hydrology, C. Kendall and J. J. McDonnell (Eds.).~~
916 ~~Elsevier Science B.V., Amsterdam, 839 p., 519-576.~~
917 Kendall, C., Elliott, E.M., Wankel, S.D., 2007. Tracing anthropogenic inputs of nitrogen
918 to ecosystems, Chapter 12. In: R.H. Michener and K. Lajtha (Eds.), Stable
919 Isotopes in Ecology and Environmental Science, 2nd edition, Blackwell
920 Publishing, pp. 375-449.
921 Koba, K., Tokuchi, N., Wada, E., Nakajima, T., Iwatsubo, G., 1997. Intermittent
922 denitrification: the application of a ^{15}N natural abundance method to a forested
923 ecosystem. Geochim. Cosmochim. Acta, 61, 5043–5050.
924 Komor, S.C., 1997. Boron contents and isotopic compositions of hog manure, selected
925 fertilizers, and water in Minnesota. J. Environ. Qual. 26, 1212–1222.
926 Krouse, H.R., Mayer, B., 2000. Sulphur and oxygen isotopes in sulphate. In: Cook,
927 P.G., Hercseg, A.L. (Eds.), Environmental Tracers in Subsurface Hydrology.
928 Kluwer Academic Press, Boston, pp. 195–231.

Li, X.-D., Liu, C.-Q., Harue, M., Li, S.-L., Liu, X.-L., 2010. The use of environmental isotopic (C, Sr, S) and hydrochemical tracers to characterize anthropogenic effects on karst groundwater quality: A case study of the Shuicheng Basin, SW China. Applied Geochemistry, 25, 1924–1936.

Mariotti, A., Germon, J.C., Hubert, P., Kaiser, P., Letolle, R., Tardieux, P., 1981. Experimental determination of nitrogen kinetic isotope fractionation: some principles, illustration for the denitrification and nitrification processes. Plant Soil, 62, 413–430.

Mariotti, A., Landreau, A., Simon, B., 1988. ^{15}N isotope biogeochemistry and natural denitrification process in groundwater: application to the chalk aquifer of northern France. Geochim. Cosmochim. Acta, 52, 1869–1878.

Mas-Pla, J., Bach, J., Montaner J., 1998. Distribución de la concentración de nitratos en el sistema hidrogeológico Baix Ter-Gavarres (Girona). In: La contaminación de las aguas subterráneas: Un problema pendiente. ITGE-AIH, pp. 139–145.

Mas-Pla, J., Vilanova, E., 2001. Dinámica del sistema hidrogeológico Baix Ter-Gavarres en base a isótopos estables. In: IGME, Las Caras del Agua, Serie Hidrogeología y Aguas Subterráneas n. 1/2001, tomo I, pp. 395-402.

Menció, A., J. Mas-Pla, A. Soler, N. Otero, O. Regàs, M. Boy-Roura, R. Puig, J. Bach, C. Domènech, A. Folch, M. Zamorano, D. Brusi (2016). Nitrate pollution of groundwater; all right …, but nothing else? Science of the Total Environment, 539C: 241-251. DOI: 10.1016/j.scitotenv.2015.08.151

Mengis, M., Walther, U., Bernasconi, S.M., Wehrli, B., 2001. Limitations of using $\delta^{18}O$ for the source identification of nitrate in agricultural soils. Environ. Sci. Technol. 35 (9), 1840–1844.

953 Michalski, G., Kolanowski, M. Rihaa, K.M., 2015. Oxygen and nitrogen isotopic
954 composition of nitrate in commercial fertilizers, nitric acid, and reagent salts.
955 Isotopes in Environmental and Health Studies 51, 382-391.
956 Mizutani, Y., Rafter, T.A., 1973. Isotopic behaviour of sulphate oxygen in the bacterial
957 reduction of sulphate. Geochemical Journal, 6, 183-191.
958 Montaner, J., Pons, P., López, J., 2010. Caracterització del flux hidrològic a la plana
959 litoral del Baix Ter. In: El flux hidrològic de la plana litoral del Baix Ter.
960 Evolució fluvial, caracterització hidrològica i pautes de gestió. Montaner, J.
961 (coord.). Càtedra d'Ecosistemes Litorals Mediterranis. Museu de la Mediterrània
962 (Ed.). Recerca i Territori, 2.
963 Neal, C., Neal, M., Warrington, A., Àvila, A., Piñol, J., Rodà, F., 1992. Stable hydrogen
964 and oxygen isotope studies of rainfall and streamwaters for two contrasting holm
965 oak areas of Catalonia, northeastern Spain. Journal of Hydrology, 140, 163–178.
966 Otero, N., Canals, A., Soler, A., 2007. Using dual-isotope data to trace the origin and
967 processes of dissolved sulphate: a case study in Calders stream (Llobregat basin,
968 Spain). Aquat. Geochem. 13, 109–126.
969 Otero, N., Soler, A., Canals, A., 2008. Controls of $\delta^{34}S$ and $\delta^{18}O$ in dissolved sulphate:
970 Learning from a detailed survey in the Llobregat River (Spain). Applied
971 Geochemistry, 23, 1166-1185.
972 Otero, N., Torrentó, C., Soler, A., Menció, A., Mas-Pla, J., 2009. Monitoring
973 groundwater nitrate attenuation in a regional system coupling hydrogeology with
974 multi-isotopic methods: the case of Plana de Vic (Osona, Spain). Agr. Ecosyst.
975 Environ. 133 (1-2), 103–113.

976 Panno, S.V., Hackley, K.C., Hwang, H.H., Kelly, W.R., 2001. Determination of the
977 sources of nitrate contamination in karst springs using isotopic and chemical
978 indicators. Chemical Geology, 179, 113-128.
979 Rivett, M.O., Buss, S.R., Morgan, P., Smith, J.W.N., Bemment, C.D., 2008. Nitrate
980 attenuation in groundwater: a review of biogeochemical controlling processes.
981 Water Res. 42, 4215–4232.
982 Rock, L., Mayer, B., 2002. Isotopic assessment of sources and processes affecting
983 sulphate and nitrate in surface water and groundwater of Luxembourg. Isotopes
984 Environ. Health Stud. 38 (4), 191-206.
985 Sacchi, E., Acutis, M., Bartoli, M., Brenna, S., Delconte. C.A., Laini, A., Pennisi, M.
986 (2013) Origin and fate of nitrates in groundwater from the central Po plain:
987 Insights from isotopic investigations. Applied Geochemistry 34, 164-180.
988 Saccon, P., Leis, A., Marca, A., Kaiser, J., Campisi, L., Böttcher, M.E., Savarino, J.,
989 Escher, P., Eisenhauer, A., Erbland, J., 2013. Multi-isotope approach for the
990 identification and characterization of nitrate pollution sources in the Marano
991 lagoon (Italy) and parts of its catchment area. Appl. Geochem., 34, 75–89.
992 Sebilo, M., Mayer, B., Nicolardot, B., Pinay, G., Mariotti, A., 2013. Long-term fate of
993 nitrate fertilizer in agricultural soils. PNAS (Proceedings of the National
994 Academy of Sciences of the United States of America).
995 www.pnas.org/cgi/doi/10.1073/pnas.1305372110
996 Seiler, R. L., 2005. Combined use of ^{15}N and ^{18}O of nitrate and ^{11}B to evaluate nitrate
997 contamination in groundwater. Applied Geochemistry, 20, 1626-1636.
998 Silva, S.R., Ging, P.B., Lee, R.W., Ebbert, J.C., Tesoriero, A.J., Inkpen, E.L., (2002)
999 Forensic applications of nitrogen and oxygen isotopes in tracing nitrate sources

in urban environments. Environ Forensic 3, 125–130. doi:10.1006/enfo.2002.0086.

Silva, S.R., Kendall, C., Wilkison, D.H., Ziegler, A.C., Chang, C.C.Y., Avanzino, R.J., 2000. A new method for collection of nitrate from fresh water and the analysis of nitrogen and oxygen isotope ratios. Journal of Hydrology, 228, 22–36.

Spivack, A.J., Edmond, J.M., 1986. Determination of boron isotope ratios by thermal ionization mass spectrometry of the dicesium metaborate cation. Anal. Chem., 58, 31-35.

Tirez, K., Brusten, W., Widory, D., Petelet, E., Bregnot, A., Xue, D., Boeckx, P., Bronders, J., 2010. Boron Isotope Ratio ($\delta^{11}B$) Measurements in Water Framework Directive Programs: Comparison between Double Focusing Sector Field ICP and Thermal Ionization Mass Spectrometry, J. Anal. At. Spectrom. 25, 964-974.

Travé, A., Labaume, P., Calvet, F., Soler, A. (1997) Sediment dewatering and pore fluid migration along thust faults in a foreland basin inferred from isotopic and elemental geochemical analyses (Eocene southern Pyrenees, Spain). Tectonophysics 282, 375-398.

Vane, C.H., Kim, A.W., McGowan, S., Leng, M.J., Heaton, T.H.E., Kendrick, C.P., Coombs, P., Yang, H., Swann, G.E.A., 2010. Sedimentary records of sewage pollution using faecal markers in contrasting peri-urban shallow lakes. The Science of the Total Environment 409, 345-356.

Van Stempvoort, D.R., Krouse, H.R., 1994. Controls of $\delta^{18}O$ in sulphate. In: Alpers, C.N., Blowes, D.W. (Eds.), Environmental Geochemistry of Sulphide Oxidation. American Chemical Society, Washington, pp. 446–480.

Vengosh, A., Heumann, K.G., Juraske, S., Kasher, R., 1994. Boron Isotope Application for Tracing Sources of Contamination in Groundwater. Environmental, Science and Technology 28, 1968-1974.

Vilanova, E., 2004. Anàlisi dels sistemes de flux a l'àrea Gavarres-Selva-Baix Empordà. Proposta de model hidrodinàmic regional. Ph.D Dissertation. Universitat Autònoma de Barcelona, 337 pp. http://www.tdx.cat/handle/10803/3437

~~Vilanova, E., Mas-Pla, J., 2004. Identificación de sistemas de flujo en base a datos isotópicos en el área Gavarres-Baix Empordà-Selva (CIC). Geotemas, 6(4), 197-202.~~

Vilanova, E., Mas-Pla, J., Menció, A., 2008. Determinación de sistemas de flujo regionales y locales en las depresiones tectónicas del Baix Empordà y La Selva (NE de España) en base a datos hidroquímicos e isotópicos. Boletín Geológico y Minero, 119 (1), 51-62.

Vitòria, L., 2004. Estudi multi-isotòpic ($\delta^{15}N$, $\delta^{34}S$, $\delta^{13}C$, $\delta^{18}O$, δD i $^{87}Sr/^{86}Sr$) de les aigües subterrànies contaminades per nitrats d'origen agrícola i ramader. Translated title: Multi-isotopic approach ($\delta^{15}N$, $\delta^{34}S$, $\delta^{13}C$, $\delta^{18}O$, δD and $^{87}Sr/^{86}Sr$) of nitrate contaminated groundwaters by agricultural and stockbreeder activities. PhD Thesis. Universitat de Barcelona, 188 pp.

Vitòria, L., Otero, N., Canals, A., Soler, A., 2004. Fertilizer characterization: isotopic data (N, S, O, C and Sr). Environ. Sci. Technol. 38, 3254–3262.

Vitòria, L., Soler, A., Aravena, R., Canals, A., 2005. Multi-isotopic approach (^{15}N, ^{13}C, ^{34}S, ^{18}O and D) for tracing agriculture contamination in groundwater (Maresme, NE Spain). In: Environmental Chemistry (Eds. E. Lichtfouse, J. Schwarzbauer and D. Robert). Springer-Verlag, Heidelberg, 43-56.

1049 Vitòria, L., Soler, A., Canals, A., Otero, N., 2008. Environmental isotopes (N, S, C, O,
1050 D) to determine natural attenuation processes in nitrate contaminated waters:
1051 example of Osona (NE Spain). Appl. Geochem. 23, 3597–3611.
1052 Waldron, S., Tatner, P., Jack, I., Arnott, C., 2001. The Impact of Sewage Discharge in a
1053 Marine Embayment: A Stable Isotope Reconnaissance. Estuarine, Coastal and
1054 Shelf Science, 52, 111–115. doi:10.1006/ecss.2000.0731.
1055 Ward, M.H., deKok, T.M., Levallois, P., Brender, J., Gulis, G., Nolan, B.T.,
1056 VanDerslice, J., 2005. Workgroup report: drinking-water nitrate and health—
1057 recent findings and research needs. Environ. Health Perspect. 113, 1607–1614.
1058 Wassenaar, L. I., 1995. Evaluation of the origin and fate of nitrate in the Abbotsford
1059 aquifer using the isotopes of ^{15}N and ^{18}O in NO_3. Applied Geochemistry, 10,
1060 391–405.
1061 Widory, D., Kloppmann, W., Chery, L., Bonnin, J., Rochdi, H., Guinamant, J.L., 2004.
1062 Nitrate in groundwater: an isotopic multi-tracer approach. Journal of
1063 Contaminant Hydrology, 72, 165-188.
1064 Widory, D., Petelet-Giraud, E., Négrel, P., Ladouche, B., 2005. Tracking the sources of
1065 nitrate in groundwater using coupled nitrogen and boron isotopes: a synthesis.
1066 Environmental, Science and Technology, 39, 539-548.
1067 Widory, D., Petelet-Giraud, E., Brenot, A., Bronders, J., Tirez, K., Boeckx, P., 2013.
1068 Improving the management of nitrate pollution in water by the use of isotope
1069 monitoring: the $\delta^{15}N$, $\delta^{18}O$ and $\delta^{11}B$ triptych. Isotopes in Environmental and
1070 Health Studies, 48, 1-19.
1071 Xu, S., Kang, P, Sun, Y., 2016. A stable isotope approach and its application for
1072 identifying nitrate source and transformation process in water. Environ Sci
1073 Pollut Res 23, 1133-1148.

Xue, D., Botte, J., De Baets, B., Accoe, F., Nestler, A., Taylor, P., Van Cleemput, O., Berglund, M., Boeckx, P., 2009. Present limitations and future prospects of stable isotope methods for nitrate source identification in surface- and groundwater. Water Research, 43, 1159-1170.

Yingkai, X., Lan, W., 2001. The effect of pH and temperature on the isotopic fractionation of boron between saline brine and sediments. Chem. Geol. 171, 253–261.

Figure captions

Figure 1. Geological map of the Baix Ter basin, sampling point locations labelled according to the hydrogeological formation where they are located. Potentiometric contour lines of the unconfined aquifer, mainly in the shallow Quaternary formations, correspond to the August 2004 survey. Dashed line represents the zero elevation potentiometric level in the deep quaternary formations (mainly leaky aquifers) affected by intensive withdrawal rates in the central area of the basin. Geology from ICGC (http:// www.icgc.cat).~~Figure 1. Baix Ter basin map showing the geology and sampling points, labelled according to their hydrogeological formation (round and triangle shapes distinguish between Quaternary and Tertiary aquifers, respectively, and light and bold points, between shallow and deep formations, respectively; square refers to the sampled spring). Potentiometric contour lines correspond to the water table measurements of the Quaternary unit (August 2004).~~

Figure 2. $\delta^{18}O_{H2O}$ and $\delta^{2}H$ of the Baix Ter groundwater samples collected in January 2004 (a) and August 2004 (b). The annual-Local Meteoric Water Line (LMWL) follows the equation $\delta^{2}H = 7.98(\pm2.71)\ \delta^{18}O + 7.85(\pm0.47)$ (r^2=0.924, n=23) (Vilanova, 2004), whose slope is equal to that of the neighbouring areas ($\delta^{2}H = 7.9\ \delta^{18}O + 9.8$; Neal et al., 1992).

Figure 3. Mn concentrations plotted against the Eh values of the groundwater samples. Eh ranges of MnO_2/Mn^{2+} and $NO_3^-/N_{2(g)}$ redox pairs are taken from Rivett et al. (2008).

Figure 4 a) NO_3^- concentration versus Cl^- concentration, b) NO_3^- concentration versus SO_4^{2-} concentration, c) SO_4^{2-} concentration versus (NO_3^-/Cl^-) ratio, and d) B concentration versus (NO_3^-/Cl^-) ratio.

Figure 5. a) Variations of the $\delta^{15}N$ and $\delta^{18}O$ of dissolved NO_3^- in groundwater according to their hydrogeological unit. Isotope ranges of the main NO_3^- sources listed in Table 4 are also represented. The extreme isotopic fractionation ~~ratios~~factors from the literature are $\varepsilon_N/\varepsilon_O$ = 2.1 (Böttcher et al., 1990) and $\varepsilon_N/\varepsilon_O$ = 1.3 (Fukada et al., 2003). b) $\delta^{18}O_{NO3}$ values plotted against ln(NO_3^-/Cl^-) according to their hydrogeological unit. R^2 values ~~of~~for the linear regressions for shallow Quat. and deep Tert. Units are also reported. ~~Variations of the $\delta^{15}N$ and $\delta^{18}O$ of dissolved NO_3^- in groundwater according to their hydrogeological unit. Isotope ranges of the main NO_3^- sources listed in Table 4 are also represented. The extreme isotopic fractionation ratios from the literature are $\varepsilon_N/\varepsilon_O$ = 2.1 (Böttcher et al., 1990) and $\varepsilon_N/\varepsilon_O$ = 1.3 (Fukada et al., 2003).~~

Figure 6. $\delta^{34}S$ and $\delta^{18}O$ of dissolved SO_4^{2-} in groundwater according to their hydrogeological unit. Isotope ranges of natural and anthropogenic SO_4 sources listed in Table 4 are also represented. The area of sulphates derived from sulphide oxidation is from Van Stempvoort and Krouse (1994). Dashed lines define the isotopic fractionation range ($\varepsilon^{34}S/\varepsilon^{18}O_{SO4}$) in SO_4 reduction reactions, varying between 2.5 and 4 (Mizutani and Rafter, 1973).

Figure 7. $\delta^{11}B$ values plotted against B concentration (a) and $\delta^{15}N$ values (b). Isotope ranges of the main NO_3^- sources listed in Table 4 are also represented. $\delta^{11}B_{seawater}$ is taken from Vengosh et al. (1994).

Figure 8. a) $\delta^{18}O_{NO3}$ values plotted against $\ln(NO_3^-/HCO_3^-)$. b) $\delta^{13}C_{HCO3}$ values plotted against HCO_3^- concentration. Isotope ranges of the main NO_3^- sources listed in Table 4 are also represented. Value for $\delta^{13}C_{HCO3}$ for marls is from Travé et al. (1997).

Table captions

Table 1. Hydrogeological formation, X and Y UTM coordinates, depth (m), hydraulic head (m.a.s.l.), and physico-chemical parameters measured in situ for the sampled points of each field campaign. See Fig. 1 for sampling locations in the Baix Ter basin. R_1 and R_2 Ter River samples are from the Colomers station, NW of the study zone (Fig. 1). (*n.d.*: Not determined).

Table 2. Hydrochemical data for the January and August 2004 field campaigns ("*" = DOC concentrations instead of TOC concentrations). R_1 and R_2 Ter River samples are from the Colomers station, NW of the study zone (Fig. 1). (*n.d.*: Not determined; *u.d.l.*: under detection limit).

Table 3. Isotope data for the January and August 2004 field campaigns. R_1 and R_2 Ter River samples are from the Colomers station, NW of the study zone (Fig. 1). (*n.d.*: Not determined).

Table 4. Ranges of nitrate, sulphate, boron and dissolved inorganic carbon isotope compositions of the main potential sources of nitrate obtained from the literature.

1155

1156

Characterizing sources and natural attenuation of nitrate contamination in the Baix Ter aquifer system (NE Spain) using a multi-isotope approach

Roger Puig[a], Albert Soler[a], David Widory[b], Josep Mas-Pla[c, d], Cristina Domènech[a] and Neus Otero[a]

[a]Grup de Mineralogia Aplicada i Geoquímica de Fluids, Dept. de Mineralogia, Petrologia i Geologia Aplicada, Facultat de Ciències de la Terra, Universitat de Barcelona (UB), c/ Martí i Franquès s/n, 08028 Barcelona, Spain.

[b]Département des Sciences de la Terre et de l'Atmosphère, Geotop/UQAM, Montréal, Canada.

[c]Grup de Geologia Aplicada i Ambiental, Centre de Geologia i Cartografia Ambiental, Dept. de Ciències Ambientals, Universitat de Girona, 17003 Girona, Spain.

[d]Catalan Institute for Water Research, c/ Emili Grahit 101, 17003 Girona, Spain.

Corresponfing author: Cristina Domenech (cristina.domenech@ub.edu)

Graphical abstract

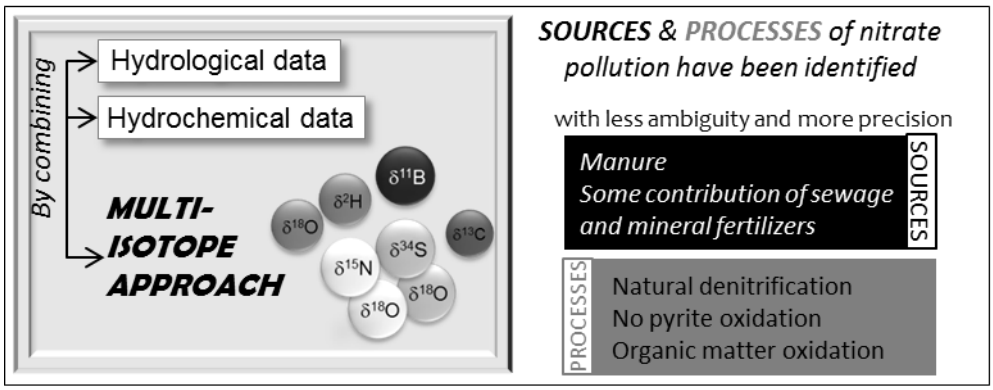

Highlights

- $\delta^{15}N$, $\delta^{18}O_{NO3}$ and $\delta^{11}B$ confirm pig manure as the main vector of NO_3- pollution.
- SO_4^{2-} and B isotopes indicate also contributions from sewage and mineral fertilizers.
- NO_3^- isotopes show that NO_3^- undergoes natural attenuation.

- SO_4^{2-} isotopes confirm that denitrification is not controlled by pyrite oxidation.
- The multi-isotope approach provides a unique and comprehensive approach that allows to characterise the origin of NO_3^- pollution as well as the processes involved.

Abstract

Nitrate pollution is a widespread issue affecting global water resources with significant economic and health effects. Knowledge of both the corresponding pollution sources and of processes naturally attenuating them is thus of crucial importance in assessing water management policies and the impact of anthropogenic activities. In this study, an approach combining hydrodynamic, hydrochemical and multi-isotope systematics (8 isotopes) is used to characterise the sources of nitrate pollution and potential natural attenuation processes in a polluted basin of NE Spain. δ^2H and $\delta^{18}O$ isotopes were used to further characterize the sources of recharge of the aquifers. Results show that NO_3^- is not homogeneously distributed and presents a large range of concentrations, from no NO_3^- to up to 480 mg L^{-1}. $\delta^{15}N$ and $\delta^{18}O$ of dissolved NO_3^- identified manure as the main source of nitrate, although sewage and mineral fertilizers can also be isotopically detected using boron isotopes ($\delta^{11}B$) and $\delta^{34}S$ and $\delta^{18}O$ of dissolved sulphate, respectively. The multi-isotope approach proved that natural denitrification is occurring, especially in near-river environments or in areas hydrologically related to fault zones. $\delta^{34}S$ and $\delta^{18}O$ indicated that denitrification is not driven by pyrite oxidation but rather by the oxidation of organic matter. This could not be confirmed by the study of $\delta^{13}C_{HCO3}$ that was buffered by the entanglement of other processes and sources.

Keywords

Stable isotopes, nitrate contamination, boron, denitrification, groundwater, manure

1. Introduction

Nitrate (NO_3^-) contamination of groundwater is a problem affecting groundwater quality worldwide (Xu et al., 2016 and references therein) that has proved to affect human health (Bryan et al., 2012; Ward et al., 2005). Because of this, considerable efforts have been made by the European authorities to promote both the reduction of NO_3^- inputs and the enhancement of attenuation processes in groundwater.

However, no decreasing trends in average European nitrate concentration in groundwater have been observed during the last 15 years (EEA, 2015). Thus, NO_3 concentrations in groundwater often exceed the 50 mg L^{-1} legal guideline set for drinking water (EC, 1998). NO_3 is currently one of the main contaminants that may hinder achieving the goals of the Water Framework (EC, 2000) and of the European Groundwater (EC, 2006) directives. This arises the need for a better knowledge on the overall nitrogen, including nitrate species cycle in surface water and groundwater.

Nitrogen is mainly incorporated into the soil as a nutrient through mineral fertilizers or manure, each of these sources accounting for nearly 50% of the N input into the European agricultural soils (EEA, 2012). However, other minor N sources such as the leakage of sewage from sewer networks in urban environments (Aravena and Mayer, 2010; Barroso et al., 2015; Sacchi et al., 2013; Vane et al., 2010) have been reported for groundwater.

Once in the soil, nitrogen is transformed through microbially mediated redox reactions (nitrogen fixation, nitrification, denitrification, dissimilatory NO_3^- reduction to ammonium, anammox; Borch et al., 2010). Nitrification represents the oxidation of nitrogen (under the form of ammonia) into nitrate. It frequently occurs in the unsaturated zone where oxygen is available and explains why most of the nitrogen that

reaches groundwater appears as NO_3^-. Denitrification is the transformation of nitrate into N_2(g). It is considered the main natural process attenuating nitrate concentration in groundwater. This requires the presence of denitrifying bacteria and electron donors (organic carbon, reduced sulphur and/or reduced iron), abundant presence of NO_3^- and an anaerobic environment (Koba et al., 1997; Rivett et al., 2008). Denitrification can be heterotrophic if linked to the oxidation of an organic compound (eq.1) or autotrophic, if linked to the oxidation of an inorganic compound, such as iron sulphide (eq.2).

$$4NO_3^- + 5CH_2O \rightarrow 2N_2 + 4HCO_3^- + CO_2 + 3H_2O \quad (1)$$

$$14NO_3^- + 5FeS_2 + 4H^+ \rightarrow 7N_2 + 10SO_4^{2-} + 5Fe^{2+} + 2H_2O \quad (2)$$

Dilution and dispersion are other processes that can result in a decrease of groundwater nitrate concentration, but contrarily to natural attenuation they do not lead to the mass-reduction of the contaminant within the aquifer.

Knowledge of both the sources of nitrogen contamination and the processes affecting nitrogen once in the aquifer is thus of the utmost importance to better design strategies to ultimately decrease nitrate pollution. The study of the isotope composition of nitrogen compounds has proved to be a viable tool to tackle both issues (e.g. Amiri et al. 2016; Vitòria et al. 2008). Denitrification reactions (eq.1 and 2) affect the isotope composition of the residual nitrate leading to an enrichment in its heavy isotopes ^{15}N and ^{18}O (Aravena and Robertson, 1998; Fukada et al., 2003; Kendall et al., 2007; Mariotti et al., 1988). The study of the $\delta^{15}N$ and $\delta^{18}O$ isotope compositions and nitrate concentrations (eq. 3 and 4) allow to determine the corresponding isotopic enrichment factor (ε), used to characterise the extension of the attenuation processes (Böttcher et al., 1990; Fukada et al., 2003; Mariotti et al., 1981). Also, as the initial NO_3^- isotope compositions differ between the different nitrate sources (inorganic fertilizers, manure, soil, …), the $\delta^{15}N$ and $\delta^{18}O$ compositions of nitrate have been used to identify its origin

in groundwater (Aravena et al., 1993; Aravena and Mayer, 2010; Clark and Fritz, 1997; Kendall et al., 2007; Panno et al., 2001).

$$\delta^{15}N_{residual} = \delta^{15}N_{initial} + \varepsilon_N \ln([NO_3^-]_{residual}/[NO_3^-]_{initial}) \quad (3)$$

$$\delta^{18}O_{residual} = \delta^{18}O_{initial} + \varepsilon_O \ln([NO_3^-]_{residual}/[NO_3^-]_{initial}) \quad (4)$$

However, in areas characterized by complex groundwater flow systems and exposed to multiple sources of nitrogen, the use of the sole $\delta^{15}N$ and $\delta^{18}O$ of NO_3^- and nitrate concentrations may result in not conclusive results.

To overcome this difficulty, as the redox transformations affecting nitrate also affect the electron donor, some authors have coupled $\delta^{15}N$ and $\delta^{18}O$ of NO_3^- data with the isotope composition of the electron donors or with other types of hydrochemical data, such as conservative elements (Xu et al., 2016). Some authors combined chloride concentration (a conservative element) with $\delta^{15}N$ and $\delta^{18}O$ of NO_3^- to identify nitrate sources and transformation processes (Silva et al. 2002, Vitòria et al. 2008). Some others used the $\delta^{34}S$ and $\delta^{18}O$ of sulphate or $\delta^{13}C_{HCO3}$ to evaluate if sulphide or organic matter oxidation processes could be linked to denitrification processes (Aravena and Robertson, 1998; Otero et al., 2009; Rock and Mayer, 2002; Saccon et al., 2013; Vitòria et al. 2005, 2008).

Moreover, in the last decade, some studies have also used the isotope composition of boron ($\delta^{11}B$) in combination with the $\delta^{15}N$ and $\delta^{18}O$ of NO_3^- to trace the origin of NO_3^- in water (Delconte et al., 2014; Komor, 1997; Saccon et al., 2013; Seiler, 2005; Widory et al., 2004, 2005, 2013). B is usually found in natural ground- and surface water as a minor constituent (<0.05 mg B L^{-1}) whereas contaminant sources are enriched in B (>0.1 mg B L^{-1}; Tirez et al., 2010). Besides the fact that groundwater affected by anthropogenic activities may present elevated B contents (Vengosh et al., 1994), $\delta^{11}B$ values are significantly discriminated between manure and wastewater. As

for nitrate isotopic composition, $\delta^{11}B$ of dissolved B can be modified by different processes. However, the processes that can shift B isotopic composition are aquifer matrix interaction (dissolution of B-bearing silicates) and adsorption-desorption interactions with clay minerals, iron and aluminium oxide surfaces, and/or organic matter (Yingkai and Lan, 2001). No effects on $\delta^{11}B$ composition are caused by volatilization and oxidation-reduction reactions (Bassett et al., 1995). Thus, the incorporation of $\delta^{11}B$ in the multi-isotope approach of nitrate polluted areas may be useful for a better identification of NO_3^- sources (manure or sewage), especially in semirural zones where agricultural and farming practices cohabitate with industrial and urban activities.

However, to our knowledge no study trying to combine these chemical/isotope approaches has ever been reported so far. Here, we aim at assessing the validity of a multi-parameter approach in which, besides the classical $\delta^{15}N$ and $\delta^{18}O$ of NO_3^-, hydrochemical data (e.g. Cl^- concentration), $\delta^{2}H$ and $\delta^{18}O$ of water, $\delta^{34}S$ and $\delta^{18}O$ of dissolved sulphate, $\delta^{13}C$ of HCO_3^- and $\delta^{11}B$ of dissolved B are used simultaneously to both identify the sources of contamination and to characterise processes affecting the nitrate budget of a given watershed. This study was undertaken in the Baix Ter aquifer (NE Spain), declared vulnerable to NO_3^- pollution in 1998 by the local government following the 91/676/EC European Nitrate Directive (EC, 1991). NO_3^- contents in groundwater exceeds the 50 mg NO_3^- L^{-1} threshold (ACA, 2007) due to the large amount of fertilizers used by local agriculture (Mas-Pla et al., 1998; Montaner et al. 2010) and pig raising practices that started in the 80's and intensified during the last decades (ACA, 2007; EEA, 1999). This aquifer is subjected to several anthropogenic pressures such as additional nitrate sources or groundwater exploitation that increases the complexity of the aquifer behaviour.

2. Study area

The Baix Ter basin is located in the Baix Empordà tectonic basin (NE Catalonia, Spain) (Fig. 1). The study zone encompasses a 200 km^2 area characterized by the Ter River alluvial plain delimited by the Montgrí Range to the north (Mesozoic limestone formations) and by the Gavarres Range to the south (Paleozoic igneous and metamorphic rocks) that turns into a fluvio-deltaic environment in its eastern margin. The foothills of the Gavarres Range, as well as the basin basement present Paleogene sedimentary materials (sandstone and limestone formations) that are severely affected by fractures (Mas-Pla and Vilanova, 2001).

The Baix Empordà basin was formed during the distensive period of the Alpine orogenesis. Detritic, fine-grained and silty formations were sedimented during the Neogene. The Quaternary fluvio-deltaic deposits originated from the Ter River as well as from some minor tributaries from the Gavarres Range (i.e., Daró River, Fig. 1). They constitute the main aquifers of the area, and lay on the Neogene sediments in the western area, and on the Paleogene in the eastern part of the basin. Fluvial deposits reach a maximum depth of 50-60 m in the central part of the basin and are constituted by three main distinguishable units according to the Holocene sedimentary sequence (Montaner et al. 2010): a deep level formed by alluvial coarse detritic material, gravel and sand; an intermediate level, formed by sandy lenticular bodies in a silty-sandy level; and a shallow level, mainly sandy formed by the present prograding alluvial deposits that transform into marsh and coastal deposits near the coast line.

Because of this lithological diversity, three distinct aquifer units are differentiated, from bottom to top: a leaky aquifer formed by the deeper coarse sediment layer, a leaky aquifer formed by the intermediate sandy layer, and an upper unconfined aquifer formed by the prograding deposits. All of them present significant lateral variations, especially

the upper aquifer that reflects the fluvio-deltaic, marsh and coastal areas presently occurring in the plain. These aquifer units are separated by loamy layers that constitute low permeability units that act as aquitards. Nevertheless, all three aquifer layers overlap in the westernmost part of the area, between Colomers and Verges.

According to Montaner et al. (2010) these aquifers are mainly recharged by local precipitation, seasonal contribution from the Ter and Daró rivers (whether natural or induced by pumping), and by irrigation returns. Moreover, igneous and metamorphic rocks at the Gavarres Range act as regional recharge areas that discharge into the fluvio-deltaic Quaternary aquifers through the preferential upward vertical flow paths of the limestone and carbonate Paleogene aquifers and, more importantly, through the fractures that affect them. Potentiometric, hydrochemical and isotope data indicate that these different aquifers are hydraulically connected (Vilanova et al., 2008).

Potentiometric maps reveal an influent (losing stream) behaviour of the Ter River in its western reach, between Colomers and Verges, and an effluent (gaining stream) behaviour of the Ter and Daró rivers downstream of Verges down to the coast line. However, intense groundwater withdrawal from these aquifers started in the 60's with the agricultural and touristic development of the area that modified the natural flow field causing a noticeable depression cone in the centre of the formation, between the villages of Gualta and Torroella de Montgrí (Fig. 1). This cone creates a downward flow from the upper unconfined aquifer, also capturing the Ter River discharge, which recharges the supply wells located in the lower aquifer levels. The total groundwater abstraction is around 21 hm^3/yr, from which 62% are for domestic use (including the touristic season), 36% for agriculture activities and 2% for the industry (ACA, 2007).

The Baix Ter basin area supports rural agriculture and livestock activities, industrial activities and several small to medium-sized urban areas that drastically increase their

population during summer due to their intense touristic activity. About 60% of the surface is covered by herbaceous dry-farmed and irrigated crops (mainly maize, sunflower and rice), 20% by forest and pasture and 7% by fruit growing (ACA, 2007).

The total nitrogen produced by livestock in the study zone is around 500 tons of N $year^{-1}$. 60% of this amount are from intensive pig rising (460 pigs/km^2; 50 m^3 ha^{-1} $year^{-1}$ of pig manure are applied onto maize crops; ACA, 2007). However, leakage from manure ponds or inappropriate spillages may also contribute to the increase of nitrogen, which is unassimilated by crops and incorporated into the saturated zone, ultimately raising NO_3^- concentrations in the groundwater. The "La Bisbal" water treatment plant discharges downstream of Daró River and produces mud that is eventually applied onto the fields, although some corrective measures were adopted to avoid wastewater spills.

3. Methodology

3.1. Sampling

Two sampling campaigns were conducted in the right bank alluvial plain of the Baix Ter basin in January 2004 (24 wells) and in August 2004 (40 wells) to cover both the wet season with fertilization and growing of dry land cereals and the dry season with cultivation of spring cereals, respectively.

All samples were taken from private wells supplied by the shallow Quaternary hydrogeological formation and the upper unconfined aquifer (Q_S), in the deep Quaternary formation and the lower unconfined aquifers (Q_D), and in the shallow (T_S) and deep (T_D) Tertiary formations located in the Paleogene materials (Fig.1). Most of the locations were sampled during both campaigns.

After measuring groundwater hydraulic head, wells were pumped until the water Eh stabilized. Then, temperature, pH and electrical conductivity (EC) were measured in situ and groundwater samples were collected in bottles that were previously rinsed several

times with groundwater. Samples were stored at 4ºC in a dark environment before analysis.

3.2. Analytical techniques

Temperature, pH, EC and Eh were measured using a flow cell to avoid contact with the atmosphere. Aqueous concentrations of chloride, nitrite, nitrate and sulphate were determined by high-performance liquid chromatography (HPLC), HCO_3^- aqueous concentration by volumetric titration, and total aqueous concentration of Na, K, Ca, Mg, Fe, Mn and B by inductive-coupled plasma optical emission spectrometry (ICP-OES). Ammonia aqueous concentration was determined by colorimetry (flow injection analysis), and total organic C (TOC) concentration by the organic matter combustion method. All these analyses were done at the Centres Científics i Tecnològics of the Universitat de Barcelona (CCiT-UB).

δ^2H and $\delta^{18}O$ of water were measured using the H_2 and CO_2 equilibration techniques respectively. H and O isotope compositions were measured by DI-IRMS on a Delta S Finnigan Mat. $\delta^{15}N$ and $\delta^{18}O$ of dissolved NO_3^- were measured using the $AgNO_3$ method (modified from Silva et al. (2000)) with an Elemental Analyser (Carlo Erba 1108) coupled with an Isochrom Continuous Flow IRMS in the case of $\delta^{15}N$ and with a Thermo-Chemical Elemental Analyser (TC/EA Thermo-Quest Finnigan) coupled with a Delta C Finnigan Mat IRMS in the case of $\delta^{18}O$ (duplicate analyses). To measure $\delta^{34}S$ and $\delta^{18}O$ of SO_4^{2-}, aqueous sulphate was precipitated as $BaSO_4$ by acidifying the sample with HCl, boiling it, and adding an excess of $BaCl_2 \cdot 2H_2O$. $\delta^{34}S$ was measured using an Elemental Analyser (Carlo Erba 1108) coupled with a Delta C Finnigan Mat, while $\delta^{18}O$ was measured with the same methodology (TC/EA-IRMS) as $\delta^{18}O$ of nitrate. In order to measure $\delta^{11}B$, sample volume was determined to ultimately yield 6 to 10 µg of B. Samples then underwent a two-step chemical purification using Amberlite

IRA-743 selective resin (method adapted from Gaillardet and Allègre (1995)). First, the sample (pH~7) was loaded on a Teflon PFA® column filled with a 1 ml resin, previously cleaned with ultrapure water and 2N ultrapure NaOH. After cleaning again the resin with water and NaOH, the purified B was collected with 15 ml of sub-boiled HCl 2N. After neutralisation of the HCl by Superpur NH_4OH (20%), the purified B was loaded again on a small 100 ml resin Teflon PFA® column. B was collected with 2 ml of HCl 2N. An aliquot corresponding to 2 mg of B was then evaporated below 70°C with mannitol ($C_6H_8(OH)_6$) in order to avoid B loss during evaporation (Ishikawa and Nakamura,1990). The dry sample was loaded onto a tantalum (Ta) single filament with graphite (C), mannitol and caesium (Cs). $\delta^{11}B$ was determined on the Cs_2BO^{2+} ion (Spivack and Edmond, 1986) by negative-ion Thermal-Ionization Mass Spectrometry (TIMS). The analysis was run in dynamic mode by switching between masses 308 and 309. Each analysis corresponded to 10 blocks of 10 ratios. Samples were always run twice. Total B blank was less than 10 ng corresponding to a maximum contribution of 0.2%, which was negligible. Seawater (IAEA-B1) was purified regularly in the same way, in order to check for a possible chemical fractionation due to an uncompleted recovery of B, and to evaluate the accuracy and reproducibility of the overall procedure. Reproducibility was obtained by repeated measurements of the NBS951 and the accuracy was controlled with the analysis of the IAEA-B1 seawater standard ($\delta^{11}B$ = 38.6±1.7‰). The $^{11}B/^{10}B$ ratio of replicate analyses of the NBS951 boric acid standard (after oxygen correction) was 4.05045±0.00130 (2σ, n=183). The reproducibility of the $\delta^{11}B$ was ±0.32‰ (2σ). The mean value obtained on $\delta^{11}B$ of seawater was 39.21±0.31‰ (2σ; n=20). In order to analyse the $\delta^{13}C$ of inorganic carbon, water samples were acidified with ortho-phosphoric acid and shaken for at least two hours to convert all bicarbonate into CO_2 and to reach equilibrium between the dissolved and

gaseous phases. Gas samples were then diluted with helium to facilitate the analysis. $\delta^{13}C$ was measured on a Gas Chromatograph-Combustion-Isotopic Ratio Mass Spectrometer (GC-C-IRMS). All isotope notations are expressed as δ per mil relative to their respective international standards: Vienna Standard Mean Ocean Water (V-SMOW), atmospheric N_2 (AIR), Vienna Canyon Diablo Troilite (V-CDT), NBS951 and Vienna Pee Dee Belemnite (V-PDB) standards. Reproducibility is ±1.5‰ for $\delta^{2}H$, ±0.2‰ for $\delta^{18}O_{H2O}$, ±0.3‰ for $\delta^{15}N$, ±0.2‰ for $\delta^{34}S$, ±0.5‰ for both $\delta^{18}O_{NO3}$ and $\delta^{18}O_{SO4}$, ±0.3‰ for $\delta^{11}B$, and ±0.3‰ for $\delta^{13}C_{HCO3}$.

For isotope analyses, samples were prepared at the laboratory of the Mineralogia Aplicada i Geoquimica de Fluids research group of the Universitat de Barcelona and the analyses were performed at the Centres Científics i Tecnològics of the Universitat de Barcelona (CCiT-UB), except those of $\delta^{11}B$ that were analysed at the BRGM (France) and those of $\delta^{13}C$ that were analysed at the Environmental Isotope Laboratory (EIL) of the University of Waterloo (Canada).

4. Results and discussion

Groundwater hydraulic head, hydrochemical and isotope data of the two campaigns are reported in Tables 1, 2 and 3.

4.1. Hydrodynamic data and potentiometric map

Hydraulic head measurements in the Quaternary aquifer conducted during the August campaign were used to draw the potentiometric contour lines shown in Fig.1, as this represents the largest pressure in the groundwater system resources. The generated potentiometric map shows that groundwater flow lines were mainly oriented along a south to north trend (from the Gavarres massif to the Ter River) (Fig. 1) although close to the Ter River, groundwater flow changed to a west-to-east direction towards the sea. The potentiometric map also reflects the depression cone of the Gualta village resulting

from the intense groundwater withdrawal activity of its supply wells. However, it was not possible to draw a consistent potentiometric plot of the Tertiary aquifer able to corroborate the upward vertical flow line connecting the underlying confined fractured Tertiary unit to the shallow Quaternary aquifer that was suggested by Vilanova et al. (2008). Potentiometric levels in the Tertiary aquifer may vary seasonally due to groundwater pumping, controlling the recharge relation with the Ter River alluvial aquifer.

4.2. δ^2H and $\delta^{18}O$ data. Sources of recharge

Fig. 2 shows that δ^2H and $\delta^{18}O$ of groundwater samples from both campaigns mostly plot under the annual Local Meteoric Water Line LMWL (Vilanova et al., 2008).

However, the wide range of δ^2H and $\delta^{18}O$ values from the Quaternary aquifer indicates the implication of several recharge flow systems affecting the aquifer. Some of the samples fall very close to the weighted mean precipitation (δ^2H = -33.5‰, $\delta^{18}O$ = -5.2‰) calculated from the Mas Badia station data (located in the Baix Ter basin; Fig. 2) showing the influence of the infiltration of rainfall into the basin. Samples located at the NW of the shallow Quaternary aquifer (Q_7, Q_8 and Q_{12}) yielded lighter isotope compositions with values similar to those of the Ter River reported by Vilanova (2004; δ^2H from -50 to -45‰, $\delta^{18}O$ from -8 to -7‰), indicating a contribution from the Ter River to the alluvial aquifer groundwater. Finally, other samples from the Quaternary aquifer present δ^2H and $\delta^{18}O$ compositions intermediate between those influenced by the rainfall and those influenced by the Ter river water (Fig. 2) but also close to those of sample T_{21}, located in the Gavarres massif foothill (south of the study area, Fig. 1). Thus, these samples can be geochemically and isotopically considered as representative of the recharge from the Gavarres massif, given its very low mineralization and its isotope composition (Fig.2). As irrigation demand is fully covered by groundwater in

the sampled area, the potential effects of irrigation returns on groundwater isotopic composition would not in any case modify the recharge model herein proposed.

In Tertiary aquifers, most of the groundwater samples fell between the weighted mean precipitation signature and the isotope composition of groundwater from the Gavarres massif (Fig. 2). They present a narrower range of δ^2H and $\delta^{18}O$ compositions, although they overlap with the intermediate isotopic composition of the Quaternary aquifer groundwater samples (Fig. 2). This overlap suggests that both aquifers share a common source of recharge or are somehow connected. This is consistent with the conceptual model described by Vilanova et al. (2008) in which an upward groundwater flow was proposed connecting the Tertiary aquifer to the deep Quaternary aquifer in the northern part of the area. Therefore, the contribution from the Tertiary units towards the Quaternary aquifer cannot be discarded despite the fact that this could not be supported by the potentiometric map.

4.3. Hydrochemical data

Chemical data for groundwater samples collected in the Baix Ter basin (Tables 1 and 2) showed a HCO_3^--Ca^{2+}-Mg^{2+} facies, in accordance with the hydrochemistry being controlled by carbonate dissolution reactions that occur throughout the Tertiary materials and alluvial formations. The rapid kinetic of carbonate dissolution hides the hydrochemical characteristics acquired from the igneous and metamorphic rocks of the Gavarres massif (Vilanova et al., 2008). Groundwater pH values were all above 7.4, HCO_3^- concentrations were between 177 and 619 mg L^{-1} and EC varied from 552 μS cm^{-1} to 2993 μS cm^{-1}.

In all the studied area, NO_3^- concentrations presented a wide range of values from below the detection limit (0.1 mg L^{-1}) to concentrations up to 480 mg L^{-1}. 60% of the studied samples had NO_3^- levels above the legal threshold of 50 mg L^{-1} for drinking

water (EC, 1998). No NO_2^- was detected. Ammonium concentration ranged between 0.08 mg L^{-1} and 0.47 mg L^{-1}. It can be observed that NO_3^- concentrations of the river samples presented values of 9 and 7 mg L^{-1}, consistent with surface water nitrate values and lower than the monthly NO_3^- average for the Ter River (15 mg L^{-1}; $\sigma = 5.1$, $n = 37$) between 2003 and 2006 (ACA, 2015). However, nitrate concentration in aquifers showed a diffuse spatial distribution. In shallow aquifers (Q_S and T_S), nitrate concentrations ranged from 6 to 480 mg L^{-1}, while in deeper aquifers they went from values below detection limit up to 265 mg L^{-1}. This distribution does not seem to be linked to any specific groundwater flow direction nor limit of the aquifer units. It can be explained by the highly complex hydrogeology of the study zone and its distinct recharge areas, and by the mixing of waters from distinct origins and qualities within the well borehole. Several factors such as the intended exploitation of different levels to increase the well efficiency, the possible lack of well casing derived from an incomplete borehole construction, and/or the presence of preferential flow paths through fractures or fault zones that connect local and regional flow systems, i.e. Quaternary and Tertiary aquifers could account for the mixing of waters. Moreover, the intensive pumping during irrigation and low rainfall periods can also enhance re-circulation between aquifer levels, mainly from the shallow to deeper ones, resulting in a decrease of the quality of the water resources stored in the deeper aquifer layers.

The lowest NO_3^- contents in the Quaternary aquifer were observed near the Ter River suggesting some influence from induced stream recharge; and in the SE area, near the Gavarres Range, in the Tertiary aquifer.

During the first sampling campaign, two samples from the shallow Quaternary aquifer (Q_4 and Q_8, Table 2) presented NO_3^- concentrations of 6 mg L^{-1} and 13 mg L^{-1}, respectively, coupled with high levels of Mn (4.4 and 0.8 mg Mn L^{-1}) and around 2 mg

L^{-1} of total organic carbon. Two samples in the Q_D (Q_1 and Q_2) and three samples in T_D aquifers (T_9, T_{10} and T_{14}) had NO_3^- below detection limit, an Eh value below 200 mV and showed the highest ammonium and manganese concentrations (Tables 1 and 2, Fig.3). Moreover, NO_3^- in Q_2 has been monitored through time and has always been below detection limit. These characteristics are typical of groundwater under reducing conditions, and would suggest that they are undergoing denitrification processes. However, measured TOC concentrations for Q_1, Q_2, T_9, T_{10} and T_{14} (between 0.4 and 1.2 mg L^{-1}) are not high enough to stoichiometrically allow the reduction of NO_3^- by oxidation of organic matter in anaerobic conditions (Rivett et al., 2008), but they may indicate the presence of organic matter that could represent a residual content after previous consumption by heterotrophic denitrifying bacteria.

Some samples with high NO_3^- concentration (Q_5, Q_{10}, Q_{15} and Q_{16} from Q_S, T_{17} and T_{20} from T_S, and T_3, T_5 and T_8 from T_D) also presented high sulphate and chloride concentrations (up to 371 and 362 mg L^{-1}, respectively) (Fig. 4a, b). Considering that Cl^- is a conservative element largely unaffected by physical, chemical and microbiological processes occurring in the groundwater (Altman and Parizek, 1995), the $[NO_3^-]/[Cl^-]$ ratio can be used to eliminate the potential effect of dilution. In Fig. 4c, sulphate concentration is plotted against the $[NO_3^-]/[Cl^-]$ ratio. Groundwater SO_4^{2-} varied between 29 and 371 mg L^{-1}, with an average value of 108 mg L^{-1} (n = 64). But a set of samples, with $1<[NO_3^-]/[Cl^-]<2$, present moderate SO_4^{2-} concentrations but also high NO_3^- and consequently high Cl^- concentrations. Samples with $[NO_3^-]/[Cl^-]>2$ had high NO_3^- but lower SO_4^{2-} concentrations (Fig. 4c).

Since no evaporitic or gypsum outcrops nor disseminated pyrite exist in the study area, these SO_4^{2-} concentrations must originate from anthropogenic sources such as manure, synthetic fertilizers or sewage. High Cl^- concentrations can be caused by the

input of organic fertilizers since they generally show elevated chloride concentrations (Karr et al., 2001; Menció et al. 2016). All these observations suggest that both the mineral and the organic fertilizers are the major vectors of contamination.

In most of samples, B concentration was below the detection limit. However, B concentrations around 0.1-0.2 mg L^{-1} have been measured in samples with high nitrate, sulphate and chloride concentrations (e.g. Q10 and Q15, Fig. 4d) suggesting sewage and manure as other potential contamination sources. However, as seen in Fig. 4d, samples with the highest B concentration (up to 232 μg/L) presented intermediate nitrate concentrations (25-45 mg NO_3^- L^{-1}), showing that the presence of B in groundwater is not necessarily linked to high NO_3^- concentrations.

Thus, our results show that groundwater is probably affected by more than one source of contamination and that natural denitrification may be acting in some areas. However, the unambiguous identification of these sources and processes based on the sole hydrochemical data is somewhat difficult as the signal may be hindered by the mixing of groundwaters from different layers and recharge flow systems.

4.4. Isotope data. Pollution sources and attenuation processes

4.4.1. $\delta^{15}N$ and $\delta^{18}O$ of NO_3^-

NO_3^- isotope composition in groundwater ranged between +5.0 and +32.5‰ for $\delta^{15}N$, with an average value of +13.0‰ (n = 58), and between +1.8 and +18.1‰ for $\delta^{18}O$, with an average value of +7.1‰ (n = 58) (Table 3).

As seen in Fig. 5a, five groundwater samples (Q_{14} and Q_{16} from Q_S, T_3 from T_D, and T_{18} and T_{21} from T_S) presented $\delta^{15}N$ values compatible with soil organic nitrogen (from +3 to +8‰), fertilizers (-4 to +8‰) and sewage (+5 to +20‰) (Table 4). Within these samples, only sample T_{21} presented low nitrate, sulphate and chloride concentration (6 mg L^{-1} NO_3^-, 36 mg L^{-1} Cl^- and 30 mg L^{-1} SO_4^{2-}). The low $\delta^{15}N$

(+5.0‰) measured in sample T_{21}, coupled with its $\delta^{2}H$ and $\delta^{18}O$, that are similar to those of the Gavarres massif (Fig. 2), indicate that the NO_3^- for these samples is consistent with a natural soil origin. T_{21} represents thus the local NO_3^- background. However, as for samples Q_{14}, Q_{16}, T_3, and T_{18}, nitrate contents range from 65 to 222 mg L^{-1}. The origin of NO_3^- for these samples cannot be solely attributed to the mineralization of soil nitrogen (as in T_{21}) which cannot explain such high concentrations.

Therefore, although a small contribution of soil organic nitrogen is possible (Wassenaar, 1995) measured isotope values may originate from synthetic fertilizers or sewage/manure sources or from a mixing of both (Fig. 5a).

Most of the samples presented $\delta^{15}N$ ranging between +8 and +16‰, indicating that NO_3^- may originate from ^{15}N-enriched anthropogenic organic matter (manure or sewage) (Fig. 5a). Finally, some samples (Q_4, Q_8 and Q_9, from Q_S, and T_2 from T_D) presented $\delta^{15}N$ values higher than +16‰,coupled to low NO_3^- contents (between 6 and 26 mg L^{-1}, Table 2) and high $\delta^{18}O_{NO3}$ values (close to +10‰). The range of $\delta^{18}O$ of NO_3^- for NH_4^+ fertilizers, soil nitrogen and manure and sewage provided in Table 4 and plotted in Fig. 5a (+3.4‰ to +4.6‰), has been estimated according to eq. 5 (Anderson and Hooper, 1983; Hollocher, 1984; Kendall et al., 2007), where the $\delta^{18}O_{H2O}$ values are the highest and lowest groundwater $\delta^{18}O$ measured in the Baix Ter basin, and the $\delta^{18}O_{O2}$ is that of the atmospheric O_2 (+23.5‰; Horibe et al., 1973).

$$\delta^{18}O_{NO3} = 2/3(\delta^{18}O_{H2O}) + 1/3(\delta^{18}O_{O2}) \quad (5)$$

$\delta^{18}O_{NO3}$ values measured in the groundwater samples ranged from +1.8‰ to +18.1‰ (Fig.5b). While nitrate fertilizers are currently applied onto local crops their direct contribution to groundwater nitrate must be discarded as $\delta^{18}O$ and $\delta^{15}N$ of groundwater NO_3^- fall very far from nitrate fertilizers values (Fig. 5a). Moreover, most

of samples had $\delta^{18}O_{NO3}$ higher than the calculated values for full equilibrium with the $\delta^{18}O$ of groundwater. Both results could be interpreted as a consequence of three different processes: i) the mineralization-immobilization-turnover (MIT) process, ii) the higher consumption of NO_3^- from mineral fertilizers compared to that of ammonium in the root zone and iii) the reduction of NO_3^- via denitrifying bacteria. The MIT process consists of a microbial-mediated immobilization of nitrate N as organic nitrogen, the subsequent mineralization of this organic nitrogen to ammonium, and finally the nitrification of this ammonium back to NO_3^- (Mengis et al., 2001). This turnover process results in an important ^{18}O depletion of the initial $\delta^{18}O_{NO3}$ of the synthetic fertilizers (+17‰ to +20‰, Table 4). As synthetic fertilizers are currently used in the area, MIT process must be very active in order to explain why our results do not show the low $\delta^{15}N$ and high $\delta^{18}O$ values of nitrate from synthetic fertilizers. This indicates all NO_3^- from synthetic fertilizers that infiltrated underwent this process and that this source cannot be dismissed.

As pig manure is mainly liquid, the infiltration of ammonium from manure through the non-saturated zone to the saturated one is faster than that of nitrate from solid synthetic fertilizers, which need to be dissolved by rain or irrigation. Ammonium soil sorption capacity can be considered negligible as the soil is already saturated due to the long-standing fertilization practices affecting the area. Ammonium is also fast and completely nitrified into nitrate in the non-saturated zone. All these elements favour ammonium from pig manure to reach the saturated zone polluting groundwater. On the contrary, nitrate from synthetic fertilizers remains on the agricultural soil, incorporated and stored in the soil organic matter pool by means of the MIT process. It could then be slowly rereleased for either uptake by crops or export into the hydrosphere (Sebilo et al., 2013). Finally, the reduction of NO_3^- via denitrifying bacteria, which is characterized by

a heavy-isotope enrichment of both the $\delta^{15}N$ and $\delta^{18}O$ of the residual nitrate, can overprint the mixing of potential end-members and can significantly alter both the NO_3^- concentration (i.e. attenuation) and corresponding N and O isotope compositions. $\delta^{15}N$ and $\delta^{18}O$ of NO_3 from the Ter River samples were in agreement with a wastewater origin.

Ten of the samples had $\delta^{18}O_{NO3}$ and $\delta^{15}N$ higher than +8‰ and +15‰, respectively. Fig. 5a shows that these samples roughly aligned following a $\varepsilon_N:\varepsilon_O$ ratio of 2, consistent with natural denitrification (Kendall et al., 2007). This means that the nitrate isotopic compositions but also the low nitrate concentration measured in those samples result from natural denitrification processes occurring in the aquifers. This is confirmed by Fig. 5b, in which a negative linear correlation between $\delta^{18}O_{NO3}$ and $\ln(NO_3^-/Cl^-)$ is observed for these samples, indicating that denitrification is taking place (Vitòria et al. 2008). The highest denitrified samples (i.e. with the higher coupled $\delta^{18}O_{NO3}$ and $\delta^{15}N$) were observed either in the shallow Quaternary levels near the Ter River (Q_4, Q_8, Q_9) or in the Tertiary aquifers (T_2). Moreover, the NO_3^- concentration measured below the detection limit in the samples Q_1, Q_2, T_9, T_{10} and T_{14} (Fig. 2) can also be interpreted as resulting of natural denitrification. Considering that no significant variations were identified in both the isotope and chemical compositions of our samples between both campaigns, it can be inferred that natural denitrification had a moderate activity and/or that NO_3^- attenuation was balanced by the input of new NO_3^- into the aquifer.

4.4.2. $\delta^{34}S$ and $\delta^{18}O$ of SO_4

SO_4^{2-} isotope compositions ranged between -16.0 and +14.7‰ for $\delta^{34}S$, with an average value of +4.5‰ (n = 64), and between +3.8 and +16.1‰ for $\delta^{18}O_{SO4}$, with an average value of +7.2‰ (n = 64) (Table 3, Fig. 6). Most of the groundwater samples fall within the area defined by the isotope signatures of local anthropogenic sources (Table

4) showing that SO_4^{2-} in the Baix Ter groundwater can be explained by a ternary mixing between: 1) mineral fertilizers, 2) sewage and 3) pig manure (Fig. 6). This comforts the conclusions from the study of sulphate and nitrate groundwater concentrations.

Still, the $\delta^{34}S$ and a $\delta^{18}O_{SO4}$ values measured between 0 and +6‰ of samples Q_{17}, T_{11}, T_{18} and T_{21} could indicate a soil origin (Table 4), in agreement with their low SO_4^{2-} concentrations (around 30 mg SO_4^{2-} L^{-1}).

Two sampling sites (T_2 and T_{14}) yielded the lowest negative $\delta^{34}S$ values and had $\delta^{18}O_{SO4}$ around +5‰, revealing a SO_4^{2-} contribution from a ^{34}S-depleted source of reduced S (Fig. 6). Moreover, both T_2 and T_{14} showed very low (9 mg L^{-1}) or below detection limit (0.1 mg L^{-1}) nitrate concentrations, respectively. On the contrary, samples Q_1, Q_2, T_9 and T_{10}, with nitrate concentration below the detection limit (0.1 mg L^{-1}) exhibited the highest $\delta^{34}S$ and $\delta^{18}O_{SO4}$ values (+14.7‰ and +16.1‰ respectively).

All these samples in which nitrate concentration is below detection limit, together with other samples with very low nitrate aqueous concentration (NO_3^- < 25 mg L^{-1}) and $\delta^{18}O_{SO4}$ higher than +8‰ define a linear trend with $\varepsilon_S/\varepsilon_O$ = 1/0.31=3.2 compatible with a bacteriogenic reduction of SO_4^{2-} (Mizutani and Rafter, 1973) (Fig. 6). This is consistent with their corresponding low Eh values and high Mn concentrations (Fig. 3). However, as the presence of pyrite and gypsum in the area is scarce, autotrophic denitrification can be discarded as the main denitrifying process occurring in the study zone.

$\delta^{34}S$ and $\delta^{18}O_{SO4}$ of the Ter River samples also indicated, in agreement with their $\delta^{15}N$ and $\delta^{18}O_{NO3}$ that the dissolved SO_4^{2-} in surface waters originated from wastewater.

4.4.3. $\delta^{11}B$

Boron isotopes measurements were performed in 12 groundwater samples, selected considering both their NO_3^- and B contents and their location in the vicinity of pig farms or urban areas with the aim of discriminating between these two origins.

Pig manure present $\delta^{11}B$ values ranging from +19.5‰ to +42.4‰, significantly higher than urban wastewater values that range from -7.7‰ to +12.9‰ (Table 4). However, mineral fertilizers are characterized by a $\delta^{11}B$ range similar to sewage (-9‰ to +15‰, Table 4). Although mineral fertilizers can present a wide range of B concentrations they usually have lower B contents compared pig manure (Fig. 7a).

$\delta^{11}B$ composition of dissolved B in selected groundwater samples ranged between +1.4‰ and +34.5‰, with an average value of +24.1‰ (n = 12). B concentrations in these samples ranged between 0.055 and 0.232 mg L^{-1}. No trends or enrichment in $\delta^{11}B$ composition of dissolved B with decreasing B content were observed (Fig. 7a), indicating that B is not explained by binary mixing relationships and that no significant sorption/desorption processes of B onto/from clay minerals are occurring. Most samples fell in the isotope range of pig manure (Fig. 7a and 7b). This is in agreement with the conclusions drawn from the NO_3^- and SO_4^{2-} isotope data. Two of the samples showed $\delta^{11}B$ values consistent with a wastewater origin. They correspond to groundwater collected in La Bisbal (Q_{20}) and Ullastret (Q_{21}) water supply wells (Fig. 1), located downstream the discharge of the La Bisbal water treatment plant into the Daró River.

Boron analyses, thus, suggest that pig manure is the main source of contamination and that the influence of sewage and mineral fertilizers is lower than the contribution from organic residues.

4.4.4. $\delta^{13}C$ of HCO_3^-

Samples presented $\delta^{13}C_{HCO3}$ values between -6.5‰ and -16.2‰ (Table 3). $\delta^{13}C_{HCO3}$ values of marine marls in the study zone are $\delta^{13}C \sim 0$‰. Typical $\delta^{13}C$ values for CO_2

dissolved in the soil are between -14‰ and -16‰; for soil HCO_3^- $\delta^{13}C$ values are around -23‰ and for pig manure, mineral fertilizers and sewage, $\delta^{13}C$ values range from -23.8‰ to -16.4‰, from -35‰ to -24‰ and from -25‰ to -13‰, respectively (Table 4).

Denitrification catalysed by organic matter oxidation induces a decrease in NO_3^- and in total organic carbon concentrations coupled with an increase in dissolved inorganic carbon concentration (eq.1), causing an increase of $\delta^{15}N$ and $\delta^{18}O_{NO3}$ and a decrease in $\delta^{13}C_{HCO3}$ (Faure, 1977).

Fig. 8a shows the evolution of the $\delta^{18}O_{NO3}$ as a function of $\ln(NO_3^-/HCO_3^-)$. A slight increase in $\delta^{18}O_{NO3}$ coupled to a decrease in $\ln(NO_3^-/HCO_3^-)$ can be observed that would suggest that denitrification may occur. Nevertheless, we were not able to observe the corresponding decrease in $\delta^{13}C_{HCO3}$ in our results (Fig. 8b). As already discussed porewaters presented HCO_3^--Ca^{2+}-Mg^{2+} facies, with saturation indices for Ca-Mg-carbonates between -1 and 1. This indicates that bicarbonate is in equilibrium with Ca-Mg-carbonates whose dissolution and precipitation will contribute to the buffering of the $\delta^{13}C_{HCO3}$ of our samples with a final isotope composition corresponding to sedimentary rocks ($\delta^{13}C$ around 0 ‰ after Travé et al., 1997). Besides these dissolution/precipitation reactions, $\delta^{13}C_{HCO3}$ can be also affected by other reactions such as equilibrium with $CO_2(g)$ and other sources such as manure or sewage (Clark and Fritz, 1997).

5. Conclusions

Here we have coupled the study of hydrochemical and multi-isotope data with hydrogeological framework information to identify the sources and to characterise processes controlling the budget of dissolved NO_3^- in ground- and surface water in a complex hydrogeological system (the Baix Ter basin).

Isotope data have shown that the sources of recharge for both the Tertiary and the Quaternary aquifers are the rainfall, the Ter River in the NW and a contribution from Les Gavarres Massif. Moreover, they showed that dissolved NO_3^- in groundwater in the study area mainly comes from pig manure application onto the fields, with minor contributions from sewage and mineral fertilizers. The study of $\delta^{11}B$ confirmed pig manure as the main vector of pollution but also identified an urban origin for two of the analysed wells. The dual-isotope ($\delta^{15}N$ and $\delta^{18}O$ of NO_3) approach indicated that mineralization-immobilization-turnover (MIT) and natural denitrification processes are occurring within the study area. The $\delta^{34}S$ and $\delta^{18}O$ of SO_4^{2-} showed that NO_3^- reduction is not controlled by the oxidation of pyrites but rather by the oxidation of organic matter. However, the role of organic matter in NO_3^- attenuation could neither be confirmed nor discarded by the study of the $\delta^{13}C_{HCO3}$ as other processes and sources ultimately buffered these isotope compositions. The consumption of organic matter in anaerobic environments is favoured by 1) the river-aquifer connection, 2) the existence of some organic layers in the Ter riversides, and 3) mixing between polluted groundwater and deep regional flows with reducing conditions.

Since the role of organic matter in the NO_3^- reduction is still an on-going research, further studies on the $\delta^{13}C$ of local contaminant sources and on the role of MnO_2 should be further investigated. Even if working with samples from exploitation wells, it has been proved that multi-isotope studies allow us to: i) describe groundwater dynamics, ii) discriminate between sources of pollution and determine their relative contribution, iii) characterise the processes affecting the overall nitrogen budget, such as natural attenuation, that in another way would go unnoticed. Still, these approaches highly depend on the knowledge of the isotopic signatures of the different potential sources of

nitrate contamination of a given area, on the complexity of the aquifers complex and on the availability of a good infrastructure (e.g. multi-piezometers).

Acknowledgements

This research was funded by the ATENUATION (CGL2011-29975-C04-01) and REMEDIATION (CGL2014-57215-C4-1-R) projects from Spanish Ministry of Economy and Competitiveness (MINECO) and the AGAUR from the Catalan Government (grant 2014SGR-1456). We would like to thank the Centres Científics i Tecnològics of the Universitat de Barcelona for its laboratory help. Authors acknowledge the fruitful comments of the three anonymous reviewers.

References

ACA, 2007. Diagnosis de la causalidad de la contaminación por nitratos de algunos abastecimientos públicos en las zonas vulnerables de Cataluña, análisis de alternativas, medidas de prevención y corrección. Área vulnerable 1 Girona. Estudio 1: Llanura aluvial de los ríos Ter y Daró, provincia de Girona. ACA (Water Catalan Agency) Internal Report. 168 pp.

ACA, 2015. Agència Catalana de l'Aigua. Generalitat de Catalunya. Consulta de dades. Available at: http://aca-web.gencat.cat/aca/appmanager/aca/aca/ (June 2016).

Altman, S.J., Parizek, R.R. 1995. Dilution of non-point source nitrate in ground water. J. Environ. Qual. 24, 707-718.

Amiri, H., Zare, M., Widory. D., 2015. Assessing sources of nitrate contamination in the Shiraz urban aquifer (Iran) using the $\delta^{15}N$ and $\delta^{18}O$ dual-isotope approach. Isotopes in Environmental and Health Studies. DOI: 10.1080/10256016.2015.1032960.

Anderson, K. K., Hooper, A. B., 1983. O_2 and H_2O are each the source of one O in NO_2^- produced from NH_3 by Nitrosomas-^{15}N-NMR evidence. FEBS Letters, 64, 236–40.

Aravena, R., Evans, M.L., Cherry, J.A., 1993. Stable isotopes of oxygen and nitrogen in source identification of nitrate from septic tanks. Ground Water, 31, 180–186.

Aravena, R., Robertson, W.D., 1998. Use of Multiple Isotope Tracers to Evaluate Denitrification in Ground Water: Study of Nitrate from a Large-Flux Septic System Plume. Ground Water, 36, 975-982.

Aravena, R., Mayer, B., 2010. Isotopes and Processes in the Nitrogen and Sulfur Cycles. In: Aelion, C.M., Höhener, P., Hunkeler, D., Aravena, R. (Eds.),

Environmental Isotopes in Biodegradation and Bioremediation. CRC Press, pp. 203–246.

Barroso, M.F., Ramalhosa, M.J., Olhero, A., Antão, M.C., Pina, M.F., Guimarães, L., Teixeira, J., Alfonso, M.J., Delerue-Matos, C., Chaminé, H.I., 2015. Assessment of groundwater contamination in an aricultural peri-urban area (NW Portugal): an integrated approach. Environ Earth Sci 73, 2881-2894.

Basset, R.L., Buszka, P.M., Davidson, G.R., Chong-Diaz, D., 1995. Identification of groundwater solute sources using boron isotopic composition. Environ. Sci. Technol. 29, 2915–2922.

Borch, T., Kretzschmar, R., Kappler, A., Van Cappellen, P., Ginder-Vogel, M., Voegelin, A., Campbell, K., 2010. Biogeochemical Redox Processes and their Impact on Contaminant Dynamics. Environmental Science and Technology, 44, 15–23.

Böttcher, J., Strebel, O., Voerkelius, S., Schmidt, H.L., 1990. Using isotope fractionation of nitrate-nitrogen and nitrate-oxygen for evaluation of microbial denitrification in sandy aquifer. Journal of Hydrology, 114, 413-424.

Bryan, N.S., Alexander, D.D., Coughlin, J.R., Milkowski, A.L., Boffetta, P., 2012. Ingested nitrate and nitrite and stomach cancer risk: An updated review. Food and Chemical Toxicology, 50, 3646–3665.

Clark, I.D., Fritz, P., 1997. Environmental Isotopes in Hydrogeology. Lewis Publishers, New York. 352 pp.

Cravotta, C.A., 1997. Use of Stable Isotopes of Carbon, Nitrogen and Sulphur to Identify Sources of Nitrogen in Surface Waters in the Lower Susquehanna River Basin, Pennsylvania. U.S. Geological Survey Water-Supply Paper 2497.

Curt, M.D., Aguado, P., Sánchez, G., Bigeriego, M., Fernández, J., 2004. Nitrogen isotope ratios of synthetic and organic sources of nitrate water contamination in Spain. Water, Air and Soil Pollution, 151, 135-142.

Delconte. C.A., Sacchi, E., Racchetti, E., Bartoli, M., Mas-Pla, J., Re, V., 2014. Nitrogen inputs to a river course in a heavily impacted watershed: a combined hydrochemical and isotopic evaluation (Oglio River Basin, N Italy). Science of the Total Environment 466-467, 924-938, DOI: 10.1016/j.scitotenv.2013.07.092.

EC (European Communities), 1991. Council Directive 91/676/EC, of 12 December 1991, concerning the protection of waters against pollution caused by nitrates from agricultural sources.

EC (European Communities), 1998. Council Directive 98/83/EC, of 3 November 1998, on the quality of water intended for human consumption.

EC (European Communities), 2000. Directive 2000/60/EC of the European Parliament and of the Council establishing a framework for the Community action in the field of water policy (Water Framework Directive). Official Journal of the European Communities, OJ L 327.

EC (European Communities), 2006. Directive 2006/118/EC of the European Parliament and of the Council on the protection of groundwater against pollution and deterioration (Groundwater Directive). Official Journal of the European Communities, OJ L 372.

EEA (European Environment Agency), 1999. Nutrients in European Ecosystems. Environmental assessment report Nº 4.

EEA (European Environment Agency), 2012. European waters: assessment of status and pressures. EEA Report Nº 8. Published: Nov 13, 2012. Copenhagen, Denmark.

EEA (European Environment Agency), 2015. Nutrients in freshwater. Indicator assessment. Data and maps. IND-8-en. CSI 020, WAT 003. Published: Sep 4th, 2015. Copenhagen, Denmark. Available as a website at http://www.eea.europa.eu/data-and-maps/indicators/nutrients-infreshwater/nutrients-in-freshwater-assessment-published-6.

Faure, G. 1997. Principles of isotope geology, Wiley, 2nd Ed, 589 pp.

Fukada, T., Hiscock, K., Dennis, P.F., Grischek, T., 2003. A dual isotope approach to identify denitrification in groundwater at a river-bank infiltration site. Water Res. 37, 3070–3078.

Gaillardet, J., Allègre, C.J., 1995. Boron isotopic compositions of corals: Seawater or diagenesis record? Earth and Planetary Science Letters 136, 665-676.

Heaton, T.H.E., 1986. Isotopic studies of nitrogen pollution in the hydrosphere and atmosphere: a review. Chem. Geol. 59, 87–102.

Hollocher, T. C., 1984. Source of oxygen atoms in nitrate in the oxidation of nitrite by *Nitrobacter agilis* and evidence against a P-O-N anhydride mechanism in oxidative phosphorylation. Archives of Biochemistry and Biophysics, 233, 721–27.

Horibe, Y., Shigehara, K., Takakuwa, Y., 1973. Isotope separation factors of carbon dioxide-water system and isotopic composition of atmospheric oxygen. Journal of Geophysical Research, 78, 2625-2629.

Ishikawa, T., Nakamura, E., 1990. Suppression of boron volatilization from a hydrofluoric acid solution using a boron-mannitol complex. Analytical Chemistry 62, 2612–2616.

Jurado, A., Vàzquez-Suñé, E., Soler, A., Tubau, I., Carrera, J., Pujades, E., Anson, I., 2013. Application of multi-isotope data (O, D, C and S) to quantify redox processes in urban groundwater. Applied Geochemistry, 34, 114–125.

Karr, J.D., Showers, W.J., Wendell Gilliam, J., Scott Andres, A., 2001. Tracing nitrate transport and environmental impact from intensive swine farming using delta nitrogen-15. J. Environ. Qual. 30, 1163–1175.

Kendall, C., Elliott, E.M., Wankel, S.D., 2007. Tracing anthropogenic inputs of nitrogen to ecosystems, Chapter 12. In: R.H. Michener and K. Lajtha (Eds.), Stable Isotopes in Ecology and Environmental Science, 2nd edition, Blackwell Publishing, pp. 375-449.

Koba, K., Tokuchi, N., Wada, E., Nakajima, T., Iwatsubo, G., 1997. Intermittent denitrification: the application of a ^{15}N natural abundance method to a forested ecosystem. Geochim. Cosmochim. Acta, 61, 5043–5050.

Komor, S.C., 1997. Boron contents and isotopic compositions of hog manure, selected fertilizers, and water in Minnesota. J. Environ. Qual. 26, 1212–1222.

Krouse, H.R., Mayer, B., 2000. Sulphur and oxygen isotopes in sulphate. In: Cook, P.G., Hercseg, A.L. (Eds.), Environmental Tracers in Subsurface Hydrology. Kluwer Academic Press, Boston, pp. 195–231.

Li, X.D., Liu, C.Q., Harue, M., Li, S.L., Liu, X.L., 2010. The use of environmental isotopic (C, Sr, S) and hydrochemical tracers to characterize anthropogenic effects on karst groundwater quality: A case study of the Shuicheng Basin, SW China. Applied Geochemistry, 25, 1924–1936.

Mariotti, A., Germon, J.C., Hubert, P., Kaiser, P., Letolle, R., Tardieux, P., 1981. Experimental determination of nitrogen kinetic isotope fractionation: some

principles, illustration for the denitrification and nitrification processes. Plant Soil, 62, 413–430.

Mariotti, A., Landreau, A., Simon, B., 1988. ^{15}N isotope biogeochemistry and natural denitrification process in groundwater: application to the chalk aquifer of northern France. Geochim. Cosmochim. Acta, 52, 1869–1878.

Mas-Pla, J., Bach, J., Montaner J., 1998. Distribución de la concentración de nitratos en el sistema hidrogeológico Baix Ter-Gavarres (Girona). In: La contaminación de las aguas subterráneas: Un problema pendiente. ITGE-AIH, pp. 139–145.

Mas-Pla, J., Vilanova, E., 2001. Dinámica del sistema hidrogeológico Baix Ter-Gavarres en base a isótopos estables. In: IGME, Las Caras del Agua, Serie Hidrogeología y Aguas Subterráneas n. 1/2001, tomo I, pp. 395-402.

Menció, A., J. Mas-Pla, A. Soler, N. Otero, O. Regàs, M. Boy-Roura, R. Puig, J. Bach, C. Domènech, A. Folch, M. Zamorano, D. Brusi (2016). Nitrate pollution of groundwater; all right …, but nothing else? Science of the Total Environment, 539C: 241-251. DOI: 10.1016/j.scitotenv.2015.08.151

Mengis, M., Walther, U., Bernasconi, S.M., Wehrli, B., 2001. Limitations of using $\delta^{18}O$ for the source identification of nitrate in agricultural soils. Environ. Sci. Technol. 35 (9), 1840–1844.

Michalski, G., Kolanowski, M. Rihaa, K.M., 2015. Oxygen and nitrogen isotopic composition of nitrate in commercial fertilizers, nitric acid, and reagent salts. Isotopes in Environmental and Health Studies 51, 382-391.

Mizutani, Y., Rafter, T.A., 1973. Isotopic behaviour of sulphate oxygen in the bacterial reduction of sulphate. Geochemical Journal, 6, 183-191.

Montaner, J., Pons, P., López, J., 2010. Caracterització del flux hidrològic a la plana litoral del Baix Ter. In: El flux hidrològic de la plana litoral del Baix Ter.

Evolució fluvial, caracterització hidrològica i pautes de gestió. Montaner, J. (coord.). Càtedra d'Ecosistemes Litorals Mediterranis. Museu de la Mediterrània (Ed.). Recerca i Territori, 2.

Neal, C., Neal, M., Warrington, A., Àvila, A., Piñol, J., Rodà, F., 1992. Stable hydrogen and oxygen isotope studies of rainfall and streamwaters for two contrasting holm oak areas of Catalonia, northeastern Spain. Journal of Hydrology, 140, 163–178.

Otero, N., Canals, A., Soler, A., 2007. Using dual-isotope data to trace the origin and processes of dissolved sulphate: a case study in Calders stream (Llobregat basin, Spain). Aquat. Geochem. 13, 109–126.

Otero, N., Soler, A., Canals, A., 2008. Controls of $\delta^{34}S$ and $\delta^{18}O$ in dissolved sulphate: Learning from a detailed survey in the Llobregat River (Spain). Applied Geochemistry, 23, 1166-1185.

Otero, N., Torrentó, C., Soler, A., Menció, A., Mas-Pla, J., 2009. Monitoring groundwater nitrate attenuation in a regional system coupling hydrogeology with multi-isotopic methods: the case of Plana de Vic (Osona, Spain). Agr. Ecosyst. Environ. 133 (1-2), 103–113.

Panno, S.V., Hackley, K.C., Hwang, H.H., Kelly, W.R., 2001. Determination of the sources of nitrate contamination in karst springs using isotopic and chemical indicators. Chemical Geology, 179, 113-128.

Rivett, M.O., Buss, S.R., Morgan, P., Smith, J.W.N., Bemment, C.D., 2008. Nitrate attenuation in groundwater: a review of biogeochemical controlling processes. Water Res. 42, 4215–4232.

Rock, L., Mayer, B., 2002. Isotopic assessment of sources and processes affecting sulphate and nitrate in surface water and groundwater of Luxembourg. Isotopes Environ. Health Stud. 38 (4), 191-206.

Sacchi, E., Acutis, M., Bartoli, M., Brenna, S., Delconte. C.A., Laini, A., Pennisi, M. (2013) Origin and fate of nitrates in groundwater from the central Po plain: Insights from isotopic investigations. Applied Geochemistry 34, 164-180.

Saccon, P., Leis, A., Marca, A., Kaiser, J., Campisi, L., Böttcher, M.E., Savarino, J., Escher, P., Eisenhauer, A., Erbland, J., 2013. Multi-isotope approach for the identification and characterization of nitrate pollution sources in the Marano lagoon (Italy) and parts of its catchment area. Appl. Geochem., 34, 75–89.

Sebilo, M., Mayer, B., Nicolardot, B., Pinay, G., Mariotti, A., 2013. Long-term fate of nitrate fertilizer in agricultural soils. PNAS (Proceedings of the National Academy of Sciences of the United States of America). www.pnas.org/cgi/doi/10.1073/pnas.1305372110

Seiler, R. L., 2005. Combined use of ^{15}N and ^{18}O of nitrate and ^{11}B to evaluate nitrate contamination in groundwater. Applied Geochemistry, 20, 1626-1636.

Silva, S.R., Ging, P.B., Lee, R.W., Ebbert, J.C., Tesoriero, A.J., Inkpen, E.L., (2002) Forensic applications of nitrogen and oxygen isotopes in tracing nitrate sources in urban environments. Environ Forensic 3, 125–130. doi:10.1006/enfo.2002.0086.

Silva, S.R., Kendall, C., Wilkison, D.H., Ziegler, A.C., Chang, C.C.Y., Avanzino, R.J., 2000. A new method for collection of nitrate from fresh water and the analysis of nitrogen and oxygen isotope ratios. Journal of Hydrology, 228, 22–36.

Spivack, A.J., Edmond, J.M., 1986. Determination of boron isotope ratios by thermal ionization mass spectrometry of the dicesium metaborate cation. Anal. Chem., 58, 31-35.

Tirez, K., Brusten, W., Widory, D., Petelet, E., Bregnot, A., Xue, D., Boeckx, P., Bronders, J., 2010. Boron Isotope Ratio ($\delta^{11}B$) Measurements in Water

Framework Directive Programs: Comparison between Double Focusing Sector Field ICP and Thermal Ionization Mass Spectrometry, J. Anal. At. Spectrom. 25, 964-974.

Travé, A., Labaume, P., Calvet, F., Soler, A. (1997) Sediment dewatering and pore fluid migration along thust faults in a foreland basin inferred from isotopic and elemental geochemical analyses (Eocene southern Pyrenees, Spain). Tectonophysics 282, 375-398.

Vane, C.H., Kim, A.W., McGowan, S., Leng, M.J., Heaton, T.H.E., Kendrick, C.P., Coombs, P., Yang, H., Swann, G.E.A., 2010. Sedimentary records of sewage pollution using faecal markers in contrasting peri-urban shallow lakes. The Science of the Total Environment 409, 345-356.

Van Stempvoort, D.R., Krouse, H.R., 1994. Controls of $\delta^{18}O$ in sulphate. In: Alpers, C.N., Blowes, D.W. (Eds.), Environmental Geochemistry of Sulphide Oxidation. American Chemical Society, Washington, pp. 446–480.

Vengosh, A., Heumann, K.G., Juraske, S., Kasher, R., 1994. Boron Isotope Application for Tracing Sources of Contamination in Groundwater. Environmental, Science and Technology 28, 1968-1974.

Vilanova, E., 2004. Anàlisi dels sistemes de flux a l'àrea Gavarres-Selva-Baix Empordà. Proposta de model hidrodinàmic regional. Ph.D Dissertation. Universitat Autònoma de Barcelona, 337 pp. http://www.tdx.cat/handle/10803/3437

Vilanova, E., Mas-Pla, J., Menció, A., 2008. Determinación de sistemas de flujo regionales y locales en las depresiones tectónicas del Baix Empordà y La Selva (NE de España) en base a datos hidroquímicos e isotópicos. Boletín Geológico y Minero, 119 (1), 51-62.

Vitòria, L., 2004. Estudi multi-isotòpic ($\delta^{15}N$, $\delta^{34}S$, $\delta^{13}C$, $\delta^{18}O$, δD i $^{87}Sr/^{86}Sr$) de les aigües subterrànies contaminades per nitrats d'origen agrícola i ramader. Translated title: Multi-isotopic approach ($\delta^{15}N$, $\delta^{34}S$, $\delta^{13}C$, $\delta^{18}O$, δD and $^{87}Sr/^{86}Sr$) of nitrate contaminated groundwaters by agricultural and stockbreeder activities. PhD Thesis. Universitat de Barcelona, 188 pp.

Vitòria, L., Otero, N., Canals, A., Soler, A., 2004. Fertilizer characterization: isotopic data (N, S, O, C and Sr). Environ. Sci. Technol. 38, 3254–3262.

Vitòria, L., Soler, A., Aravena, R., Canals, A., 2005. Multi-isotopic approach (^{15}N, ^{13}C, ^{34}S, ^{18}O and D) for tracing agriculture contamination in groundwater (Maresme, NE Spain). In: Environmental Chemistry (Eds. E. Lichtfouse, J. Schwarzbauer and D. Robert). Springer-Verlag, Heidelberg, 43-56.

Vitòria, L., Soler, A., Canals, A., Otero, N., 2008. Environmental isotopes (N, S, C, O, D) to determine natural attenuation processes in nitrate contaminated waters: example of Osona (NE Spain). Appl. Geochem. 23, 3597–3611.

Waldron, S., Tatner, P., Jack, I., Arnott, C., 2001. The Impact of Sewage Discharge in a Marine Embayment: A Stable Isotope Reconnaissance. Estuarine, Coastal and Shelf Science, 52, 111–115. doi:10.1006/ecss.2000.0731.

Ward, M.H., deKok, T.M., Levallois, P., Brender, J., Gulis, G., Nolan, B.T., VanDerslice, J., 2005. Workgroup report: drinking-water nitrate and health—recent findings and research needs. Environ. Health Perspect. 113, 1607–1614.

Wassenaar, L. I., 1995. Evaluation of the origin and fate of nitrate in the Abbotsford aquifer using the isotopes of ^{15}N and ^{18}O in NO_3. Applied Geochemistry, 10, 391–405.

Widory, D., Kloppmann, W., Chery, L., Bonnin, J., Rochdi, H., Guinamant, J.L., 2004. Nitrate in groundwater: an isotopic multi-tracer approach. Journal of Contaminant Hydrology, 72, 165-188.

Widory, D., Petelet-Giraud, E., Négrel, P., Ladouche, B., 2005. Tracking the sources of nitrate in groundwater using coupled nitrogen and boron isotopes: a synthesis. Environmental, Science and Technology, 39, 539-548.

Widory, D., Petelet-Giraud, E., Brenot, A., Bronders, J., Tirez, K., Boeckx, P., 2013. Improving the management of nitrate pollution in water by the use of isotope monitoring: the $\delta^{15}N$, $\delta^{18}O$ and $\delta^{11}B$ triptych. Isotopes in Environmental and Health Studies, 48, 1-19.

Xu, S., Kang, P, Sun, Y., 2016. A stable isotope approach and its application for identifying nitrate source and transformation process in water. Environ Sci Pollut Res 23, 1133-1148.

Xue, D., Botte, J., De Baets, B., Accoe, F., Nestler, A., Taylor, P., Van Cleemput, O., Berglund, M., Boeckx, P., 2009. Present limitations and future prospects of stable isotope methods for nitrate source identification in surface- and groundwater. Water Research, 43, 1159-1170.

Yingkai, X., Lan, W., 2001. The effect of pH and temperature on the isotopic fractionation of boron between saline brine and sediments. Chem. Geol. 171, 253–261.

Figure captions

Figure 1. Geological map of the Baix Ter basin, sampling point locations labelled according to the hydrogeological formation where they are located. Potentiometric contour lines of the unconfined aquifer, mainly in the shallow Quaternary formations, correspond to the August 2004 survey. Dashed line represents the zero elevation potentiometric level in the deep quaternary formations (mainly leaky aquifers) affected by intensive withdrawal rates in the central area of the basin. Geology from ICGC (http:// www.icgc.cat).

Figure 2. $\delta^{18}O_{H2O}$ and $\delta^{2}H$ of the Baix Ter groundwater samples collected in January 2004 (a) and August 2004 (b). The annual-Local Meteoric Water Line (LMWL) follows the equation $\delta^{2}H = 7.98(\pm2.71)\ \delta^{18}O + 7.85(\pm0.47)$ (r^2=0.924, n=23) (Vilanova, 2004), whose slope is equal to that of the neighbouring areas ($\delta^{2}H = 7.9\ \delta^{18}O + 9.8$; Neal et al., 1992).

Figure 3. Mn concentrations plotted against the Eh values of the groundwater samples. Eh ranges of MnO_2/Mn^{2+} and $NO_3^-/N_{2(g)}$ redox pairs are taken from Rivett et al. (2008).

Figure 4 a) NO_3^- concentration versus Cl^- concentration, b) NO_3^- concentration versus SO_4^{2-} concentration, c) SO_4^{2-} concentration versus (NO_3^-/Cl^-) ratio, and d) B concentration versus (NO_3^-/Cl^-) ratio.

Figure 5. a) Variations of the $\delta^{15}N$ and $\delta^{18}O$ of dissolved NO_3^- in groundwater according to their hydrogeological unit. Isotope ranges of the main NO_3^- sources listed in Table 4 are also represented. The extreme isotopic fractionation factors from the literature are $\varepsilon_N/\varepsilon_O = 2.1$ (Böttcher et al., 1990) and $\varepsilon_N/\varepsilon_O = 1.3$ (Fukada et al., 2003). b) $\delta^{18}O_{NO3}$

values plotted against ln(NO_3^-/Cl^-) according to their hydrogeological unit. R^2 values for the linear regressions for shallow Quat. and deep Tert. Units are also reported.

Figure 6. $\delta^{34}S$ and $\delta^{18}O$ of dissolved SO_4^{2-} in groundwater according to their hydrogeological unit. Isotope ranges of natural and anthropogenic SO_4 sources listed in Table 4 are also represented. The area of sulphates derived from sulphide oxidation is from Van Stempvoort and Krouse (1994). Dashed lines define the isotopic fractionation range ($\varepsilon^{34}S/\varepsilon^{18}O_{SO4}$) in SO_4 reduction reactions, varying between 2.5 and 4 (Mizutani and Rafter, 1973).

Figure 7. $\delta^{11}B$ values plotted against B concentration (a) and $\delta^{15}N$ values (b). Isotope ranges of the main NO_3^- sources listed in Table 4 are also represented. $\delta^{11}B_{seawater}$ is taken from Vengosh et al. (1994).

Figure 8. a) $\delta^{18}O_{NO3}$ values plotted against ln(NO_3^-/HCO_3^-). b) $\delta^{13}C_{HCO3}$ values plotted against HCO_3^- concentration. Isotope ranges of the main NO_3^- sources listed in Table 4 are also represented. Value for $\delta^{13}C_{HCO3}$ for marls is from Travé et al. (1997).

Table captions

Table 1. Hydrogeological formation, X and Y UTM coordinates, depth (m), hydraulic head (m.a.s.l.), and physico-chemical parameters measured in situ for the sampled points of each field campaign. See Fig. 1 for sampling locations in the Baix Ter basin. R_1 and R_2 Ter River samples are from the Colomers station, NW of the study zone (Fig. 1). (*n.d.*: Not determined).

Table 2. Hydrochemical data for the January and August 2004 field campaigns ("*" = DOC concentrations instead of TOC concentrations). R_1 and R_2 Ter River samples are from the Colomers station, NW of the study zone (Fig. 1). (*n.d.*: Not determined; *u.d.l.*: under detection limit).

Table 3. Isotope data for the January and August 2004 field campaigns. R_1 and R_2 Ter River samples are from the Colomers station, NW of the study zone (Fig. 1). (*n.d.*: Not determined).

Table 4. Ranges of nitrate, sulphate, boron and dissolved inorganic carbon isotope compositions of the main potential sources of nitrate obtained from the literature.

Table 1

Click here to download Table: Table 1.docx

Table 1. Hydrogeological formation, X and Y UTM coordinates, depth (m), hydraulic head (m.a.s.l.), and physico-chemical parameters measured in situ for the sampled points of each field campaign. See Fig. 1 for sampling locations in the Baix Ter basin. R_1 and R_2 Ter River samples are from the Colomers station, NW of the study zone (Fig. 1). (*n.d.*: Not determined)

Sample	Field campaign	Hydrogeological formation	X (UTM)	Y (UTM)	Depth (m)	Hydraulic head (m.a.s.l.)	T (ºC)	EC (25 ºC) (mS/cm)	pH	Eh (mV)
Q_1	1	Q_D	504970	4654520	28	13.1	14.0	787	7.9	89
Q_2	1	Q_D	508910	4653880	46	-1.4	14.4	596	8.0	46
Q_3	1	Q_D	508790	4648620	72	16.9	16.7	955	7.7	397
Q_2	2	Q_D	508910	4653880	46	-3.0	18.3	812	7.8	188
Q_3	2	Q_D	508790	4648620	72	15.6	18.2	1225	7.7	393
Q_4	1	Q_S	506280	4653300	7	10.8	15.0	1594	7.4	276
Q_5	1	Q_S	502300	4649320	10	27.4	16.0	1640	7.6	376
Q_6	1	Q_S	503340	4649390	10	22.4	14.6	899	7.6	332
Q_7	1	Q_S	501670	4655680	21	13.4	17.0	843	7.7	368
Q_8	1	Q_S	504920	4656490	20	10.9	16.9	862	7.9	366
Q_9	1	Q_S	505460	4652860	10	12.6	14.0	772	7.9	267
Q_{10}	1	Q_S	504340	4644620	8	60.3	16.3	1180	7.7	425
Q_{11}	1	Q_S	507820	4647100	6	32.0	13.3	722	8.2	361
Q_{12}	1	Q_S	501970	4655900	20	12.3	16.1	773	7.9	340

Q_{13}	1	Q_S	504290	4652570	16	13.1	14.9	836	7.8	449
Q_{14}	1	Q_S	504920	4646740	6	37.7	13.2	886	8.2	378
Q_{15}	1	Q_S	509180	4650980	6	5.2	15.3	2523	7.6	409
Q_{16}	1	Q_S	510970	4644350	6	36.4	14.7	1004	7.8	392
Q_5	2	Q_S	502300	4649320	10	24.8	16.8	2359	7.6	386
Q_6	2	Q_S	503340	4649390	10	n.d.	17.3	1125	7.8	318
Q_7	2	Q_S	501670	4655680	21	10.2	17.1	1164	7.5	413
Q_8	2	Q_S	504920	4656490	20	10.7	17.7	1383	7.8	332
Q_9	2	Q_S	505460	4652860	10	n.d.	16.2	1070	7.7	395
Q_{10}	2	Q_S	504340	4644620	8	60.4	16.2	1320	7.4	428
Q_{13}	2	Q_S	504290	4652570	16	8.7	16.2	1219	7.4	395
Q_{14}	2	Q_S	504920	4646740	12	36.1	17.6	949	7.5	365
Q_{15}	2	Q_S	509180	4650980	6	3.8	17.3	2993	8.0	388
Q_{16}	2	Q_S	510970	4644350	6	35.7	22.9	1007	7.8	443
Q_{17}	2	Q_S	501720	4647990	n.d.	29.5	17.6	809	7.9	386
Q_{18}	2	Q_S	510230	4648070	6	14.2	17.9	875	7.7	408
Q_{19}	2	Q_S	508410	4647030	12	32.8	16.4	999	7.6	348
Q_{20}	2	Q_S	503580	4647920	17	19.0	15.8	661	7.8	727
Q_{21}	2	Q_S	505090	4650800	17	15.0	16.2	980	7.5	445
S	1	spring	507650	4645200	0	55.0	15.0	629	7.7	319

S	2	spring	507650	4645200	0	55.0	15.4	748	7.9	334
T_1	1	T_D	508930	4648350	90	21.6	19.5	552	8.0	348
T_2	1	T_D	508830	4651340	100	7.2	14.9	908	8.0	369
T_3	1	T_D	503340	4651590	100	27.7	17.5	1176	7.8	378
T_4	1	T_D	505912	4646025	110	27.4	16.6	725	8.1	n.d.
T_5	1	T_D	504420	4647820	125	27.1	16.5	1325	7.8	343
T_6	1	T_D	511510	4646260	110	-4.5	18.5	736	7.8	362
T_1	2	T_D	508930	4648350	90	21.6	20.0	935	7.7	366
T_2	2	T_D	508830	4651340	100	11.4	19.8	1095	7.7	426
T_3	2	T_D	503340	4651590	100	22.1	17.2	1500	7.7	370
T_5	2	T_D	504420	4647820	125	24.4	19.1	1330	7.9	301
T_6	2	T_D	511510	4646260	110	-4.5	19.0	600	8.2	326
T_7	2	T_D	499910	4647360	70	42.0	21.2	1164	7.7	425
T_8	2	T_D	501790	4643590	156	n.d.	18.1	1374	8.0	357
T_9	2	T_D	507880	4644460	85	53.9	18.4	971	7.9	157
T_{10}	2	T_D	510025	4649000	125	n.d.	20.7	1053	7.9	183
T_{11}	2	T_D	501590	4647810	130	23.8	19.4	824	8.0	916
T_{12}	2	T_D	498230	4653260	110	n.d.	19.3	994	7.8	456
T_{13}	2	T_D	512180	4645340	175	n.d.	17.1	1137	7.6	393
T_{14}	2	T_D	508150	4649930	60	19.3	17.0	1449	7.6	159

T_{15}	2	T_D	501970	4653420	80	n.d.	19.1	1389	7.8	331
T_{16}	1	T_S	510930	4647500	22	-6.5	16.1	1006	7.9	363
T_{16}	2	T_S	510930	4647500	22	-5.8	16.8	1219	7.5	408
T_{17}	2	T_S	502650	4652480	40	23.7	19.2	2414	7.6	321
T_{18}	2	T_S	499460	4652480	34	126.0	18.0	837	8.0	357
T_{19}	2	T_S	500770	4651700	10	106.3	17.8	944	8.0	352
T_{20}	2	T_S	508550	4653010	9	9.0	17.7	1528	7.7	357
T_{21}	2	T_S	504505	4643350	5	102.5	22.2	649	7.7	385
T_{22}	2	T_S	499640	4645180	n.d.	n.d.	17.9	1055	7.6	327
T_{23}	2	T_S	502340	4646230	40	35.0	17.5	1438	7.5	372
R_1	-	Ter River	505699	4654685	-	-	n.d.	636	7.8	n.d.
R_2	-	Ter River	499361	4658519	-	-	n.d.	664	7.8	n.d.

Table 2

Click here to download Table: Table 2.docx

Table 2. Hydrochemical data for the January and August 2004 field campaigns ("*" = DOC concentrations instead of TOC concentrations). R_1 and R_2 Ter River samples are from the Colomers station, NW of the study zone (Fig. 1). (*n.d.*: Not determined; *u.d.l.*: under detection limit).

Sample	Field campaign	Hydrogeological formation	HCO_3^- (mg/L)	SO_4^{2-} (mg/L)	Cl^- (mg/L)	NO_3^- (mg/L)	Na^+ (mg/L)	K^+ (mg/L)	Ca^{2+} (mg/L)	Mg^{2+} (mg/L)	NH_4^+ (mg/L)	TOC (mg/L)	Mn (mg/L)	Fe (mg/L)	B (mg/L)
Q_1	1	Q_D	413	66	138	*u.d.l.*	43	*u.d.l.*	157	23	0.15	1.2	0.056	0.015	*u.d.l.*
Q_2	1	Q_D	349	48	51	*u.d.l.*	44	3	90	19	0.47	1.0	0.289	0.020	*u.d.l.*
Q_3	1	Q_D	361	117	79	115	37	*u.d.l.*	181	18	0.15	1.2	0.002	0.010	*u.d.l.*
Q_2	2	Q_D	341	41	61	*u.d.l.*	45	3	99	19	0.41	0.6	0.335	0.016	*u.d.l.*
Q_3	2	Q_D	335	129	79	144	36	*u.d.l.*	184	17	0.14	0.9	0.002	*u.d.l.*	*u.d.l.*
Q_4	1	Q_S	473	227	269	6	92	4	239	40	0.25	2.3	4.380	0.019	0.127
Q_5	1	Q_S	463	223	200	215	88	*u.d.l.*	291	28	0.13	2.1	0.002	0.019	*u.d.l.*
Q_6	1	Q_S	388	71	62	88	31	2	153	18	0.15	1.6	0.003	0.015	*u.d.l.*
Q_7	1	Q_S	353	111	76	48	30	*u.d.l.*	159	22	0.13	1.0	0.001	0.013	*u.d.l.*
Q_8	1	Q_S	347	136	99	13	60	3	128	25	0.12	1.4	0.783	0.016	*u.d.l.*
Q_9	1	Q_S	372	86	84	25	63	4	122	17	0.16	1.2	0.002	0.012	0.217
Q_{10}	1	Q_S	384	114	60	325	41	*u.d.l.*	245	15	0.18	1.3	0.001	0.014	0.113

Q_{11}	1	Q_S	253	60	52	31	31	3	94	13	0.17	3.3	0.003	0.018	*u.d.l.*
Q_{12}	1	Q_S	324	134	81	12	43	2	141	20	0.18	1.1	0.001	0.011	0.055
Q_{13}	1	Q_S	401	89	106	51	44	*u.d.l.*	167	20	0.15	1.9	0.001	0.017	0.089
Q_{14}	1	Q_S	210	77	52	147	29	*u.d.l.*	128	12	0.15	1.7	0.002	*u.d.l.*	*u.d.l.*
Q_{15}	1	Q_S	427	277	294	387	94	72	283	76	0.14	3.2	0.001	0.011	0.168
Q_{16}	1	Q_S	351	124	76	168	57	*u.d.l.*	183	19	0.17	1.9	0.001	*u.d.l.*	*u.d.l.*
Q_5	2	Q_S	483	321	226	328	123	*u.d.l.*	331	30	0.14	1.6	0.001	*u.d.l.*	*u.d.l.*
Q_6	2	Q_S	366	88	59	129	28	2	165	18	0.16	0.6	0.006	*u.d.l.*	*u.d.l.*
Q_7	2	Q_S	399	112	79	122	30	*u.d.l.*	201	26	0.11	0.5	0.001	0.011	*u.d.l.*
Q_8	2	Q_S	337	204	139	51	71	3	174	31	0.08	1.1	0.971	*u.d.l.*	*u.d.l.*
Q_9	2	Q_S	358	86	84	26	58	4	130	17	0.11	0.6	0.002	*u.d.l.*	0.209
Q_{10}	2	Q_S	440	76	50	241	45	*u.d.l.*	225	13	0.12	0.9	0.002	0.012	0.189
Q_{13}	2	Q_S	405	120	86	66	44	2	178	21	0.08	1.2	0.001	*u.d.l.*	0.123
Q_{14}	2	Q_S	195	66	55	201	29	*u.d.l.*	140	13	0.08	0.5	0.002	0.011	*u.d.l.*
Q_{15}	2	Q_S	413	371	362	480	111	68	345	85	0.14	3.4	0.001	*u.d.l.*	0.150
Q_{16}	2	Q_S	356	93	55	65	47	*u.d.l.*	143	14	0.14	0.6	0.001	*u.d.l.*	*u.d.l.*

Q_{17}	2	Q_S	301	29	28	60	18	*u.d.l.*	116	12	0.13	0.4	0.001	*u.d.l.*	*u.d.l.*
Q_{18}	2	Q_S	390	102	47	83	38	6	163	14	0.13	0.6	0.001	*u.d.l.*	*u.d.l.*
Q_{19}	2	Q_S	304	55	52	205	24	*u.d.l.*	166	14	0.15	0.7	0.001	0.022	*u.d.l.*
Q_{20}	2	Q_S	177	52	52	50	29	5	83	11	0.12	0.9	0.001	0.012	0.082
Q_{21}	2	Q_S	313	95	71	45	55	4	124	16	0.21	0.6	0.002	0.011	0.232
S	1	spring	298	64	47	37	29	*u.d.l.*	110	12	0.18	1.4	0.001	0.011	*u.d.l.*
S	2	spring	268	58	50	68	31	*u.d.l.*	117	13	0.15	1.0	0.001	0.013	*u.d.l.*
T_1	1	T_D	417	68	43	10	42	3	131	13	0.13	0.8	0.001	0.012	*u.d.l.*
T_2	1	T_D	470	156	87	9	51	3	129	54	0.13	1.3	0.018	0.019	*u.d.l.*
T_3	1	T_D	276	116	123	222	55	*u.d.l.*	185	22	0.15	1.9	0.001	0.014	*u.d.l.*
T_4	1	T_D	383	110	60	15	33	49	118	24	0.16	1.2	0.025	0.016	0.071
T_5	1	T_D	430	152	119	222	105	12	178	36	0.20	2.8	0.007	0.012	0.066
T_6	1	T_D	382	59	76	46	57	3	118	20	0.14	1.2	0.007	0.014	*u.d.l.*
T_1	2	T_D	402	55	41	23	35	3	136	12	0.16	0.4	0.001	*u.d.l.*	*u.d.l.*
T_2	2	T_D	435	157	74	11	44	3	127	51	0.12	0.7	0.026	*u.d.l.*	0.081
T_3	2	T_D	376	91	180	221	68	4	214	30	0.12	1.7	0.001	*u.d.l.*	0.065

T_5	2	T_D	514	118	99	61	162	11	94	23	0.18	0.6	0.010	*u.d.l.*	0.104
T_6	2	T_D	354	34	70	3	54	3	100	18	0.14	0.3	0.007	*u.d.l.*	0.051
T_7	2	T_D	368	83	66	139	32	*u.d.l.*	183	14	0.14	0.9	0.001	*u.d.l.*	*u.d.l.*
T_8	2	T_D	222	107	135	265	58	9	181	24	0.12	1.1	0.007	0.016	*u.d.l.*
T_9	2	T_D	384	31	118	*u.d.l.*	75	5	81	39	0.16	0.9	0.197	0.013	0.055
T_{10}	2	T_D	533	74	52	*u.d.l.*	63	2	168	16	0.10	0.4	0.064	0.013	0.053
T_{11}	2	T_D	323	32	46	69	41	3	106	16	0.11	0.8	0.001	0.013	*u.d.l.*
T_{12}	2	T_D	379	52	62	71	33	3	104	45	0.12	0.4	0.002	0.013	*u.d.l.*
T_{13}	2	T_D	392	86	96	46	55	2	146	28	0.12	0.7	0.001	0.010	0.051
T_{14}	2	T_D	619	87	126	*u.d.l.*	74	4	102	94	0.33	0.5	0.042	0.016	0.061
T_{15}	2	T_D	401	95	130	152	114	3	110	42	0.21	1.2	0.002	0.014	0.095
T_{16}	1	T_S	388	149	93	63	55	2	162	37	0.12	1.4	0.002	0.014	*u.d.l.*
T_{16}	2	T_S	371	146	102	71	49	*u.d.l.*	169	32	0.23	0.9	0.002	0.012	*u.d.l.*
T_{17}	2	T_S	372	245	231	419	122	59	223	70	0.11	2.6	0.003	*u.d.l.*	0.084
T_{18}	2	T_S	249	30	31	147	15	*u.d.l.*	121	19	0.14	0.6	0.001	*u.d.l.*	*u.d.l.*
T_{19}	2	T_S	348	56	39	89	33	7	137	13	0.14	1.2	0.003	*u.d.l.*	*u.d.l.*

T_{20}	2	T_S	350	210	108	212	56	6	200	38	0.17	2.2	0.001	*u.d.l.*	0.123
T_{21}	2	T_S	300	30	36	6	22	*u.d.l.*	104	9	0.14	1.0	0.002	0.012	*u.d.l.*
T_{22}	2	T_S	371	81	49	153	29	*u.d.l.*	193	8	0.16	1.1	0.002	0.012	*u.d.l.*
T_{23}	2	T_S	355	66	181	190	75	*u.d.l.*	216	24	0.26	0.7	0.004	0.010	*u.d.l.*
R_1	-	Ter River	194	73	50	7	38	5	75	11	*n.d.*	4.3*	0.029	0.010	0.075
R_2	-	Ter River	204	74	50	9	40	5	78	12	n.d.	4.5*	0.025	0.012	0.090

Table 3

Click here to download Table: Table 3.docx

Table 3. Isotope data for the January and August 2004 field campaigns. R_1 and R_2 Ter River samples are from the Colomers station, NW of the study zone (Fig. 1). (*n.d.*: Not determined).

Sample	Field campaign	Hydrogeological formation	$\delta^{18}O$-H_2O (‰)	$\delta^{2}H$ (‰)	$\delta^{15}N$ (‰)	$\delta^{18}O$-NO_3 (‰)	$\delta^{34}S$ (‰)	$\delta^{18}O$-SO_4 (‰)	$\delta^{13}C$-DIC (‰)	$\delta^{11}B$ (‰)
Q_1	1	Q_D	-5.2	-35.8	*n.d.*	*n.d.*	14.7	16.1	-14.9	*n.d.*
Q_2	1	Q_D	-5.5	-37.8	*n.d.*	*n.d.*	13.9	13.6	-13.7	*n.d.*
Q_3	1	Q_D	-5.4	-35.4	11.6	8.3	0.4	5.6	-13.6	*n.d.*
Q_2	2	Q_D	-5.9	-37.6	*n.d.*	*n.d.*	10.3	12.4	-13.8	*n.d.*
Q_3	2	Q_D	-5.5	-34.9	12.3	8.4	0.9	5.5	-13.7	*n.d.*
Q_4	1	Q_S	-5.1	-33.6	32.5	18.1	8.2	13.0	-13.2	34.5
Q_5	1	Q_S	-5.3	-34.6	15.9	8.9	12.2	10.1	-12.9	*n.d.*
Q_6	1	Q_S	-5.3	-33.9	11.3	6.8	6.2	6.8	-13.2	*n.d.*
Q_7	1	Q_S	-6.0	-40.8	12.2	7.7	6.3	7.8	-11.3	*n.d.*
Q_8	1	Q_S	-6.5	-44.1	20.5	13.7	9.1	10.1	-12.7	*n.d.*
Q_9	1	Q_S	-5.4	-35.3	19.1	10.1	6.8	8.9	-14.0	23.3
Q_{10}	1	Q_S	-5.8	-39.5	10.4	4.4	5.9	4.8	-12.5	25.7

Q_{11}	1	Q_S	-6.3	-39.6	13.6	8.7	5.1	7.8	-16.0	*n.d.*
Q_{12}	1	Q_S	-6.3	-41.9	13.3	8.1	8.2	8.9	-12.4	26.0
Q_{13}	1	Q_S	-5.3	-35.9	14.7	9.2	6.3	8.2	-13.9	28.3
Q_{14}	1	Q_S	-5.6	-36.8	7.7	5.5	4.0	5.4	-11.3	*n.d.*
Q_{15}	1	Q_S	-4.8	-31.8	13.5	7.5	2.6	5.8	-14.6	30.4
Q_{16}	1	Q_S	-5.5	-36.9	8.7	4.2	5.3	5.3	-14.0	*n.d.*
Q_5	2	Q_S	-5.3	-33.5	18.9	5.3	12.7	10.2	-15.5	*n.d.*
Q_6	2	Q_S	-5.3	-33.8	12.3	7.2	6.1	7.0	-13.6	*n.d.*
Q_7	2	Q_S	-5.3	-36.3	12.3	6.5	3.0	6.0	-12.0	*n.d.*
Q_8	2	Q_S	-6.6	-43.9	16.3	9.5	8.0	7.8	-11.8	*n.d.*
Q_9	2	Q_S	-5.5	-34.8	21.6	10.6	7.7	9.9	-14.1	*n.d.*
Q_{10}	2	Q_S	-6.0	-40.6	13.4	4.6	6.4	5.1	-16.0	*n.d.*
Q_{13}	2	Q_S	-5.3	-33.8	15.7	9.1	5.9	8.5	-13.6	*n.d.*
Q_{14}	2	Q_S	-5.2	-34.8	9.9	4.4	4.6	5.0	-14.7	*n.d.*
Q_{15}	2	Q_S	-4.9	-31.8	16.2	4.6	3.3	5.3	-14.1	*n.d.*
Q_{16}	2	Q_S	-5.8	-37.3	7.2	4.3	4.7	6.1	-14.1	*n.d.*

Q_{17}	2	Q_S	-5.4	-35.6	8.4	4.8	7.2	6.6	-15.0	*n.d.*
Q_{18}	2	Q_S	-5.6	-38.0	8.2	4.5	-1.4	6.3	-12.2	*n.d.*
Q_{19}	2	Q_S	-5.5	-38.2	10.5	5.5	3.1	4.9	-13.4	*n.d.*
Q_{20}	2	Q_S	-5.6	-36.2	13.6	7.4	5.6	6.6	-14.9	9.0
Q_{21}	2	Q_S	-5.6	-36.9	16.6	9.9	5.4	7.5	-14.7	1.4
S	1	spring	-5.8	-37.4	8.6	5.0	5.3	7.3	-14.3	*n.d.*
S	2	spring	-5.9	-37.7	9.6	6.8	5.4	7.2	-13.5	*n.d.*
T_1	1	T_D	-5.6	-37.8	8.9	6.8	1.6	8.2	-10.2	*n.d.*
T_2	1	T_D	-5.2	-35.1	16.0	8.0	-13.5	3.8	-9.0	*n.d.*
T_3	1	T_D	-5.1	-33.1	7.6	4.7	4.9	6.0	-13.7	*n.d.*
T_4	1	T_D	-5.5	-36.3	14.9	10.1	4.9	10.1	-13.3	31.7
T_5	1	T_D	-5.3	-34.7	11.1	5.3	4.2	4.8	-12.5	23.9
T_6	1	T_D	-5.6	-35.7	12.8	6.9	2.3	8.0	-12.0	*n.d.*
T_1	2	T_D	-5.8	-36.4	10.8	6.8	1.5	7.6	-11.2	*n.d.*
T_2	2	T_D	-5.3	-35.3	22.6	10.9	-13.4	4.2	-9.1	*n.d.*
T_3	2	T_D	-5.2	-36.1	11.0	7.0	5.5	6.2	-13.9	*n.d.*

T_5	2	T_D	-5.9	-37.5	13.7	6.5	5.8	7.9	-8.5	*n.d.*
T_6	2	T_D	-5.9	-37.1	12.1	9.1	-2.6	11.1	-11.9	*n.d.*
T_7	2	T_D	-5.5	-36.3	10.8	5.2	5.2	6.6	-13.4	*n.d.*
T_8	2	T_D	-5.6	-35.7	13.8	6.1	5.3	4.6	-15.4	*n.d.*
T_9	2	T_D	-6.1	-39.0	*n.d.*	*n.d.*	14.2	12.0	-11.5	*n.d.*
T_{10}	2	T_D	-5.7	-37.6	*n.d.*	*n.d.*	10.0	10.6	-10.2	*n.d.*
T_{11}	2	T_D	-5.4	-39.7	11.6	6.6	6.3	6.2	-13.0	*n.d.*
T_{12}	2	T_D	-5.2	-37.5	13.8	7.1	-1.8	4.5	-12.1	*n.d.*
T_{13}	2	T_D	-5.7	-37.6	11.9	5.6	1.7	5.8	-12.5	*n.d.*
T_{14}	2	T_D	-5.4	-36.4	*n.d.*	*n.d.*	-16.0	4.9	-6.5	*n.d.*
T_{15}	2	T_D	-5.4	-36.6	12.2	5.0	6.2	5.2	-13.1	*n.d.*
T_{16}	1	T_S	-5.4	-34.8	10.7	8.5	-4.1	5.8	-11.3	*n.d.*
T_{16}	2	T_S	-5.0	-35.1	13.3	9.4	-1.7	5.5	-11.9	*n.d.*
T_{17}	2	T_S	-5.1	-34.3	16.1	1.8	5.9	6.3	-14.5	29.5
T_{18}	2	T_S	-5.0	-33.9	6.3	3.5	4.1	5.0	-13.5	*n.d.*
T_{19}	2	T_S	-5.9	-38.1	9.3	6.2	7.3	9.2	-16.2	*n.d.*

T_{20}	2	T_S	-5.4	-36.0	12.2	5.1	3.3	5.6	-13.2	25.5
T_{21}	2	T_S	-6.2	-36.8	5.0	6.3	6.9	5.1	-14.9	*n.d.*
T_{22}	2	T_S	-5.7	-36.2	11.5	6.2	6.6	4.9	-15.6	*n.d.*
T_{23}	2	T_S	-5.6	-38.2	16.1	6.1	9.4	4.3	-14.8	*n.d.*
R_1	-	Ter River	*n.d.*	*n.d.*	13.2	4.2	11.3	9.5	*n.d.*	*n.d.*
R_2	-	Ter River	*n.d.*	*n.d.*	*n.d.*	*n.d.*	*n.d.*	*n.d.*	*n.d.*	*n.d.*

Table 4

Click here to download Table: Table 4.docx

Table 4. Ranges of nitrate, sulphate, boron and dissolved inorganic carbon isotope compositions of the main potential sources of nitrate obtained from the literature.

NO_3^- source Isotope ratio (‰)	Pig manure	Mineral fertilizers	Sewage	Soil
$\delta^{15}N$	+8 — +16	-4 — +8	+5 — +20	+3 — +8
	Vitòria (2004)	Michalski et al. (2015), Vitòria et al. (2004)	Aravena and Mayer (2010), Curt el al. (2004), Vane et al. (2010)	Aravena and Mayer (2010), Heaton (1986), Kendall et al. (2007)
$\delta^{18}O_{NO3}$	+3.4 — +4.6	+17 — +25	+3.4 — +4.6	+3.4 — +4.6
	Estimated in this study according to eq.5	Aravena and Mayer (2010), Vitòria et al. (2004), Xue et al. (2009)	Estimated in this study according to eq.5	Estimated in this study according to eq.5
$\delta^{34}S$	-0.9 — +5.8	0 — +10	+7.6 — +11.7	0 — +6
	Cravotta (1997)	Vitòria et al. (2004)	Otero et al. (2008)	Krouse and Mayer (2000)
$\delta^{18}O_{SO4}$	+3.8 — +6	+9 — +15	+9 — +11.1	0 — +6
	Otero et al. (2007), Vitòria (2004)	Vitòria et al. (2004)	Otero et al. (2008)	Krouse and Mayer (2000)

$\delta^{11}B$	+19.5 — +42.4	-9 — +15	-7.7 — +12.9	-
	Widory et al. (2005)	Komor (1997), Widory et al. (2005), (2013)	Bassett et al. (1995), Vengosh et al. (1994), Widory et al. (2013), Xue et al. (2009)	-
$\delta^{13}C_{HCO3}$	-23.8 — -16.4	-35 — -24	-25 — -13	-23
	Cravotta (1997), Vitòria (2004)	Vitòria et al. (2004)	Jurado et al. (2013), Li et al. (2010), Waldron et al. (2001)	Clark and Fritz (1997)

Figure 1

Click here to download high resolution image

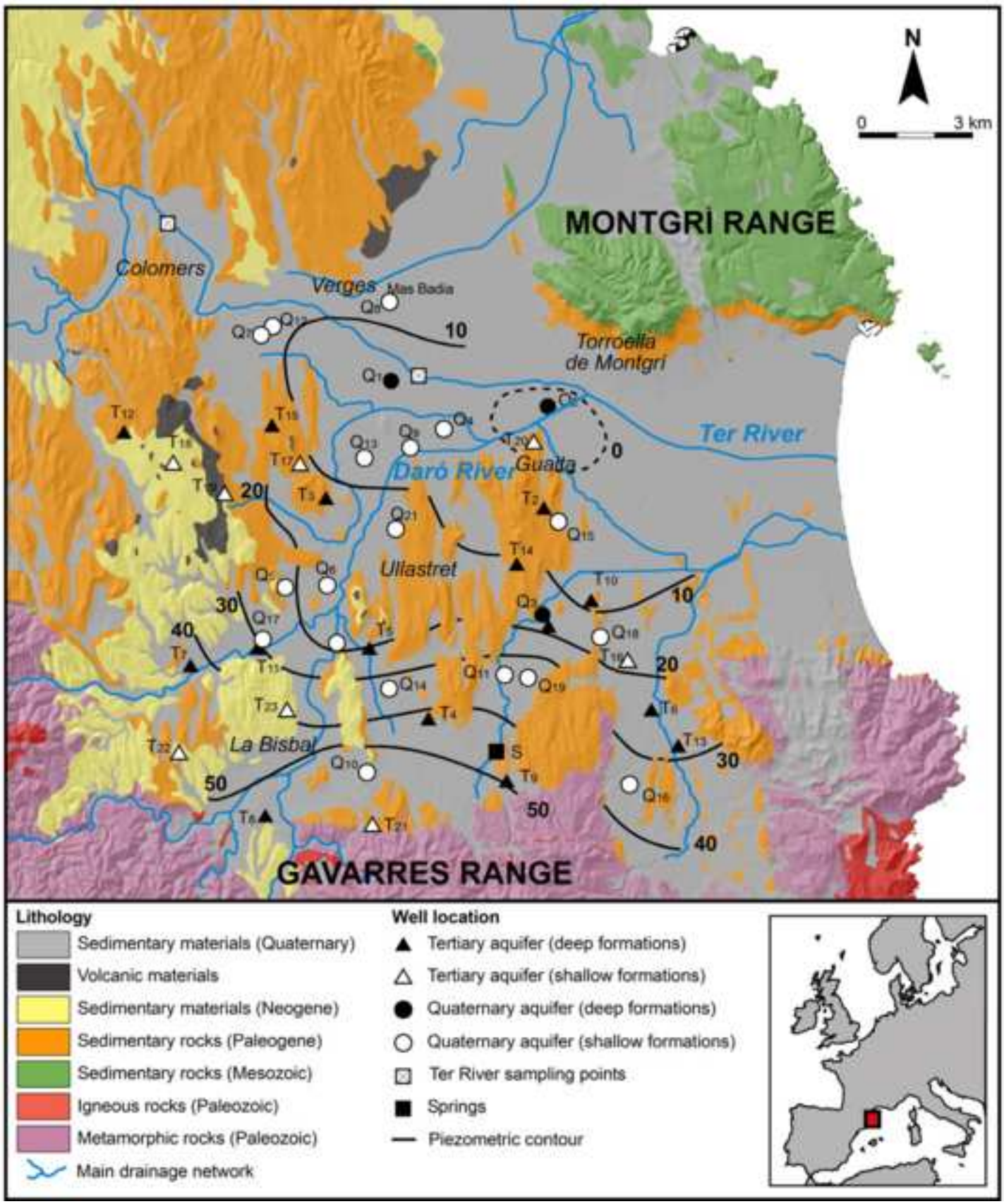

Figure 2

Click here to download Figure: figure2.docx

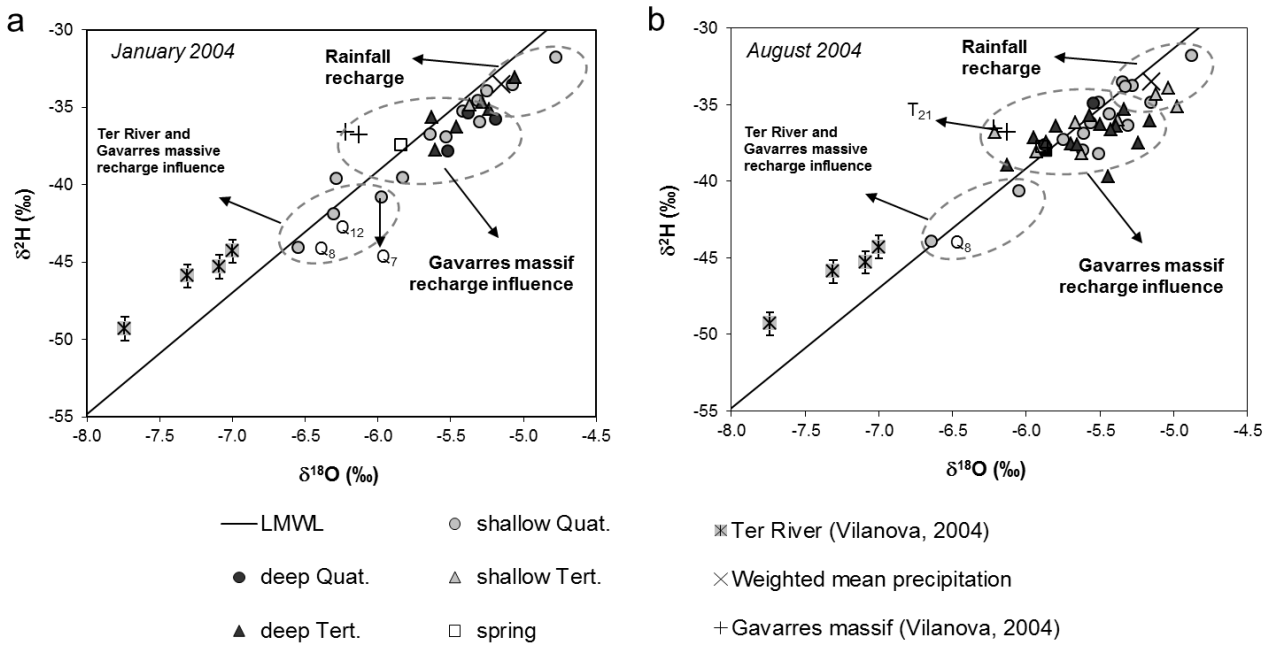

Figure 3

Click here to download Figure: figure3.docx

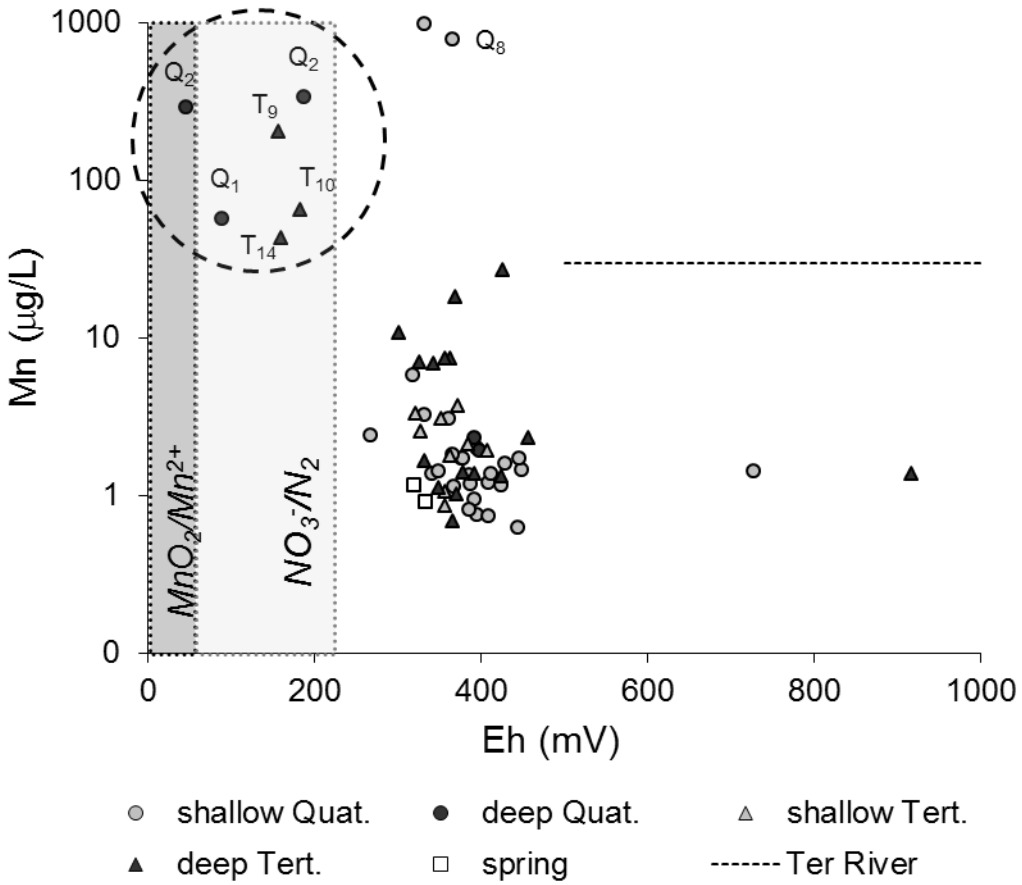

Figure 4

Click here to download Figure: figure4.docx

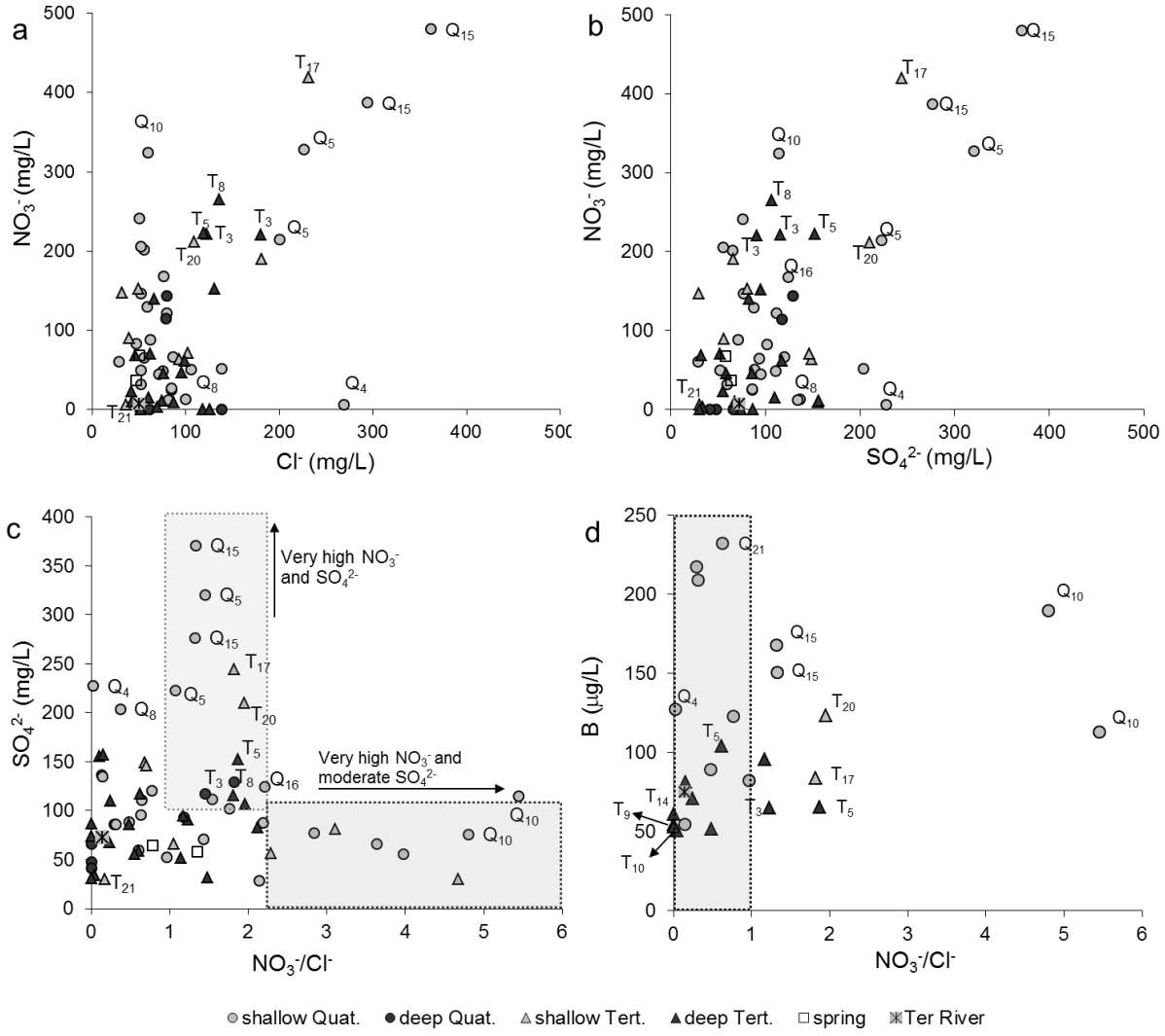

Figure 5

Click here to download Figure: figure5.docx

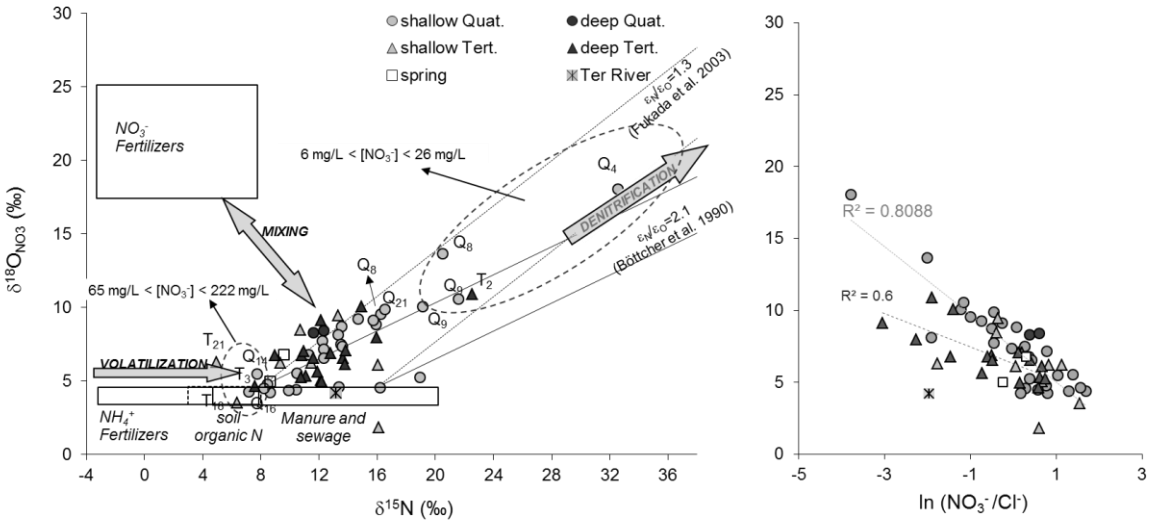

Figure 6

Click here to download Figure: figure6.docx

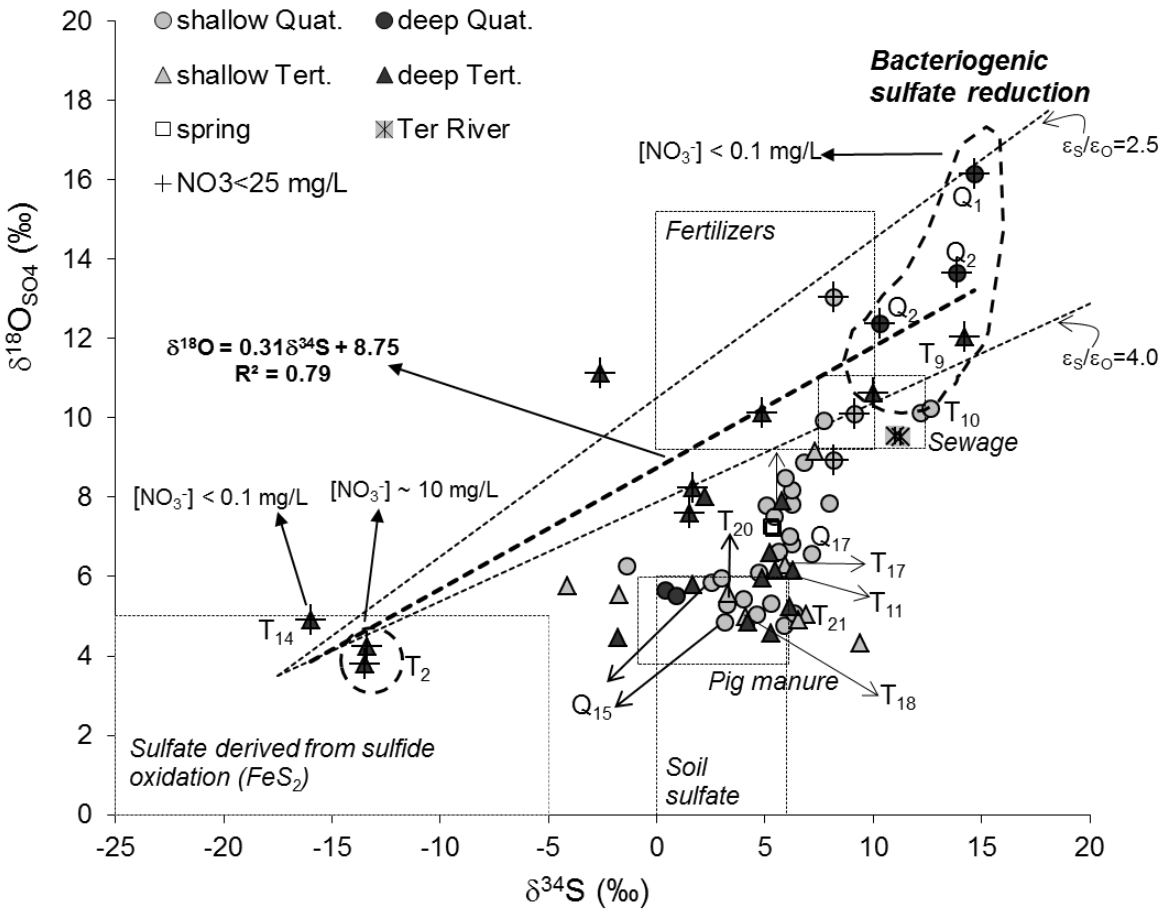

Figure7

Click here to download Figure: figure7.docx

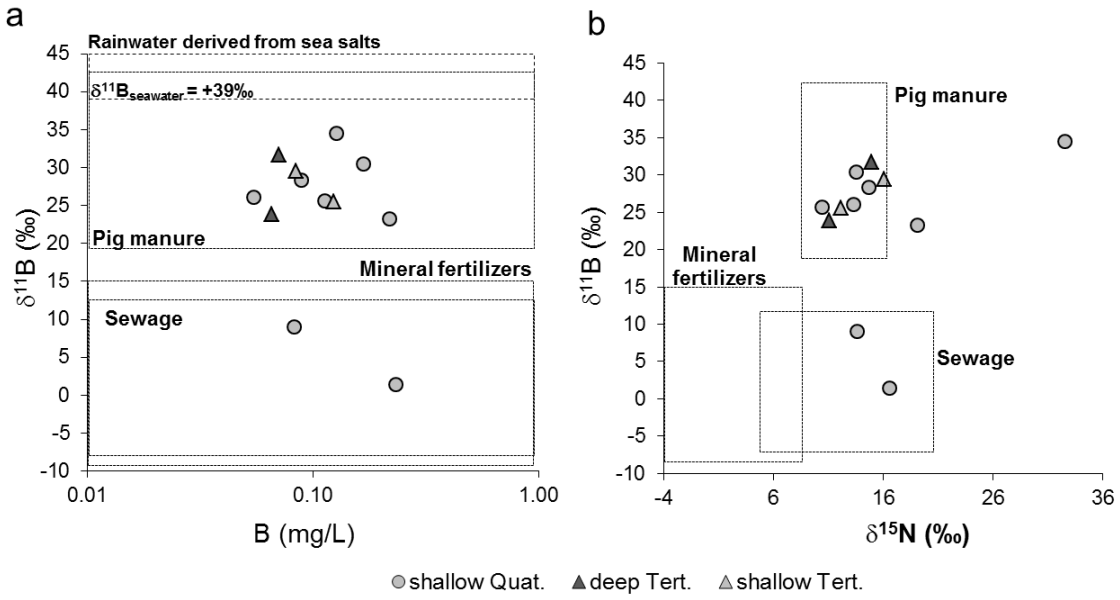

Figure 8

Click here to download Figure: figure8.docx